Dynamic Modelling of CO_2 Sequestration in the Harvey Area

A Report by ODIN Reservoir Consultants

For

DMIRS 2018/7

ODIN
Reservoir Consultants

June 2018

List of Figures

List of Tables

Declaration

ODIN Reservoir Consultants has been commissioned to undertake to provide a reservoir modelling study for the South West Hub CO2 Sequestration Project on behalf of The Department of Mines, Industry Regulation and Safety (DMIRS)

Our note must be considered in its entirety and reflects ODIN's informed professional judgment based on accepted standards of professional investigation and, as applicable, the data and information provided by DMIRS, the limited scope of engagement, and the time permitted to conduct the evaluation. The opinions expressed herein are subject to and fully qualified by the generally accepted uncertainties associated with the interpretation of geoscience and engineering data and do not reflect the totality of circumstances, scenarios and information that could potentially affect decisions made by the report's recipients and/or actual results. In line with those accepted standards, this document does not in any way constitute or make a guarantee or prediction of results, and no warranty is implied or expressed that actual outcome will conform to the outcomes presented herein.

ODIN has not independently verified any information provided by or at the direction of DMIRS, and has accepted the accuracy and completeness of these data. ODIN has no reason to believe that any material facts have been withheld from it, but does not warrant that its inquiries have revealed all of the matters that a more extensive examination might otherwise disclose.

ODIN has not undertaken a site visit and inspection because it is not necessary for such an evaluation. As such, ODIN is not in a position to comment on the operations or facilities in place, their appropriateness and condition and whether they are in compliance with the regulations pertaining to such operations. Further, ODIN is not in a position to comment on any aspect of health, safety or environment of such operation.

Neither ODIN Reservoir Consultants nor its employees have any pecuniary interest or other interest in the assets evaluated other than to the extent of the professional fees receivable for the preparation of this report.

Note:

ODIN has conducted the attached independent technical evaluation with the following internationally recognised specialists:

***David Lim** is a member of the Society of Petroleum Engineers (SPE). He has over 30 years of international reservoir engineering experience in Europe, North and South America, North and West Africa, Middle East, Asia and Australasia. David is an internationally recognised expert in reservoir simulation and reservoir engineering. David has been the Reservoir Simulation and Reservoir Engineering Advisor to NOCs, major and independent operators in Australia and SE Asia. David has also chaired SPE committees and forums on reservoir simulation, well testing and field development planning.*

1. EXECUTIVE SUMMARY

ODIN Reservoir Consultants was commissioned by the Department of Mines, Industry Regulation and Safety (DMIRS) to provide a multi-disciplinary group with sub-surface skill sets to:

1) Undertake an interpretation of the 3D seismic data;
2) provide support through reservoir model building and updating of the South West Hub Project in the southern Perth Basin; and
3) provide on-going technical support.

As an integral part of the above, ODIN Reservoir Consultants conducted reservoir simulation studies to assess the suitability of the Lesueur Formation in the South West Region of Western Australia as a potential carbon dioxide geological sequestration site.

The objective of the simulation study was to provide a suite of full field simulation models which cover a range of subsurface uncertainties that provides confidence that the CO_2 plume stays below 800mTVDss and within the storage complex for 1000 years. The results of this study will enable a Go/No Go decision on additional data acquisition in the Harvey area.

Dynamic modelling of the CO_2 sequestration process in the Harvey area was conducted in two ways:

- “Black Oil” Modelling – A simplified description of the physics of the fluids based on simple interpolation of PVT properties as a function of pressure.
- Compositional modelling - Using a "compositional" approach based on a thermodynamically-consistent model such as a cubic equation of state (EOS).

In the Harvey area, most of the modelling was conducted using the “Black Oil” formulation. Specific cases were tested in a compositional model as a sense check. The results of the Black Oil and compositional modelling show that it could be feasible to inject 800,000 tpa of CO_2 over 30 years in the Lesueur Formation in the Harvey area. Our modelling studies show that all of the injected CO_2 remains in the area of interest and that the main factors controlling CO_2 plume migration are:

- the solubility of CO_2 in brine

and

- The combination of the transmissibility of fluids across the faults, and high vertical permeability fracture zones close to faults.

The results of the modelling also show that communication between the Wonnerup and Yalgorup Members, through faults or sand-to-sand communication does result in migration of CO_2 into the Yalgorup Member. Nevertheless, the injected CO_2 remains in the Lesueur Formation and within the area of interest even in pessimistic geological and fluid flow realisations, which have a low chance of occurring.

2. INTRODUCTION

ODIN Reservoir Consultants was commissioned by the Department of Mines, Industry Regulation and Safety (DMIRS) to provide a multi-disciplinary group with sub-surface skill sets to:

1) Undertake an interpretation of the 3D seismic data;
2) provide support through reservoir model building and updating of the South West Hub Project in the southern Perth Basin; and
3) provide on-going technical support.

As an integral part of the above, ODIN Reservoir Consultants conducted reservoir simulation studies to assess the suitability of the Lesueur Formation in the South West Region of Western Australia as a potential carbon dioxide geological sequestration site capable of injecting 800,000 tonnes per annum of CO_2 and containing the CO_2 for at least 1000 years after injection ceases. The location and area of interest of the study is shown in Figure 2-1.

The objective of the simulation study is to provide suite of full field simulation models which cover uncertainties and demonstrate plume profiles over 1,000 years and containment of the plume below 800mTVDss and within the storage complex for 1000 years that will enable a Go/No Go decision on additional data acquisition.

Dynamic Modelling or Simulation is a key step within the modelling workflow (Figure 2-2) which is the study of fluid flow within the Static 3D Geological Model. The results are analysed and compared to expected reality. The findings of the simulation study may be fed back into building another version of the 3D geological model to either refine the results or assist with defining the uncertainties/sensitivities of the reservoir.

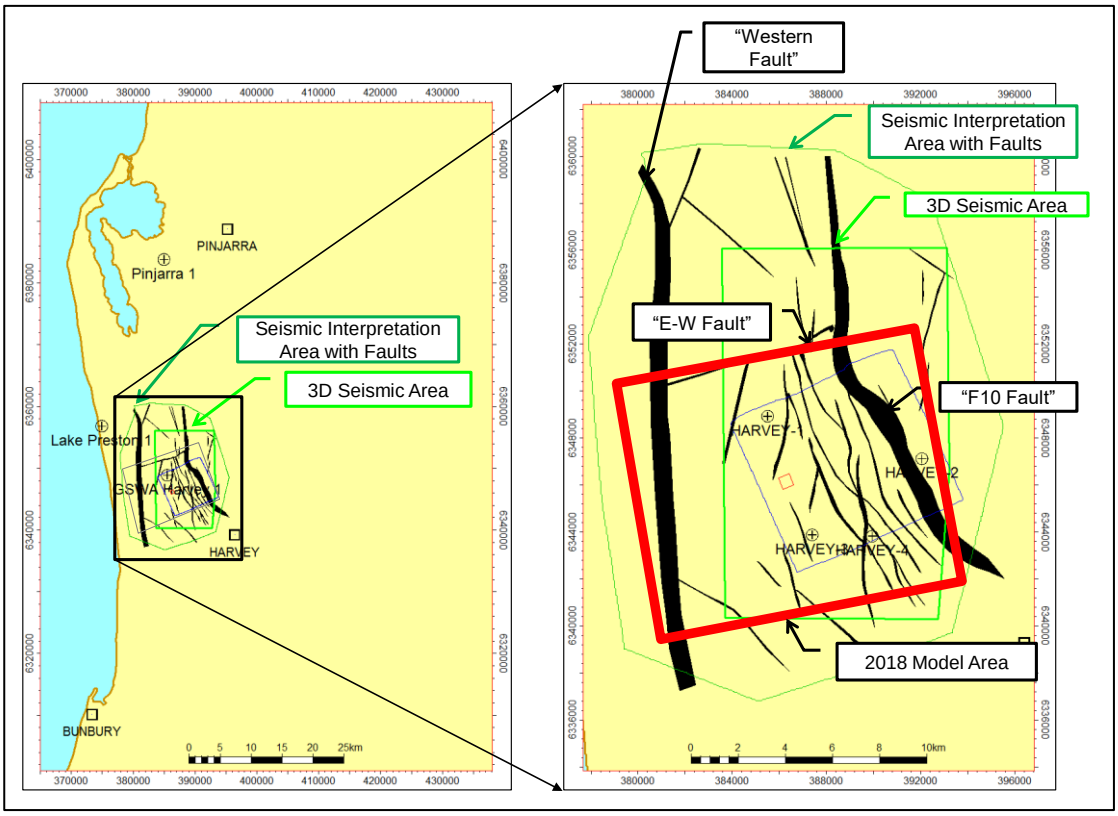

Figure 2-1 Location Map of the Harvey Area showing the Area of Interest

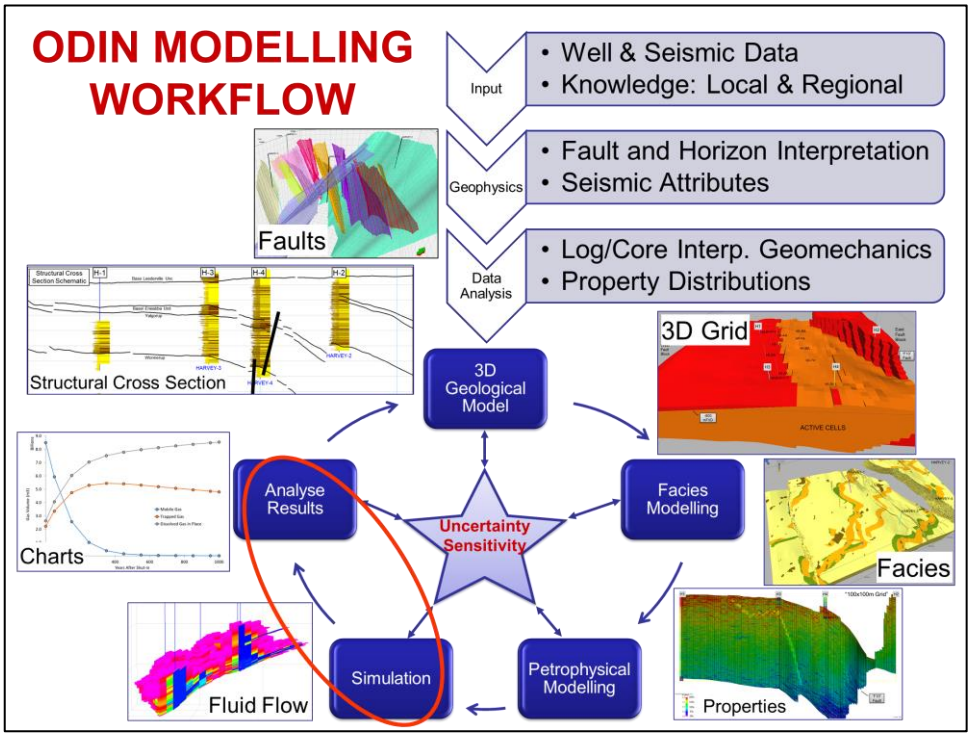

Figure 2-2 ODIN Modelling Workflow

3. INPUT FOR MODELLING

3.1 Temperature Regime

Bottom hole temperatures were recorded on all the wireline logging runs in GSWA Harvey 1, DMP Harvey-2, DMP Harvey-3 and DMP Harvey-4 (Figure 3-1). The maximum temperature recorded was nearly 76º C at a measured depth of about 2860m in GSWA Harvey 1. This represents a geothermal gradient of between 20-25 ºC/km.

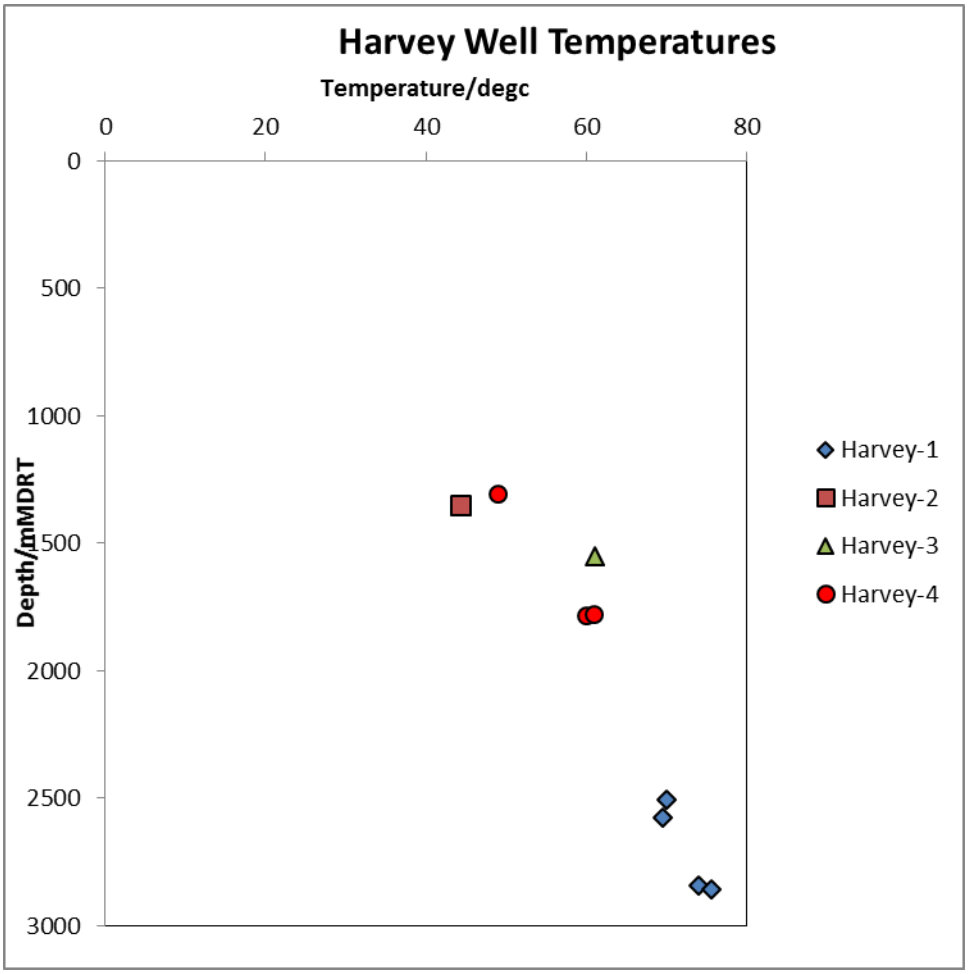

Figure 3-1 Temperature Measurements for the Harvey wells

3.2 Pressure Regime

Pressure measurements were made with the formation pressure sampling tools in GSWA Harvey 1 and DMP Harvey-4 are summarised in Figure 3-2. The data are consistent with a normally pressured aquifer extending to surface.

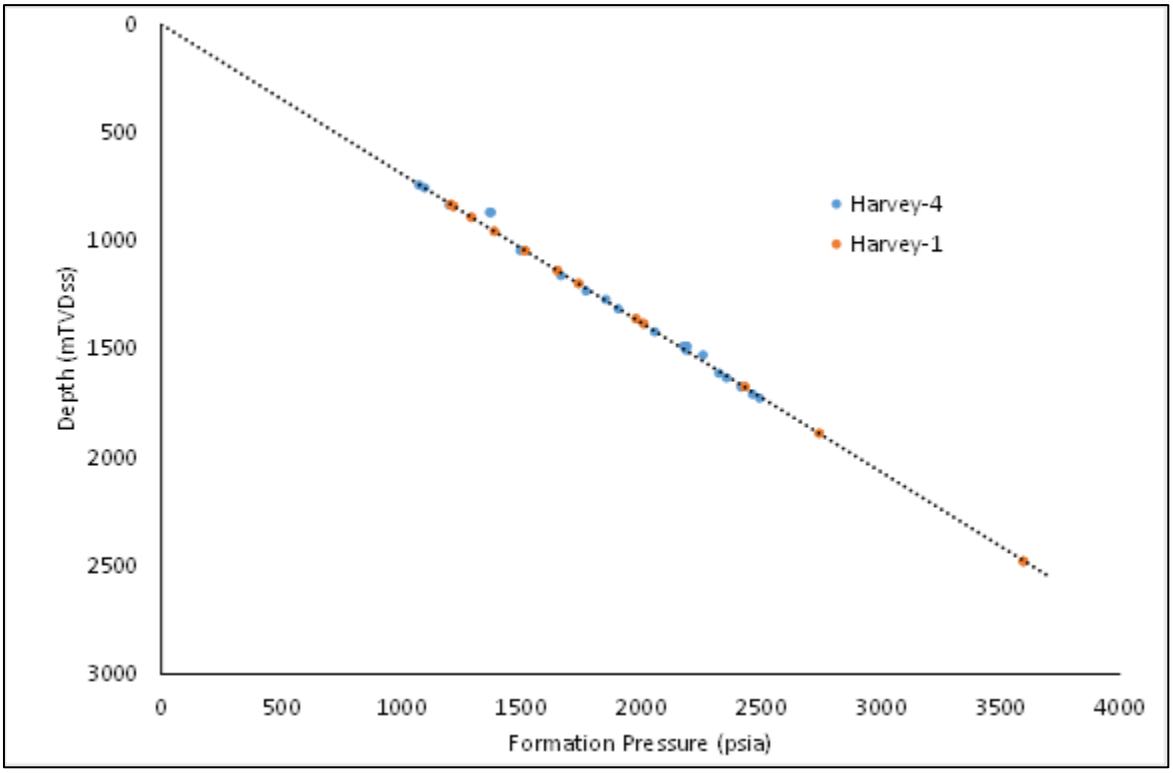

Figure 3-2 Pressure data from Harvey-4 and -1

3.3 Relative Permeability Data

Twenty seven core plugs from the GSWA Harvey 1, DMP Harvey-2, DMP Harvey-3 and DMP Harvey-4 wells were nominated for special core analysis (SCAL). The core plugs underwent computed tomography (CT) scans to ensure that the samples were not compromised by internal fractures or heterogeneities which could affect the SCAL (Appendix 1, Reference 2). Sixteen core plugs were selected for SCAL from the results CT scans (Table 3-1).

Well	Sample Number	Sample Depth, meters	Kair mD	Facies
Harvey-1	12A	2528.07	50.7	HE
Harvey-1	13A	2530.03	104	HE
Harvey-1	7A	1911.84	0.838	LE
Harvey-1	15A	2518.42	0.39	LE
Harvey-1	7B	1911.89	0.9	LE
Harvey-1	8B	1919.9	2.6	LE
Harvey-1	9B	2491.78	257.0	HE
Harvey-1	11A	2522.54	22.0	LE
Harvey-3	20	1429	22	LE
Harvey-3	4A	1369.84	114.0	HE
Harvey-3A	1A	1427.47	269	LE
Harvey-3A	3B	1392.35	7.2	LE
Harvey-4	6B	1794.27	1360	HE
HE= High Energy				
LE=Low Energy				

Table 3-1 Samples Selected for SCAL

3.3.1 Steady State Relative Permeability

Six of the plugs underwent steady state CO_2-Brine drainage and imbibition[i] experiments (Table 3-2). Figure 3-3 and Figure 3-4 show the drainage and imbibition relative permeability data for the Harvey wells. Hysteresis of the non-wetting phase is evident in all samples. The wetting phase exhibits negligible hysteresis.

Steady State Data								
Well	Sample Number	Sample Depth, meters	Kair mD	Porosity, fraction:	Specific Permeability to Water, mD	Specific Permeability to gas, mD	Sg Max Fraction	SGT Fraction
Harvey-4	6B	1794.27	1360	0.22	258.3	22.400	0.578	0.258
Harvey-1	12A	2528.07	50.7	0.12	15.8	2.600	0.467	0.234
Harvey-1	13A	2530.03	104	0.14	18.6	3.070	0.567	0.298
Harvey-3A	1A	1427.47	269	0.23	94.9	7.900	0.461	0.137
Harvey-1	7A	1911.84	0.838	0.11	0.3	0.074	0.442	0.238
Harvey-3	20	1429	22	0.22	4.2	0.079	0.508	0.265
Harvey-1	15A	2518.42	0.39	0.10	0.2	0.014	0.389	0.222

Table 3-2 Steady State Data

[i] Sample 20 from Harvey-3 was analysed in 2016 (Reference 3).

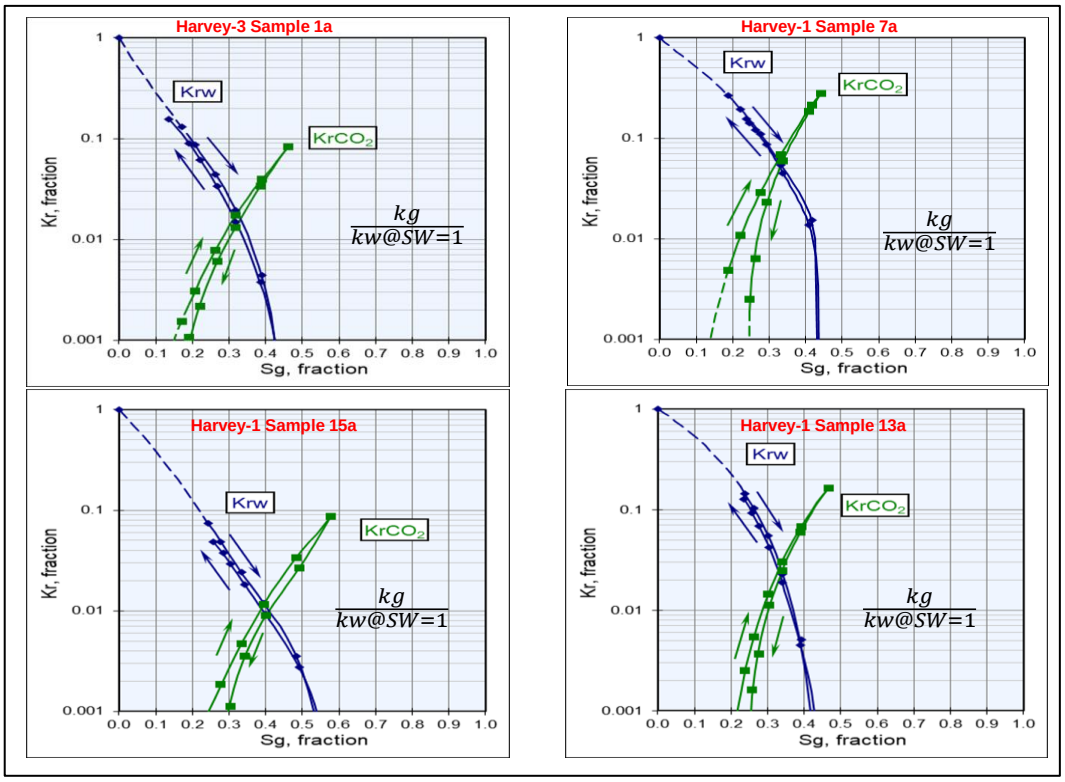

Figure 3-3 Steady State Drainage and Imbibition Relative Permeability - Samples 1A, 7A, 15A and 13a

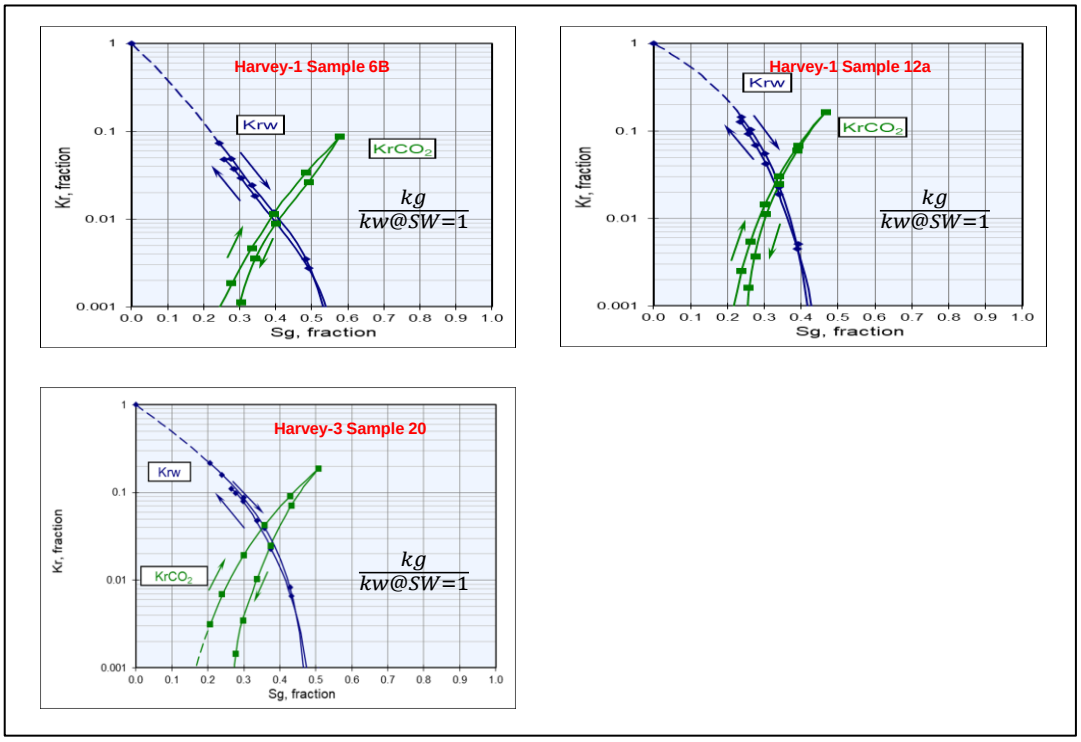

Figure 3-4 Steady State Drainage and Imbibition Relative Permeability Samples 6B, 12A and 20

3.3.2 Unsteady State Relative Permeability Data

Ten plugs underwent unsteady state CO_2-Brine relative permeability experiments (Table 3-3). Only end point data was reported from Reference 2. The unsteady state samples 206647, 206660, 206669, 11, 135, 4 and 8 were reviewed in Reference 19.

Unsteady State Data								
Well	Sample Number	Sample Depth, meters	Kair mD	Porosity, fraction:	Specific Permeability to Water, mD	Specific Permeability to gas, mD	Sg Max Fraction	SGT Fraction
Harvey-1	206647	1901.61	525.0	0.155	48	10.7	0.55	0.23
Harvey-1	206660	1935.5	128.2	0.156	16.5	3.4	0.6	0.43
Harvey-1	206669	2491.56	298.1	0.126	238	40.94	0.58	0.34
Harvey-1	7B	1911.89	0.9	0.108	0.297	0.240	0.574	0.213
Harvey-1	8B	1919.9	2.6	0.126	0.875	0.187	0.416	0.172
Harvey-1	9B	2491.78	257.0	0.135	62.730	23.460	0.467	0.145
Harvey-1	11A	2522.54	22.0	0.133	9.029	7.598	0.685	0.317
Harvey-3	4A	1369.84	114.0	0.218	1.209	0.915	0.309	0.122
Harvey-3A	3B	1392.35	7.2	0.142	0.076	0.034	0.381	0.201
Harvey-3	11	1420	42.5	0.234	19.500	4.570	0.467	0.191
Harvey-3	135	1544	1130.0	0.191	530.00	58.000	0.434	0.374
Harvey-4	4	1793	2720.0	0.217	2180.00	251.000	0.352	0.296
Harvey-4	8	1799	67.7	0.174	18.00	2.630	0.581	0.180

Table 3-3 Unsteady State Data

3.3.3 Relationship of SCAL Results to Rock Properties

3.3.3.1 End Point Relative Permeability

Figure 3-3 to Figure 3-7 plots the end point relative permeability data against rock classification. The plots show that there is no discernible correlation between the end point relative permeability data of the samples to facies, rock classifications such as Flow Zone Indicators (FZI) or Hydraulic Flow Units (HFU). An average value of the non-wetting phase end point data of 0.08 and wetting phase end point of 0.32 was used in the modelling. Figure 3-7 shows that the end point data from the Harvey plugs are comparable to the data from Reference 4.

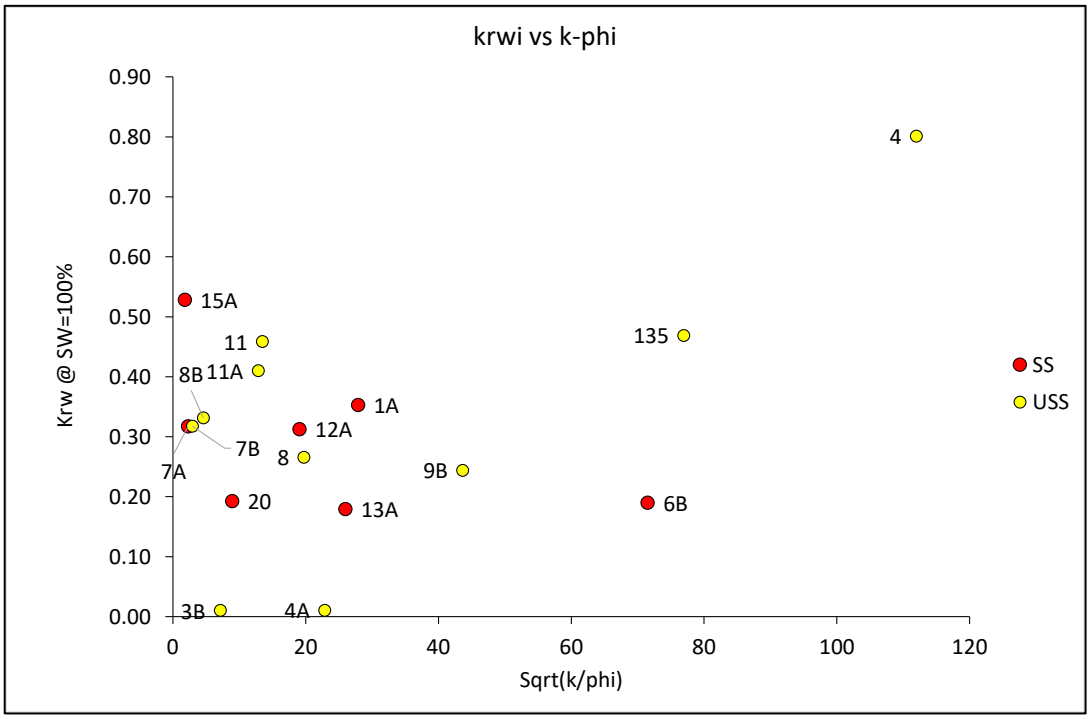

Figure 3-5 End Point Relative Permeability to Water @ 100% SW vs k/phi

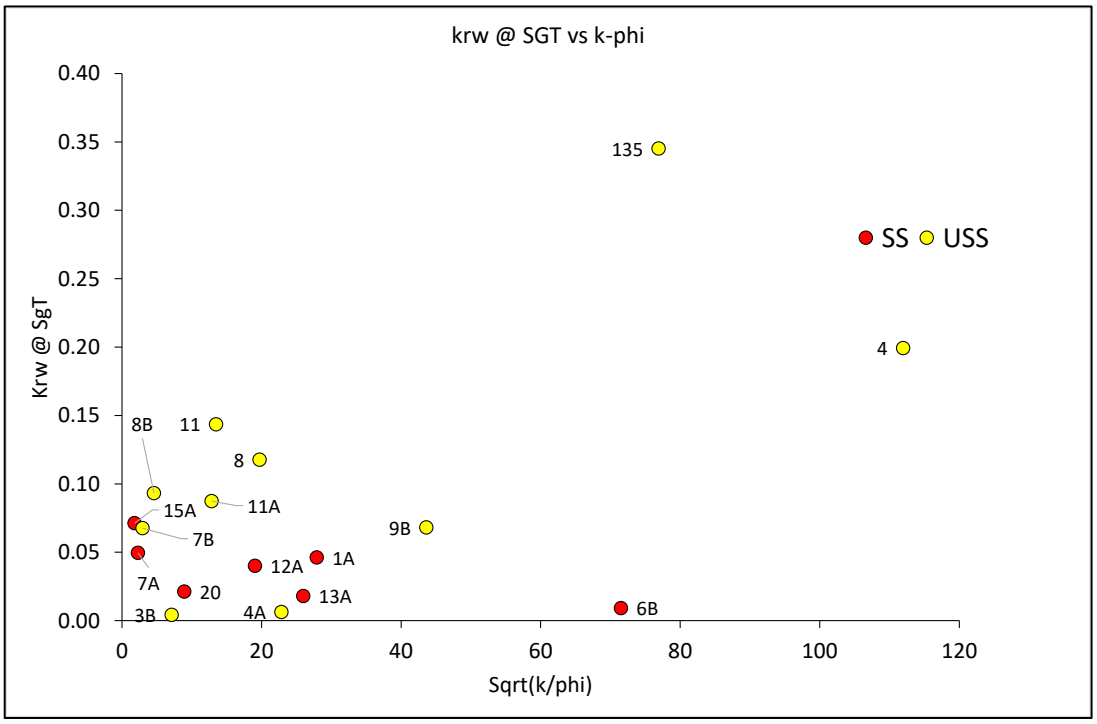

Figure 3-6 End Point Relative Permeability to Water @ Sg_T vs k/phi

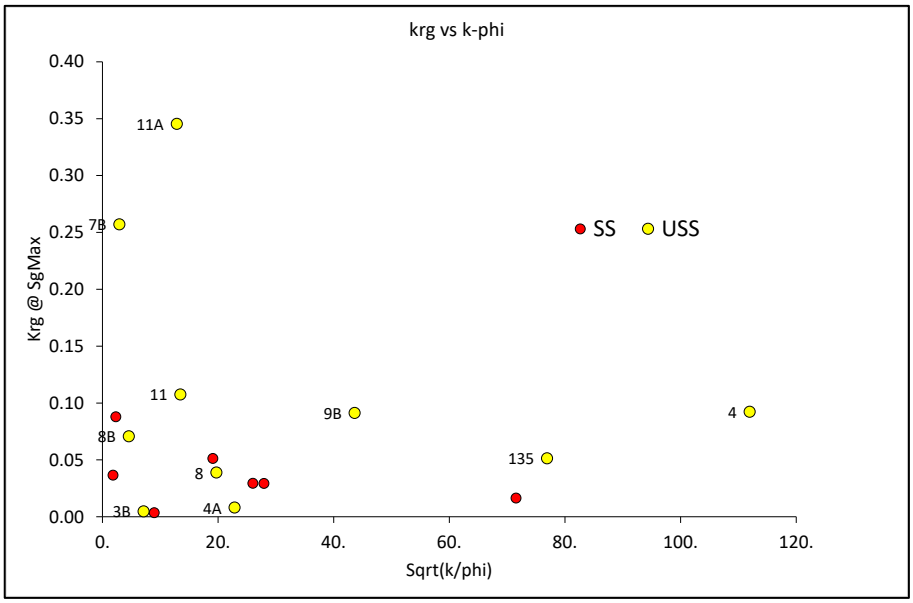

Figure 3-7 End Point Relative Permeability to Gas @ SgMax vs k/phi

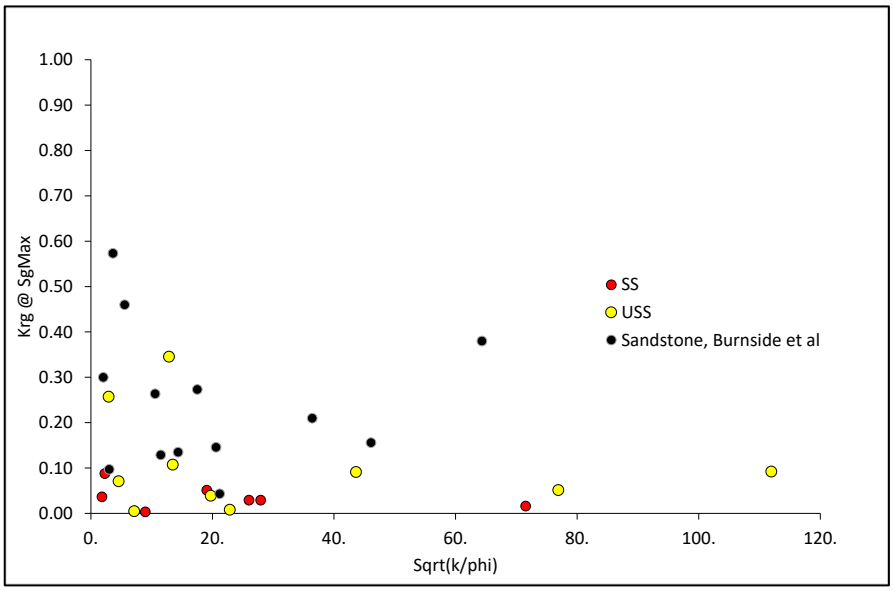

Figure 3-8 Comparison of End Point Relative Permeability to Gas @ SgMax and published data

3.3.3.2 Maximum Gas Saturation (SgMax)

Figure 3-9 shows the initial gas saturation as a function of permeability. The plot shows that a correlation can be discerned which links the initial gas saturation to the permeability of the rock and provides a reasonable basis for populating the dynamic model with flow properties.

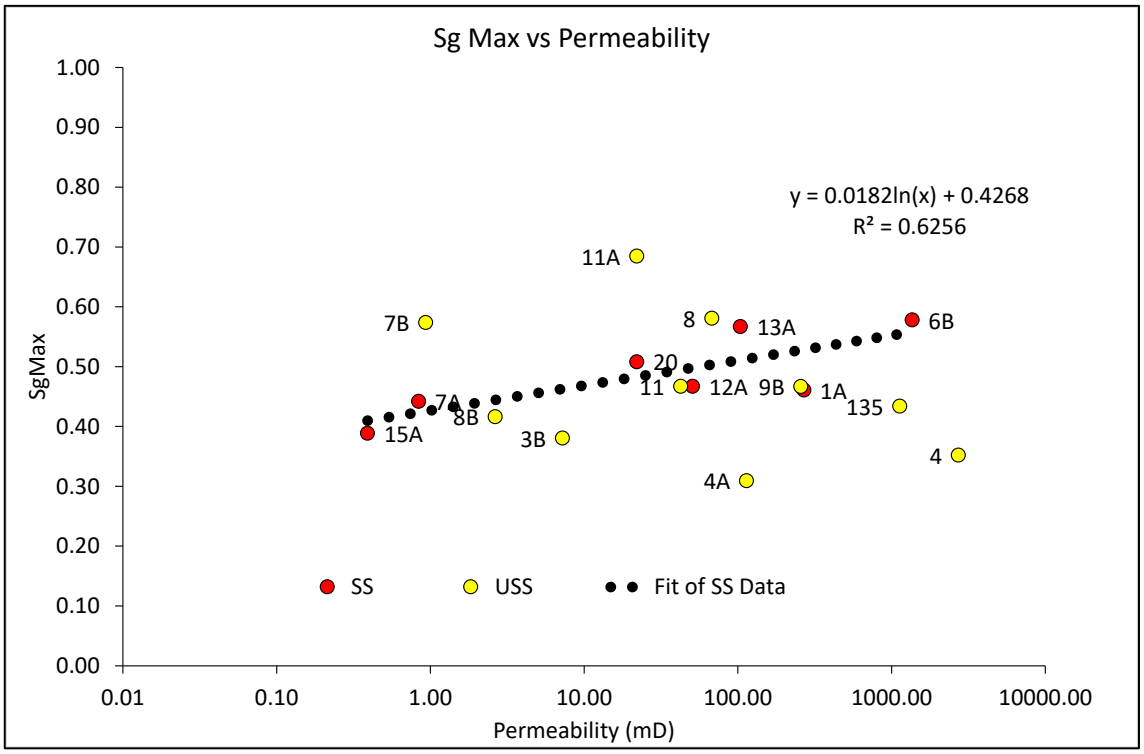

Figure 3-9 SgMax vs. Permeability

3.3.3.3 Trapped Gas Saturation

Figure 3-10 shows the trapped gas saturation as a function of SgMax for steady and unsteady state data from the Harvey wells. The observed trapped gas saturation (SgT) from the steady state data is a good fit to the Land Correlation (Reference 5). The best fit was obtained with a correlation parameter, C, of 1.95. There was too much scatter in the unsteady state data to obtain a meaningful fit to the Land Correlation. Figure 3-11 compares the trapped gas data from Harvey with the data from Reference 4 . The plot shows that the scatter in the trapped gas data from Reference 4 is comparable to the scatter observed from the unsteady state data from Harvey. Figure 3-12 shows that there is no correlation between trapped gas saturation and facies.

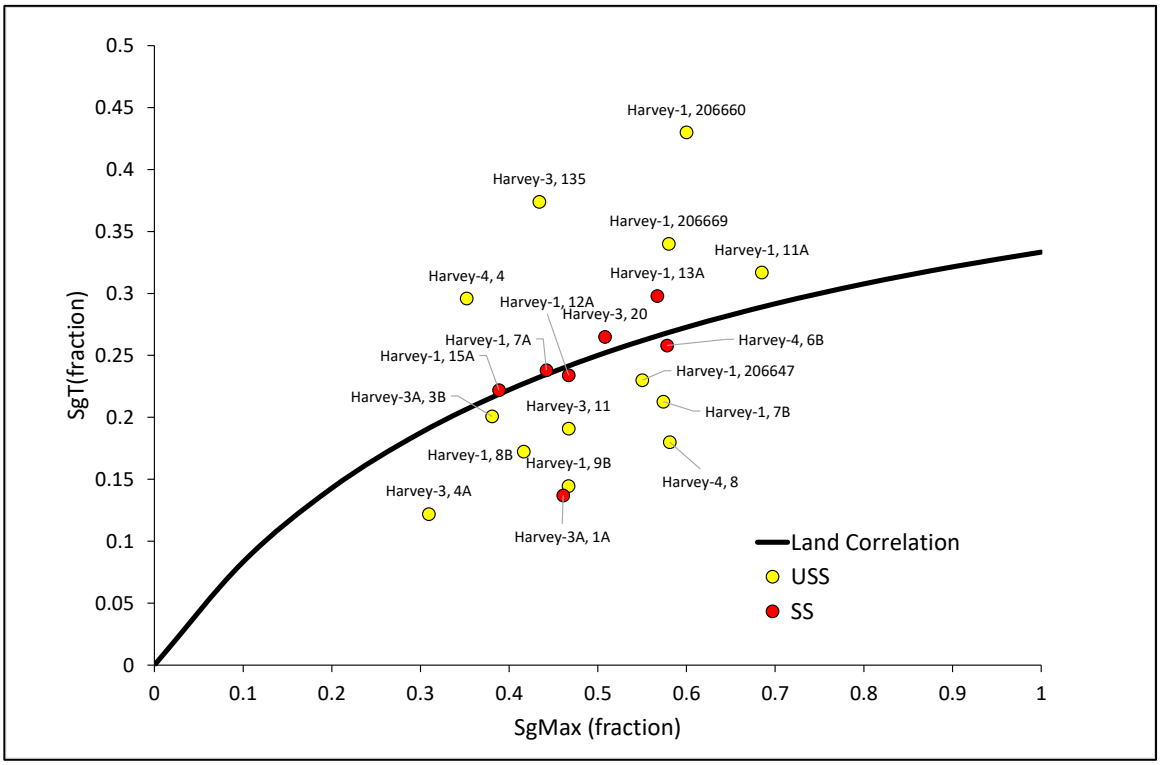

Figure 3-10 Trapped Gas Saturation vs. SgMax

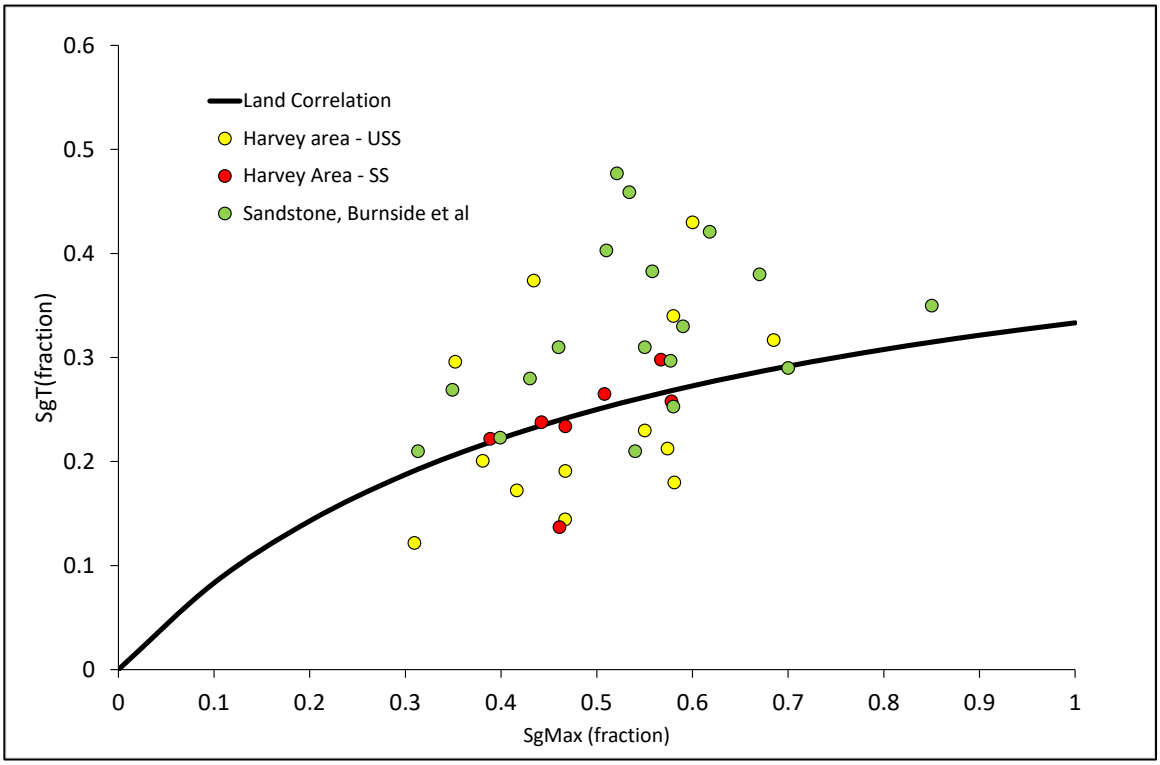

Figure 3-11 Comparison of Trapped Gas Saturation vs SgMax and published data

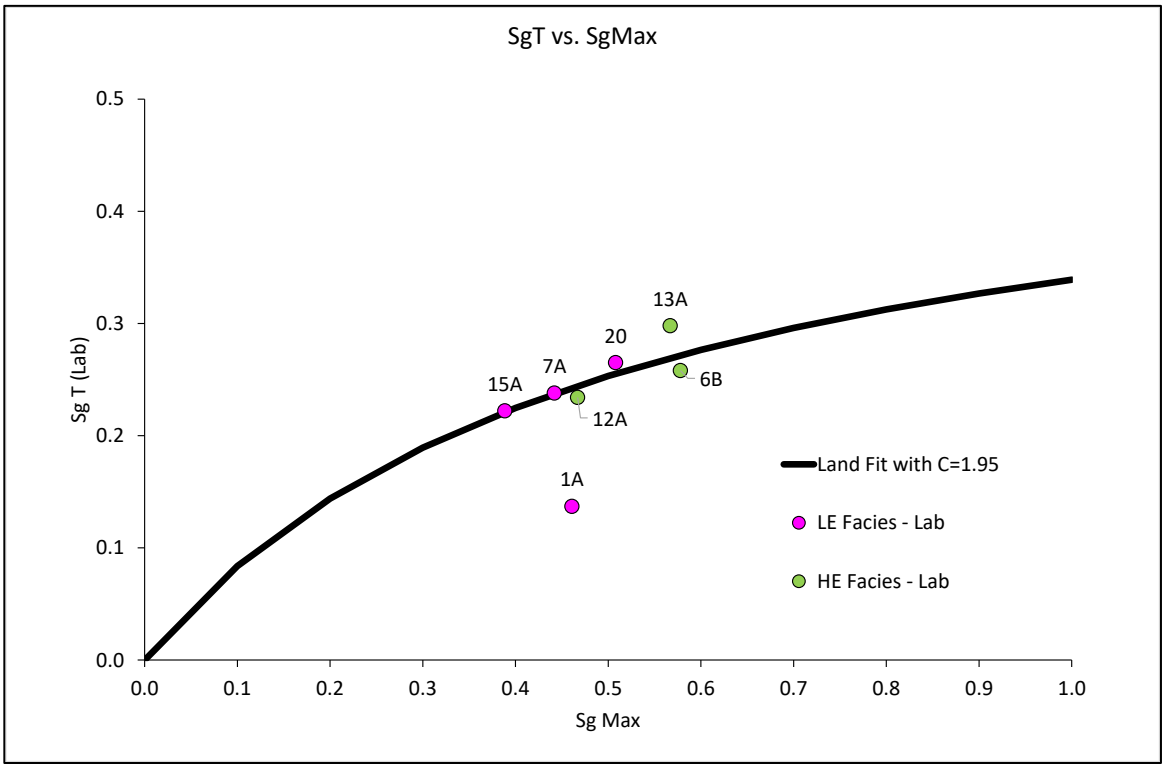

Figure 3-12 of Trapped Gas Saturation vs SgMax by facies

3.3.4 Relative Permeability Relationships

3.3.4.1 CO_2 Relative Permeability

Figure 3-13 shows the CO_2 relative permeability curves for the drainage cycle from the steady state core data from Harvey. There is a good fit between the observed data and the Brooks-Corey model (Reference 7) using λ of 1.2. The Brooks-Corey model with λ of 1.2 is also a reasonable fit of the relative permeability data from the imbibition cycle (Figure 3-14).

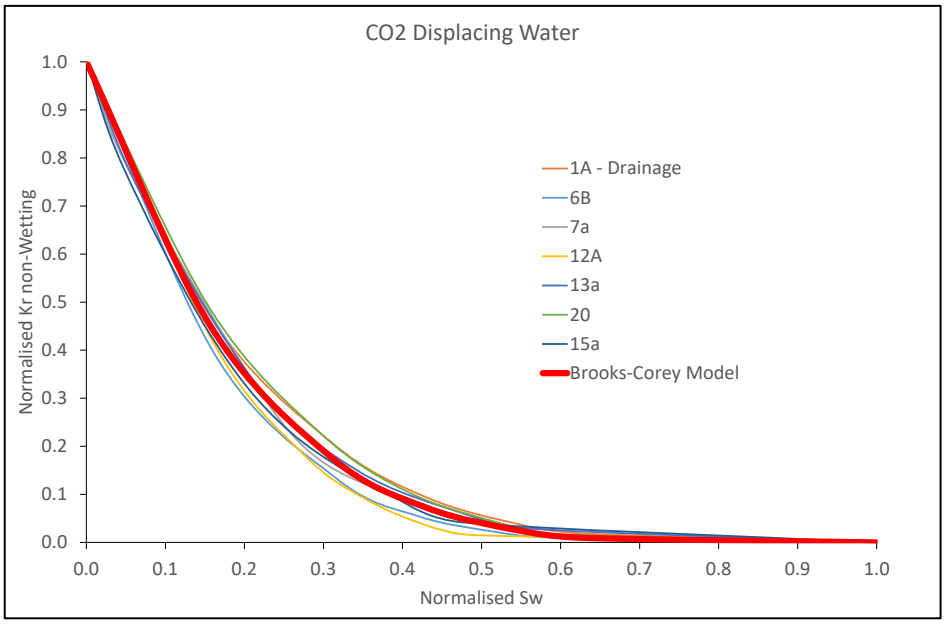

Figure 3-13 Comparison of CO_2 Relative Permeability Curves and Brooks-Corey Model (CO_2 Displacing Water)

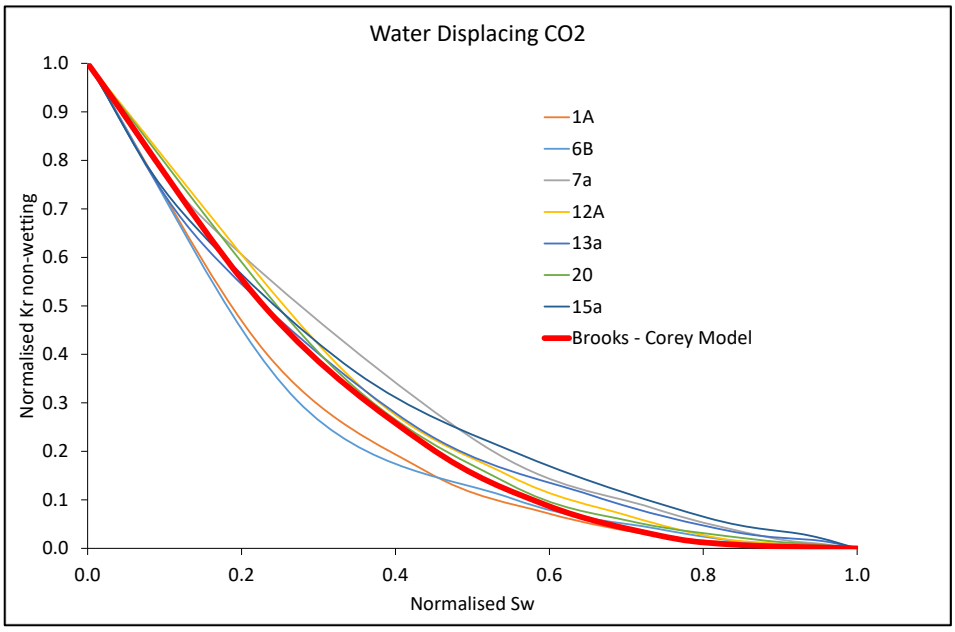

Figure 3-14 Comparison of CO_2 Relative Permeability Curves and Brooks-Corey Model (Water Displacing CO_2)

3.3.4.2 Water Relative Permeability

Figure 3-15 shows the water relative permeability curves for the imbibition and drainage cycle from the steady state core data from Harvey. A good fit between the observed data and the Purcell model (Reference 8) using λ of 1.2. Reference 9 and 10 indicated that the Purcell relative permeability model fits the wetting phase relative permeability well and the Brooks-Corey model is a better fit of the non-wetting phase relative permeability.

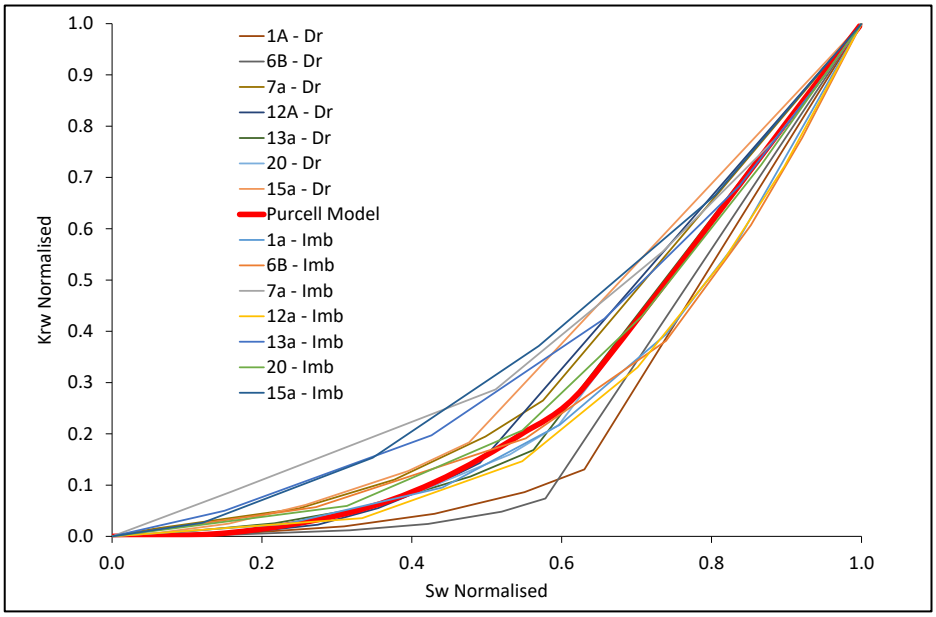

Figure 3-15 Comparison of Water Relative Permeability Curves and Purcell Model

3.3.5 Capillary Pressure Data

No CO_2-brine capillary pressure data was obtained for the Harvey plugs. Air-Mercury capillary pressure data for five samples (Table 3-4) with a wide range of rock properties were reported in Reference 2. The air-mercury capillary pressure data were converted to CO_2-brine capillary pressure data at reservoir conditions using IFT*Cosine Contact Angle of 19 dyne/cm (Reference 2). An example of the converted data for Sample 20 is shown in Figure 3-16.

Figure 3-17 and Figure 3-18 show the fit of the converted MICP data with Brooks-Corey model. In most instances, a good fit was obtained with λ=1.2 as in the relative permeability data. In one case a good fit was achieved with λ=1.3.

Sample	Facies	Permeability (mD)	Porosity (fraction)
20	Low Energy	22	0.220
11	Low Energy	42.5	0.234
135	High Energy	1130	0.191
4	High Energy	2720	0.196
8	Low Energy	53.2	0.149

Table 3-4 Samples used Air-Mercury Capillary Pressure

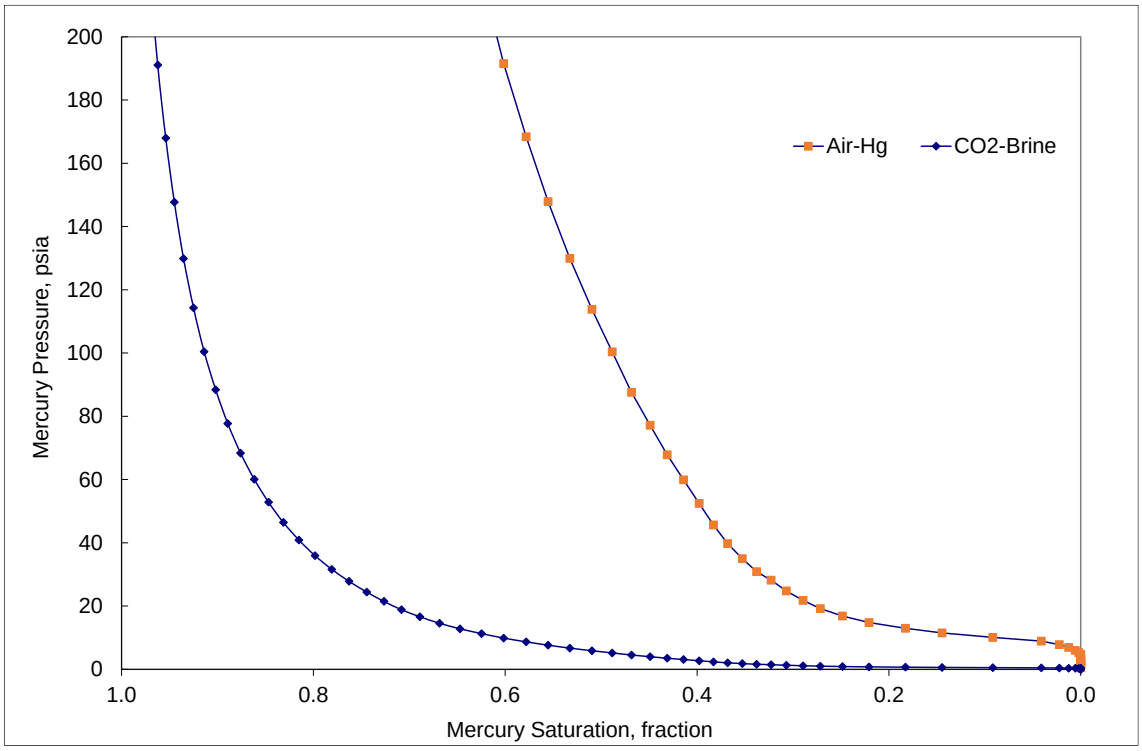

Figure 3-16 Air-Mercury and CO_2-Brine Capillary Pressure (Reference 2).

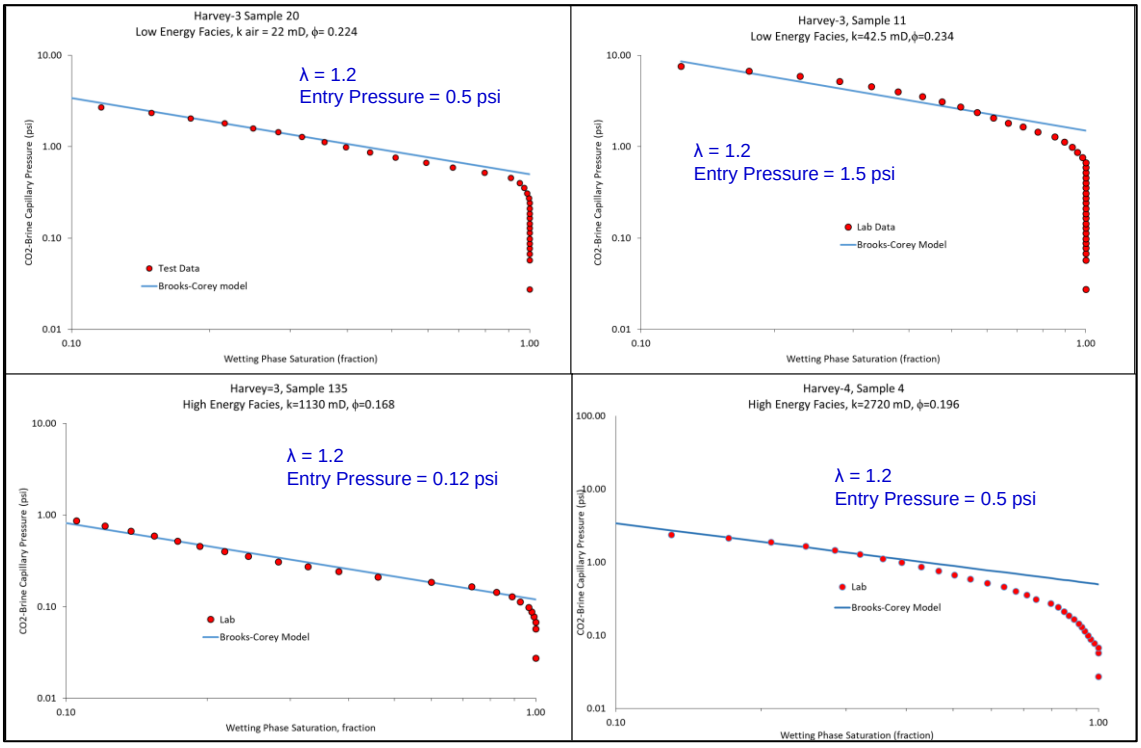

Figure 3-17 Fit of CO_2-Brine Capillary Pressure vs Normalised Wetting Phase Saturation with Brooks-Corey Model (Samples 20, 135, 4 and 11)

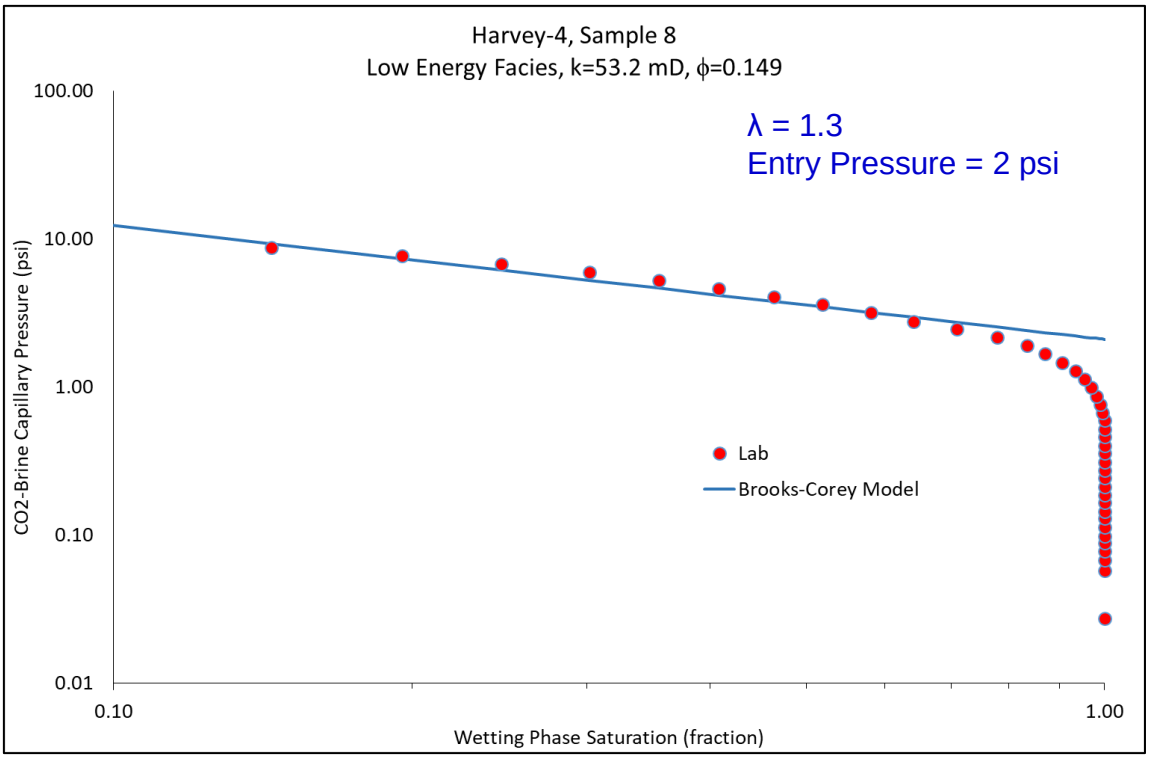

Figure 3-18 Fit of CO_2-Brine Capillary Pressure vs Normalised Wetting Phase Saturation with Brooks-Corey Model (Sample 8)

3.3.6 Observations

The drainage and imbibition relative permeability curves can be fit to the Brooks-Corey and Purcell models with a λ=1.2. This λ also fits the MICP data from the Wonnerup.

There is a lot of scatter in Sg_T and Sg_{Max} from unsteady state data. It is recommended that only steady state data be acquired in any future relative permeability experiments.

3.4 Brine Salinity

Five water samples were retrieved from DMP Harvey-3 and DMP Harvey-4: two from DMP Harvey-3 and three from DMP Harvey-4. All five samples were likely contaminated, as suggested by elevated potassium and chloride figures (Reference 11). Both samples from DMP Harvey-3 were heavily contaminated and are not reliable (Reference 13). The three samples were retrieved from DMP Harvey-4 and analysed by Core Laboratories (Reference 12). It was suggested that the contamination of Sample 1 from DMP Harvey-4 was not as severe as the samples from DMP Harvey-3. Core Laboratories used the sample from the Wonnerup as the basis of a synthetic “uncontaminated” brine composition for the Wonnerup.

Table 3-5 is a list of the water samples from Harvey. The synthetic sample from Core Laboratories was used in the full field simulation.

Well	Sample	TDS mg/L H2O	NaCl Equivalent ppm	Comments
Harvey-3	EP1511686-001	59900	51025	Contaminated sample from Wonnerup
Harvey-3	EP1511686-002	62600	58979	Contaminated sample from Wonnerup
Harvey-4	Sample 1 (1632.0 m)	45230	43650	RDT sample from Wonnerup
Harvey-4	Sample 3 (742.05 m)	70500	72046	RDT sample from Eneabba
Harvey-4	Sample 2 (1270.1 m)	156960	214782	RDT sample from Yalgorup
Synthetic	Core Lab	50001	46422	Synthetic Sample from Core Lab

Table 3-5 Water Samples from Harvey

3.5 Geological Model

Reservoir property and structural information for the Harvey model were imported directly from Petrel.

4. BLACK OIL MODELLING OF CO_2 SEQUESTRATION

The use of a "Black Oil" model to model CO_2 sequestration is well established and a number of studies have been conducted using this technique (Reference 15 and 16). Black Oil Modelling uses a simplified description of the physics of the fluids based on simple interpolation of PVT properties as a function of pressure. This method of modelling CO_2 sequestration is attractive as it allows reservoir uncertainties and development sensitivities to be evaluated relatively quickly compared to compositional modelling. Nevertheless, it was recommended that selected cases in the full field modelling study are checked against a fully compositional model (Reference 14).

4.1 Full Field Model of the Harvey Area

4.1.1 Grid Dimensions

The full field model of the Harvey Area of Interest (Figure 2-1) was constructed with grid blocks of 250X250 metres in the I- and J-directions with the resolution of the layers in the Yalgorup retained at the geological model scale of 1 metre. In the Wonnerup, the 4 metre layers were used (Figure 4-1). Extensive grid sensitivity studies indicated that indicate that the Wonnerup sands can be upscaled successfully to vertical resolution of 4 metres (Reference 19).

To further reduce the number of cells in the full field model, all cells with a depth shallower than 800mTVDss was made void. Migration of CO_2 shallower than 800mTVDss is considered a breach of containment as the CO_2 changes from a supercritical state to a gaseous state at depths shallower than 800mTVDss. The dimensions of the model are summarised below:

- 48 cells in the I-direction
- 39 cells in the J-direction
- 1,050 cells in the K-direction
- 1,965,600 cells of which 1,196,457 are active cells
- Cell sizes of 250mX250mX1m in the Yalgorup
- Cell sizes of 250mX250mX4m in the Wonnerup
- The Yalgorup is modelled in Layers 1 to 700
- The Wonnerup is modelled in Layers 701-1,050

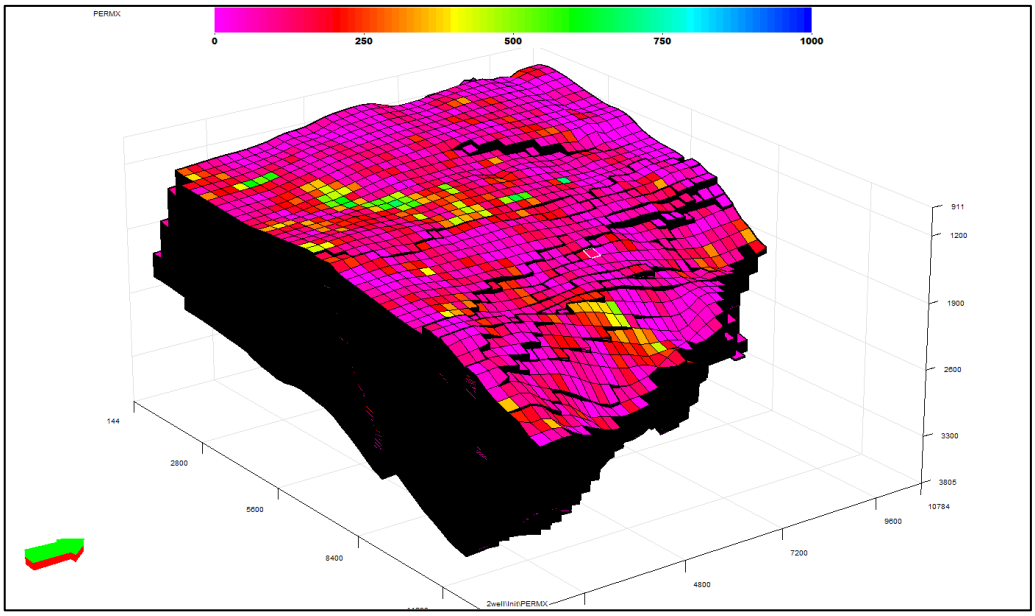

Figure 4-1 View of Model Showing Permeability Distribution

4.2 Initialisation Parameters

The full field model was initialised with the following parameters:

- Initial Pressure
  - Initial pressure based on the RCI data from Harvey-1.
  - Reference pressure of 19327 kpa at 1900 metres.
- The model was initialised as completely oil saturated with the initial solution gas-oil ratio, Rsi, set to zero.

For this study, the Black Oil version of the reservoir simulation package from Reservoir Fluid Dynamics, tNav™, was selected. The Black Oil models constructed in this study are fully compatible with Schlumberger's simulator Eclipse™.

4.3 Modelling Temperature

Black oil models are isothermal and reservoir temperature is not required. Fluid properties are calculated at a single temperature and input as a table. The PVT data for the Black Oil model of the Reference Case was calculated at 55°C which is the reservoir temperature at a depth of about 1600mTVDss. This depth is roughly the mid-point of the Pore Volume of the model (i.e. 50% of the pore volume of the model is shallower than 1600mTVDss and 50% is deeper).

4.4 CO_2 and Water Properties

In Black Oil simulation of CO_2 sequestration in aquifers the oil is assigned the properties of the water phase and gas are assigned the properties of CO_2. The input to the Black Oil model was generated using software created by CSIRO (*J. Ennis-King 2017, personal communication, 22 September*). In Eclipse, the properties of the brine and CO_2 are represented by Live Oil tables (Figure 4-2) and dry gas (Figure 4-3). The solubility of CO_2 in the 44,600 ppm brine was represented by the solution gas ratio as a function of pressure.

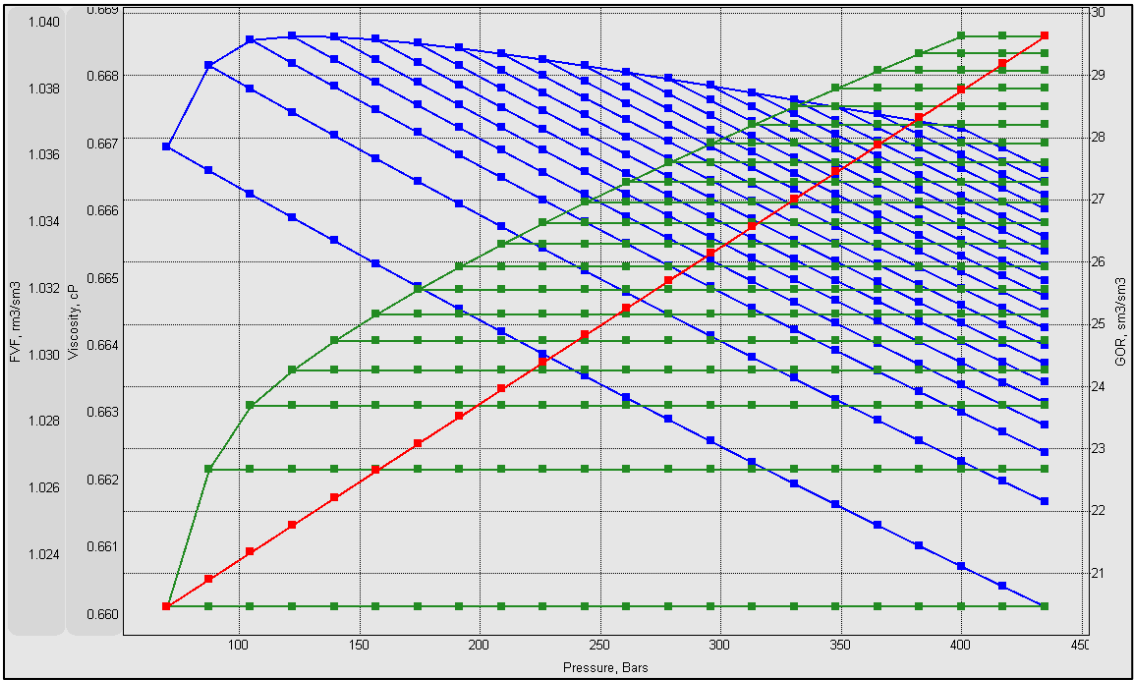

Figure 4-2 PVT Properties – Oil (PVTO)

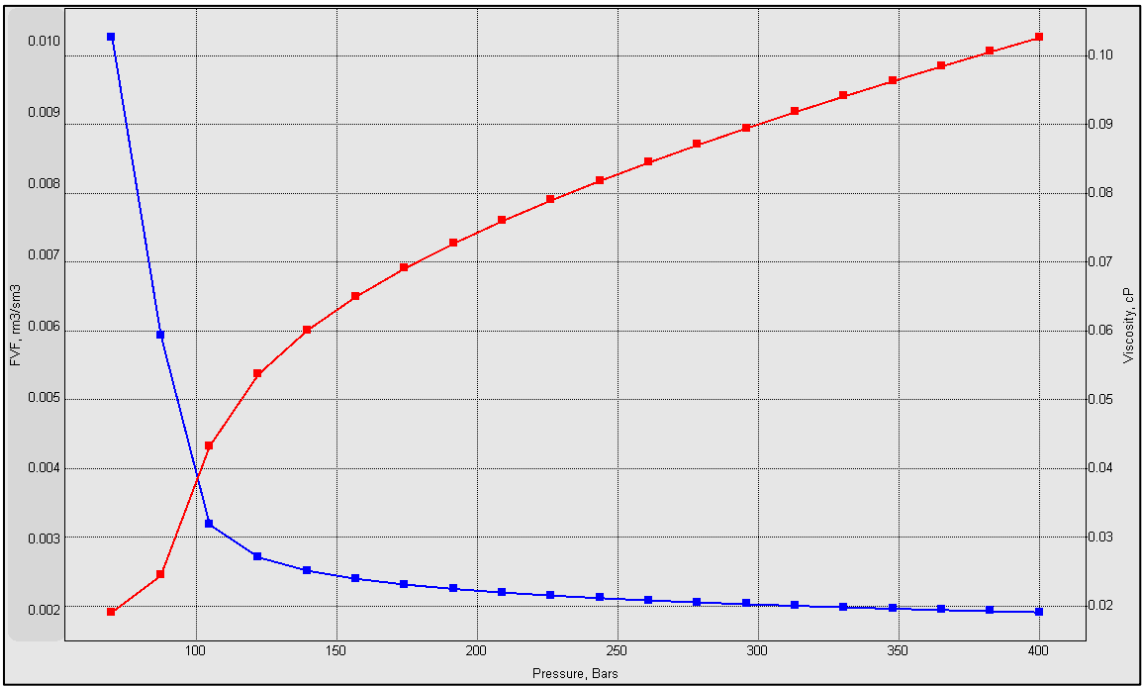

Figure 4-3 Dry Gas PVT Properties (PVTG)

4.5 Fluid Flow Data for Simulation

Figure 4-4 shows a plot of the distribution of permeability in the Best Technical Case (Reference Case) model of the Area of Interest. The plots shows that the distribution of permeability can be subdivided into seven groups:

1. Permeability < 50 mD
2. Permeability between 50 and 100 mD.
3. Permeability between 100 and 150 mD.
4. Permeability between 150 and 200 mD.
5. Permeability between 200 and 250 mD.
6. Permeability between 250 and 300 mD.
7. Permeability greater than 300 mD.

Seven sets of relative permeability and capillary pressure curves for each of the groups with the following parameters:

- The wetting phase relative permeability curves were generated using the Purcell equation with λ of 1.2.
- Non-Wetting phase relative permeability curves were generated using the Brooks-Corey model with λ of 1.2.

- Drainage capillary pressure curves were generated using the Brooks-Corey model and imbibition capillary pressure curves were generated using the Li-Horne model (Reference 10).
- Trapped gas saturation, Sg_T, for each of the permeability classes was generated using the Land Correlation with C=1.95.
- Sg_{Max} for each class was generated using the relationship observed from the core data (Section 3.3.3.2).

The relative permeability and capillary pressure curves were assigned to the simulation model using saturation regions (SATNUMs) according to the permeability ranges (Table 4-1). Figure 4-5 to Figure 4-7 show examples of the drainage and imbibition wetting and non-wetting phase relative permeability, and capillary pressure curves

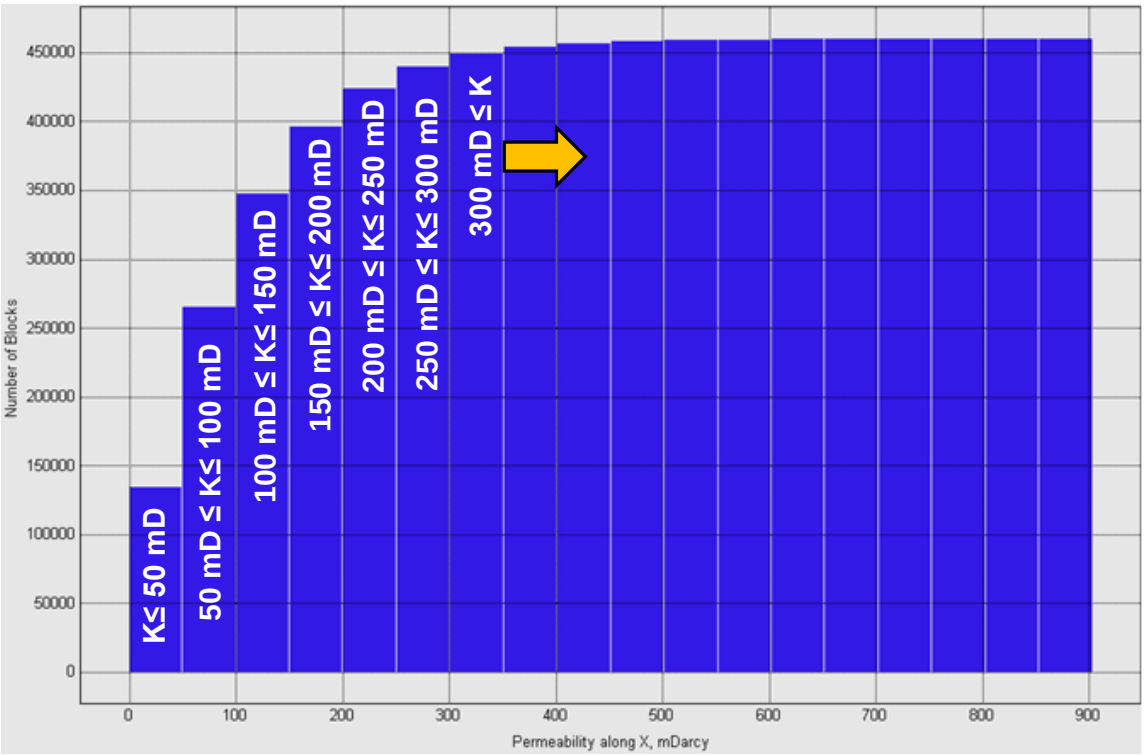

Figure 4-4 Cumulative Distribution of Permeability in the Harvey Dynamic Model

SATNUM	Permeability Range (mD)	SgT (fraction)	SgMax (fraction)
1	Permeability<50	0.249	0.485
2	50<Permeability<100	0.255	0.505
3	100<Permeability<150	0.257	0.515
4	150<Permeability<200	0.258	0.521
5	200<Permeability<250	0.259	0.525
6	250<Permeability<300	0.260	0.529
7	300<Permeability	0.262	0.536

Table 4-1 Saturation Table Assignments (SATNUM) in the Harvey Dynamic Model

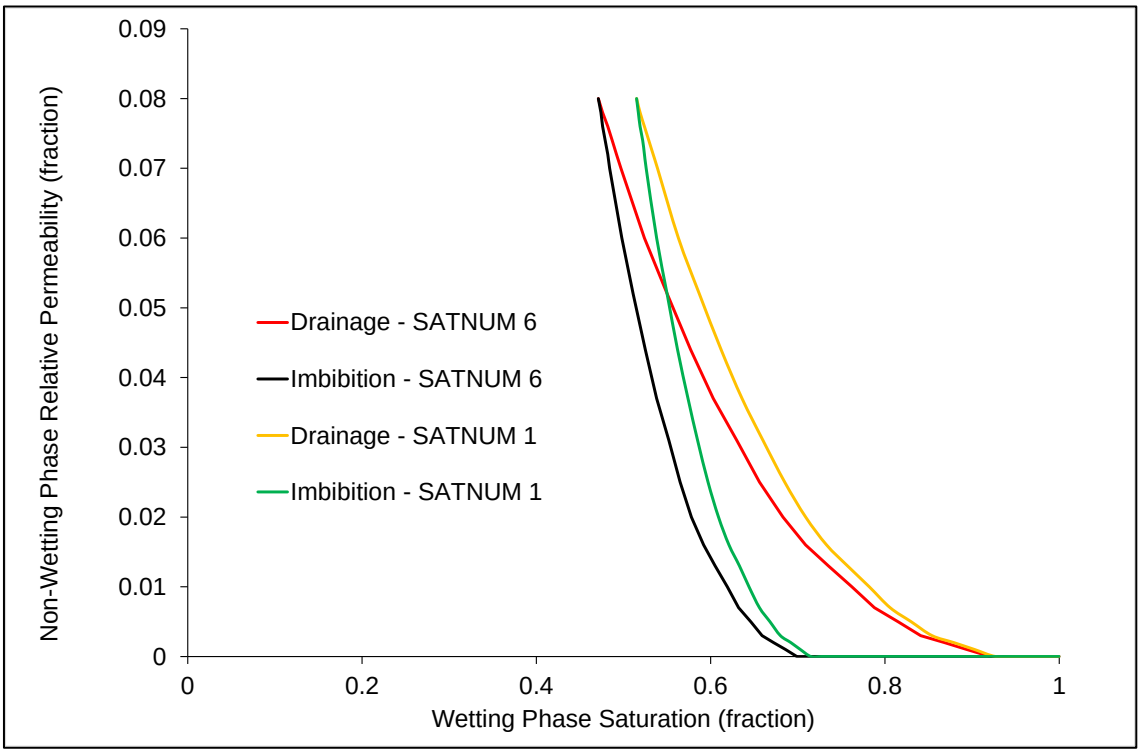

Figure 4-5 Example of Drainage and Imbibition Relative Permeability Curves (Non-Wetting Phase, SATNUM 6)

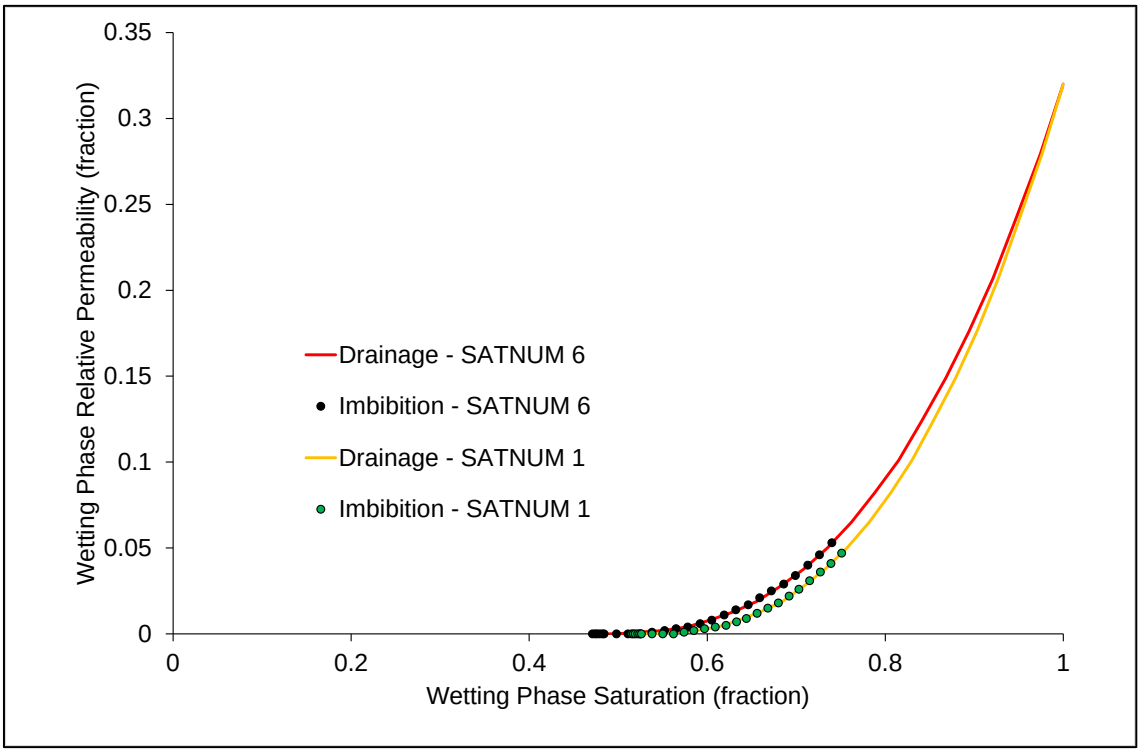

Figure 4-6 Example of Drainage and Imbibition Relative Permeability Curves (Wetting Phase, SATNUM 6)

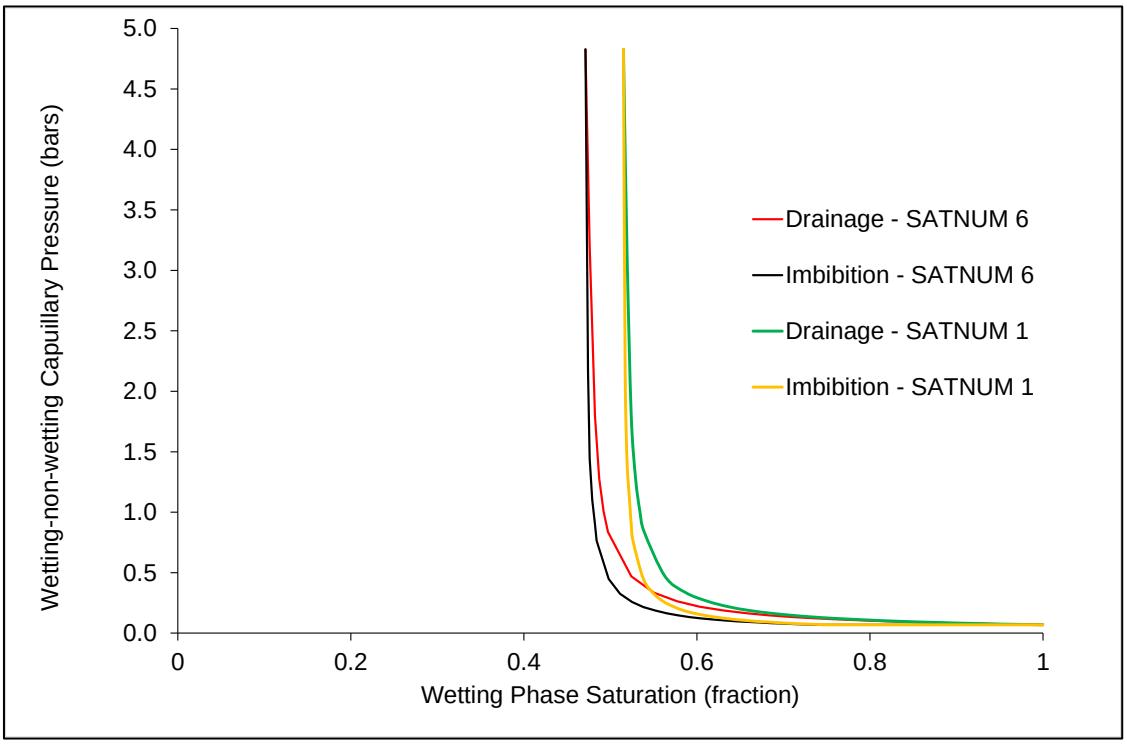

Figure 4-7 Example of Drainage and Imbibition Capillary Pressure Curves (Non-Wetting Phase, SATNUM 6)

4.6 Aquifer Extent

The full field model of the Harvey area by no means captures the full extent of the Wonnerup and Yalgorup aquifers. Figure 4-8 shows that the Yalgorup and Wonnerup (Reference 1) are unconstrained at least 50km to the north and 25km to the south of the area of interest. To model the likely extent of the aquifer the pore volume of the columns at the end of the model were increased (Figure 4-9) using multipliers.

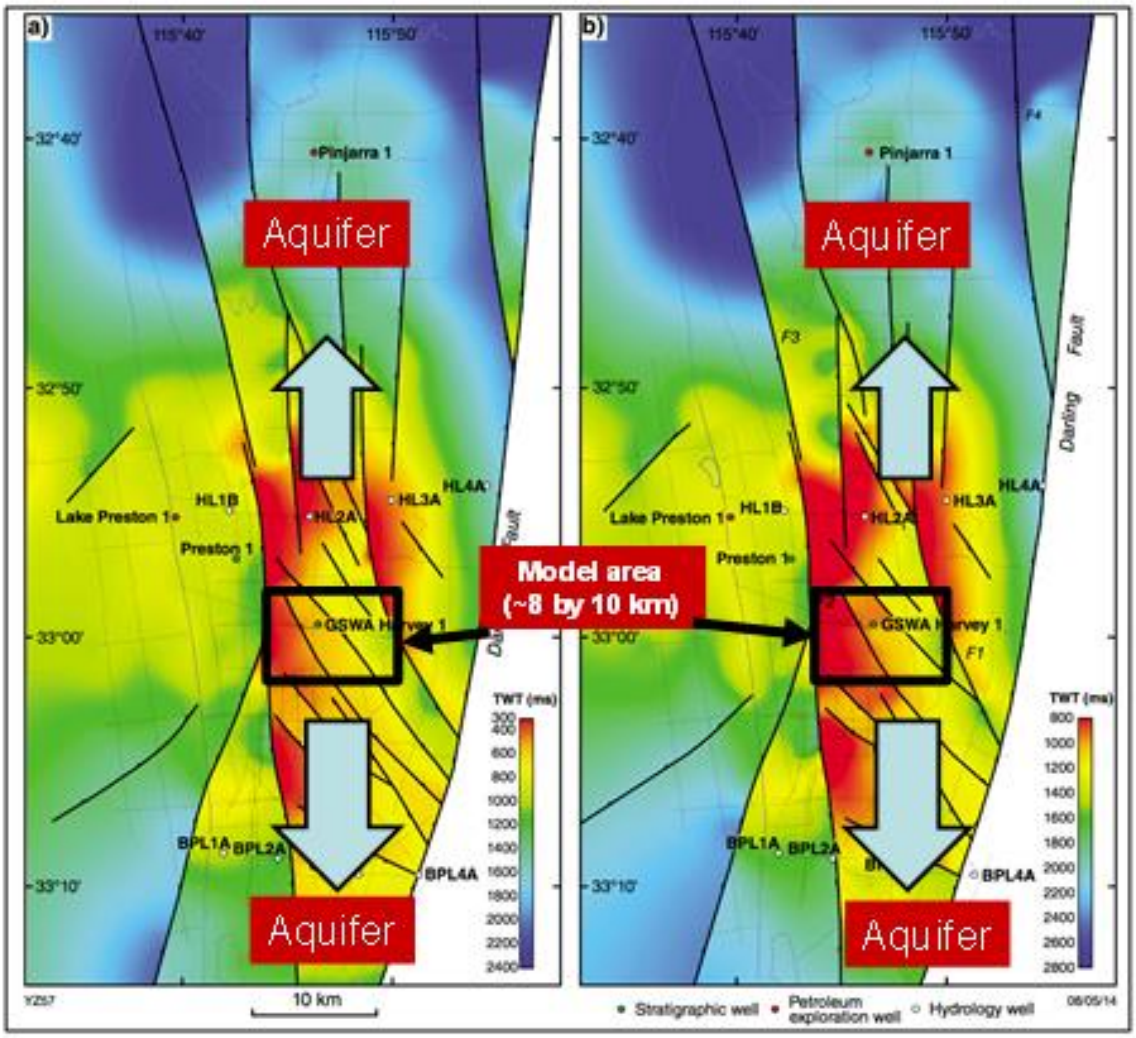

Figure 4-8 Time Structure maps of the: a) top Yalgorup Member; b) top Wonnerup Member (After Reference 1)

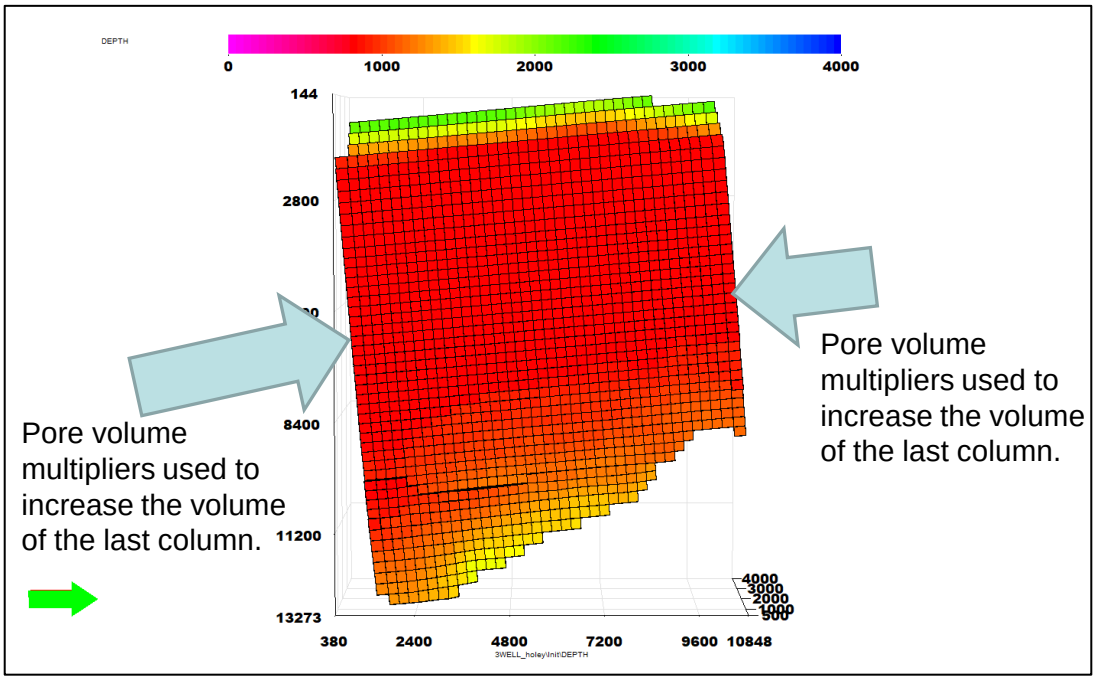

Figure 4-9 Modelling the Extent of the Wonnerup and Yalgorup Aquifers

5. CO_2 PLUME – BLACK OIL MODEL

5.1 Reference Case Definition

The conceptual development plan for the Harvey area envisages injection of 800,000 tonnes of CO_2 per year for 30 years. At the end of the 30 year injection period, the wells are shut-in and the CO_2 is allowed to dissipate through the aquifer. In this work, it was assumed that 3 wells laid out in a line-drive configuration would be used to inject CO_2 into the Wonnerup reservoir (Figure 5-1). All of the wells are completed in the bottom 250m of the Wonnerup at a depth of over 3,000mTVDss (Figure 5-2).

The Reference Case for the study is defined as follows:

- Reservoir
  - All faults are assumed to be not sealing
  - Wonnerup and Yalgorup are assumed to be in communication
- Model built in Eclipse™ Black Oil format.
- PVT Properties
  - Oil properties calculated using a salinity of 46 g/L H_2O
  - Temperature of 55°C
- Rock-Fluid
  - Hysteresis of the gas phase is assumed based on the results of the SCAL
  - No hysteresis of the water phase based on the results of the SCAL
- Injection
  - Dry gas ("CO_2") is injected at rate of 1.2 million m^3/day
  - Injection begins on an arbitrary date of 1/1/2020 and ends on 10/1/2050
- Bottom hole pressure constraint = 360 bars @ mid-point injection depth of 3250m [34 bars above pore pressure]
- Fluid flow:
  - Carlson's Hysteresis Model chosen as default

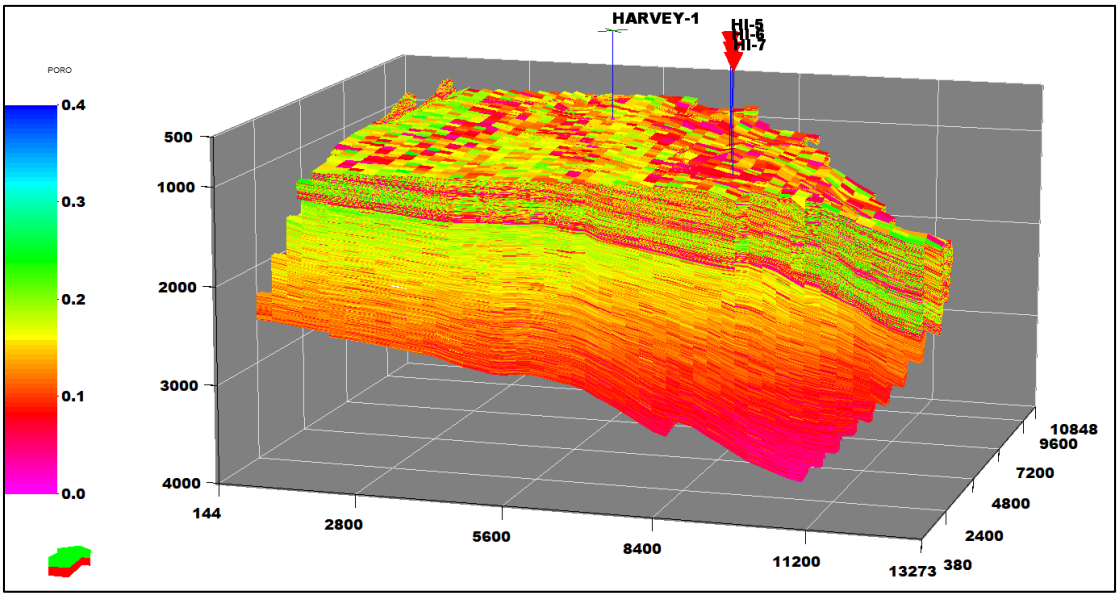

Figure 5-1 Porosity Grid Showing Well Locations in the Model

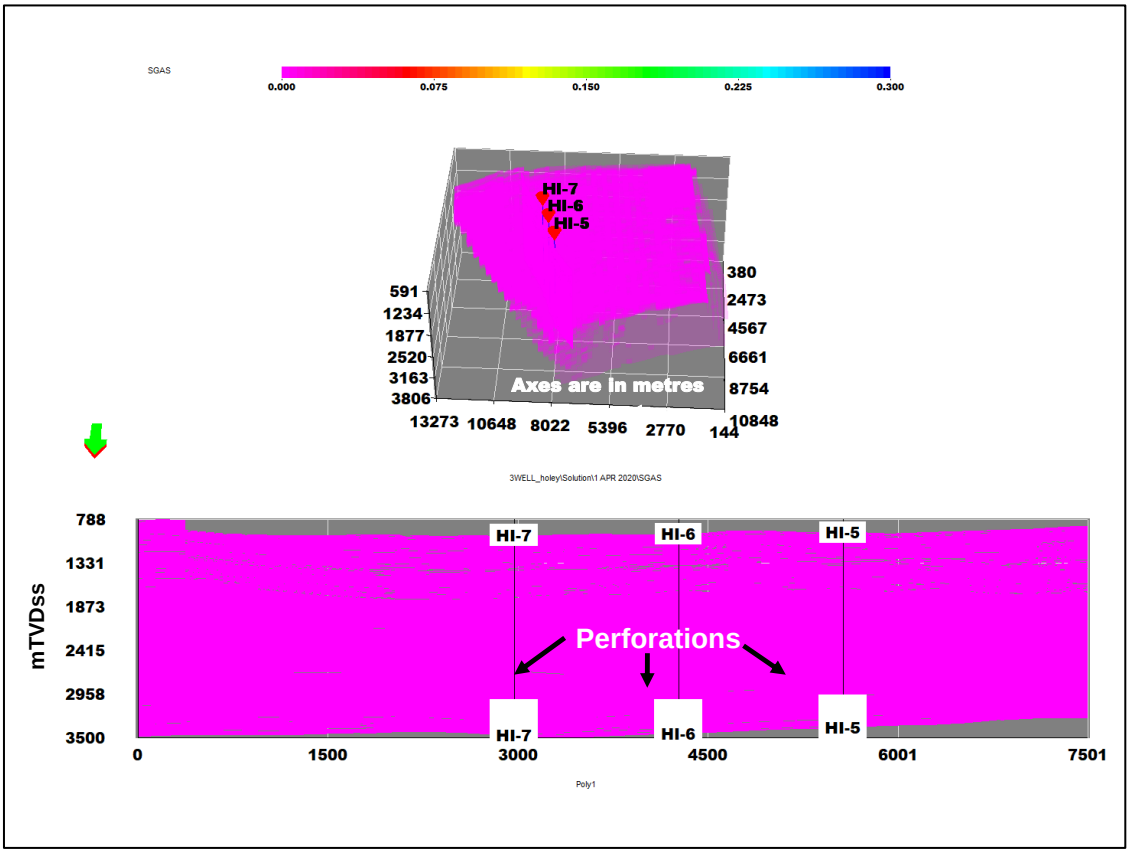

Figure 5-2 Cross Section through Injectors Showing Completion Intervals

Figure 5-3 show the injection profile for the Reference Case. The results of the modelling show that 800,000 tonnes/year of CO_2 was injected into the Wonnerup in the model for 30

years for a cumulative injection of 24 million tonnes of CO_2. The bottom hole pressures during the injection period (Figure 5-4) are lower than the bottom hole pressure constraint.

Figure 5-5 shows the CO_2 distribution in the model 1,000 years after injection. The plots show that the CO_2 front does not reach the location of GSWA Harvey-1 even after, 1000 years. An East-West cross section shows that the CO_2 front rose to a depth of 2,154mTVDss and remains within the Wonnerup. The Wonnerup is considered the primary containment unit and the Yalgorup the secondary for the CO_2.

Figure 5-6 shows that the movement of CO_2 in the model effectively stops after about 600 years. The volume of trapped gas peaks at about 400 years and declines as the gas dissolves in the liquid phase. Consequently, the volume of gas dissolved in the liquid phase continues to increase over the time period modelled.

The material balance accounting of the CO_2 injected in the Reference Case model after 1,000 years (Table 5-1) show that about 59% of injected CO_2 is dissolved in water. The remainder is in a supercritical phase.

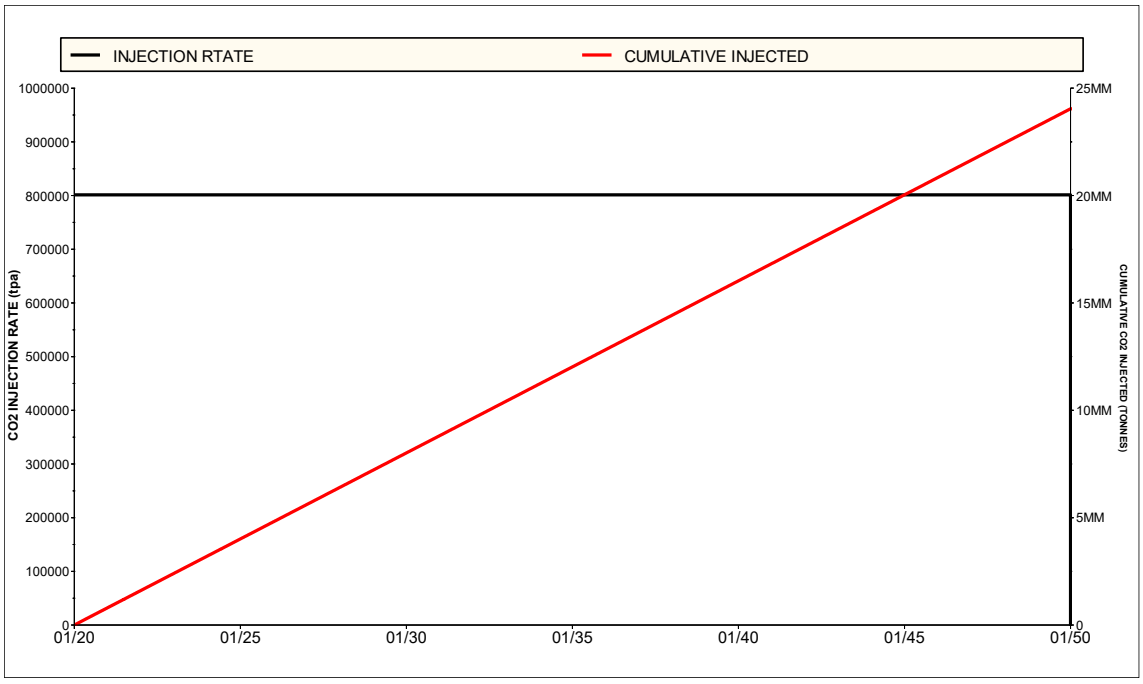

Figure 5-3 Injection Profile - Reference Case (Black Oil)

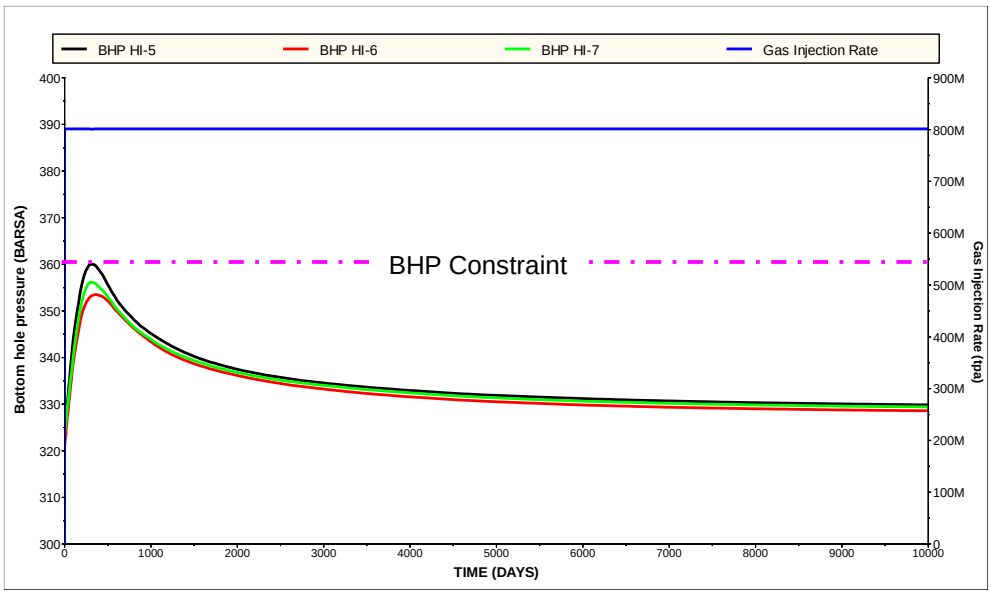

Figure 5-4 Bottom hole pressure profile during the Injection period

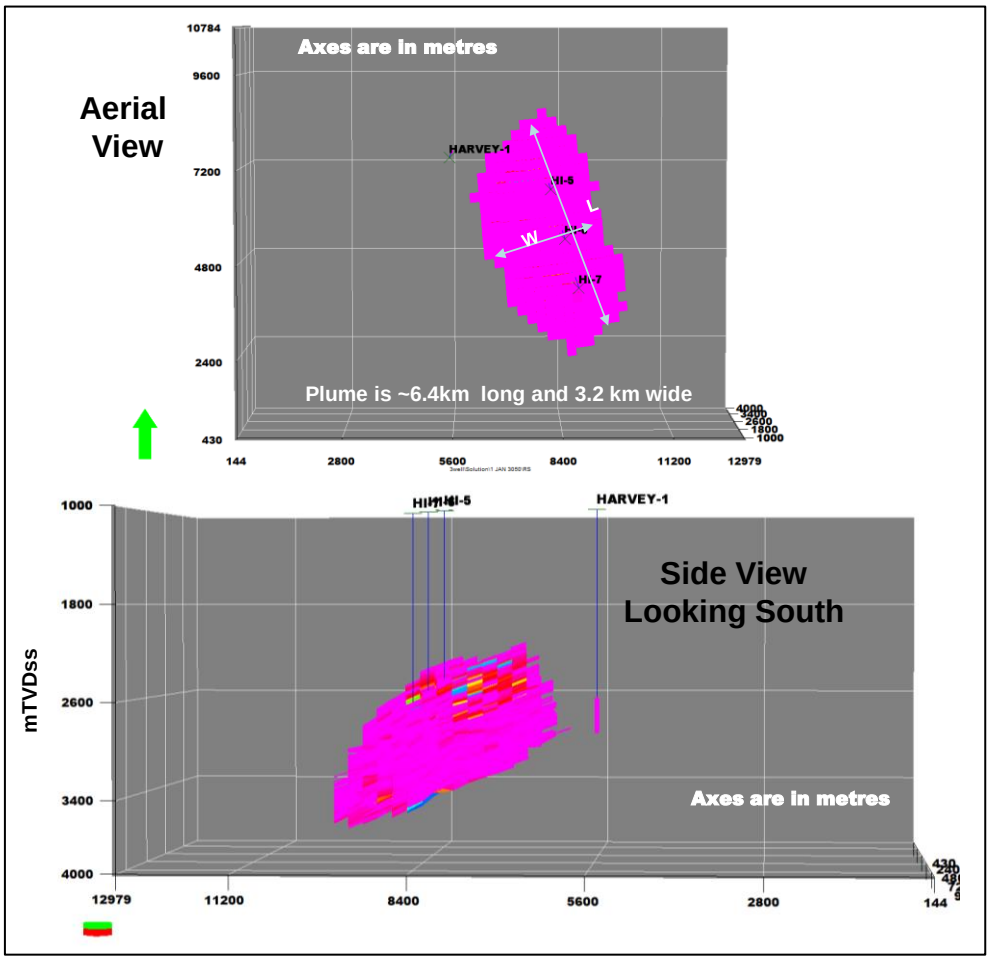

Figure 5-5 CO_2 Plume Shape Reference Case (After 1000 years of shut-in)

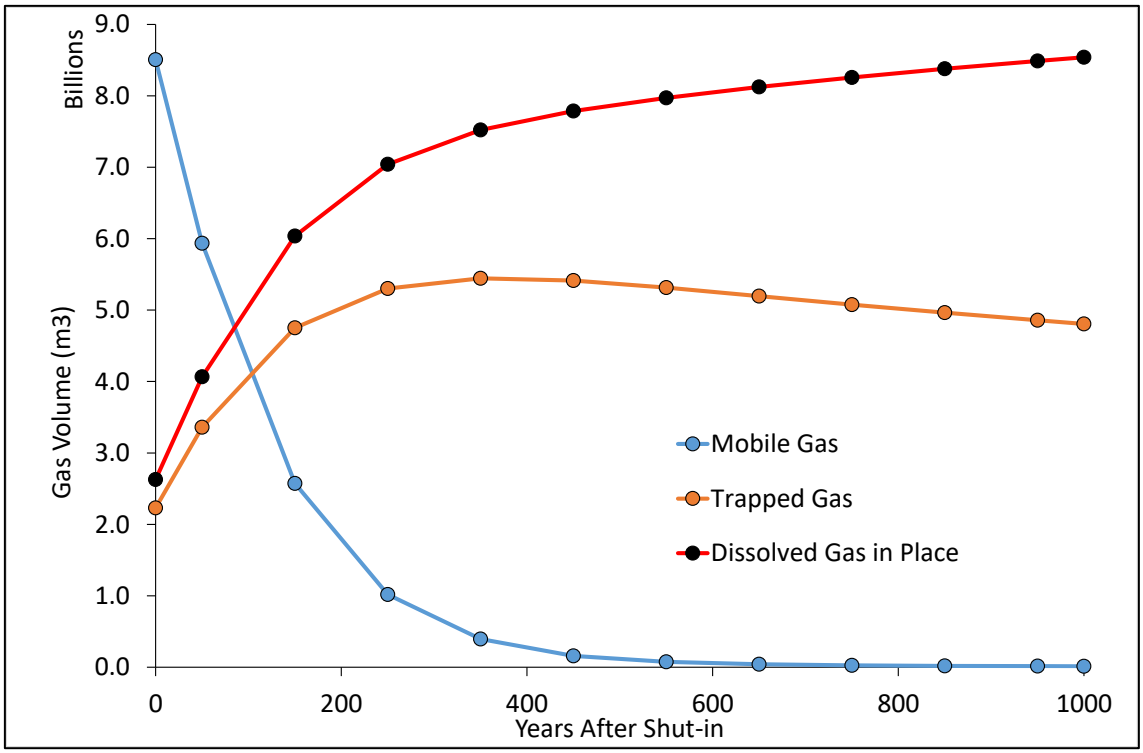

Figure 5-6 CO2 Material Balance vs. Time – Reference Case

	Supercritical CO2			
	Trapped Gas (Sm3)	Mobile Free Gas (Sm3)	Total CO2 Dissolved (Sm3)	Total CO2 (Sm3)
Gas Material Balance	5.4E+09	2.0E+07	7.7E+09	1.3E+10
% of Injected	40.9%	0.2%	59.0%	100%

Table 5-1 Material Balance Accounting @ 1000 years – Reference Case Model

5.2 Grid Sensitivity Check

In Reference 14, grid sensitivity studies concluded that the solubility of the injected gas can be reasonably calculated using the coarse scale model with cell dimensions of 250X250m. Reference 14 indicated that a finer grid size, 100X100m, could be used if it is important to have an understanding of the shape of the injected gas plume. Figure 5-7 and Figure 5-8 compare the shape of the plume in the model with Reference Case parameters and 250X250m grid cells with a model with 100X100m grid cells. The figures show that the plumes in the 100X100m and 250X250m models are similar, confirming the results in Reference 14. Table 5-2 compares the CO_2 material balance in the 100X100m and 250X250m model. The table shows that at the end of the 1,000-year shut-in time, the 100X100m model had slightly less gas dissolved in the liquid phase compared to the 250X250m model. The differences in

the distribution of gas in the models is small and confirms that the results of the modelling are relatively insensitive to grid block dimensions.

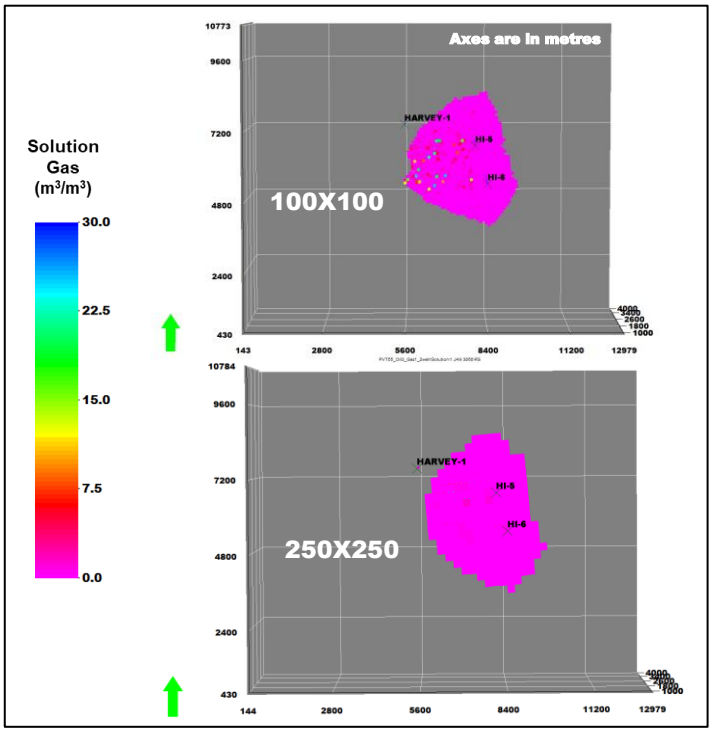

Figure 5-7 Areal View of Plume Distribution (Comparison between 250X250m and 100X100m Models @ 1000 years)

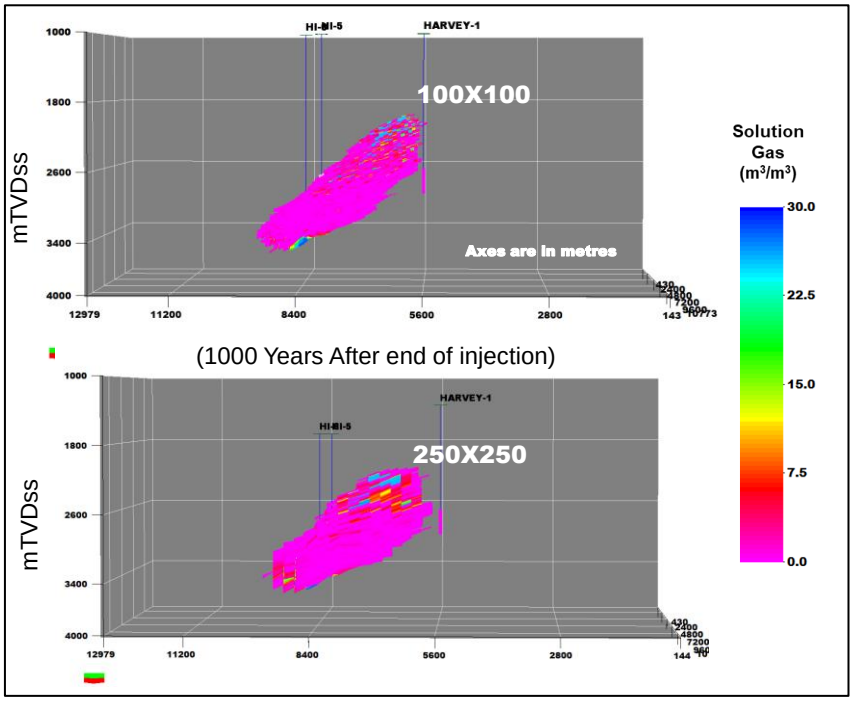

Figure 5-8 Plume Distribution Looking South (Comparison between 250X25m0 and 100X100m Models)

100X100 Model

	Supercritical CO2			
	Trapped Gas (Sm3)	Mobile Free Gas (Sm3)	Total CO2 Dissolved (Sm3)	Total CO2 (Sm3)
Gas Material Balance	5.6E+09	2.1E+08	7.5E+09	1.3E+10
% of Injected	41.9%	1.6%	56.5%	100%

250X250 Model

	Supercritical CO2			
	Trapped Gas (Sm3)	Mobile Free Gas (Sm3)	Total CO2 Dissolved (Sm3)	Total CO2 (Sm3)
Gas Material Balance	5.4E+09	2.0E+07	7.7E+09	1.3E+10
% of Injected	40.9%	0.2%	59.0%	100%

Table 5-2 Material Balance Accounting (Comparison Between 100X100m and 250X250m Models)

6. IMPACT OF RESERVOIR UNCERTAINTIES ON THE MOVEMENT OF THE CO_2 PLUME

It is impossible to have precise knowledge of subsurface parameters that can affect the movement of CO_2 in the reservoir. The key risk is that the CO_2 plume breaks out of the Area of Interest or rises to a depth shallower than 800m.

A number of models of the Harvey area were constructed to investigate the effects of the reservoir uncertainties on containment failure and the location of the CO_2 plume. The model is tested with a number of subsurface parameters and combinations of these parameters to test the robustness of the development concept. The intent of the uncertainty modelling is to "break" the model and identify the mechanism or subsurface parameters that are responsible for the failure. Action can then be undertaken to reduce or eliminate the uncertainties responsible for the failure of containment. Table 6-1 is a summary of the reservoir uncertainties investigated and the parameters used in the investigations.

Case	Case Name	Geological Model	Description
Reference	3Well	Reference	800,000 tpa. Brine salinity=45600 ppm (NaCl Equivalent) SgT based on Land Correlation C=1.95
1	3Well_NoPC	Reference	800,000 tpa. Brine salinity=45600 ppm (NaCl Equivalent) No capillary pressures SgT based on Land Correlation C=1.95
2	3Well_highkrg	Reference	800,000 tpa. Brine salinity=45600 ppm (NaCl Equivalent) Krg=0.25 SgT based on Land Correlation C=1.95
3	3Well_bland	Wonneup is homogeneous	800,000 tpa. Brine salinity=45600 ppm (NaCl Equivalent) SgT based on Land Correlation C=1.95
4	3Well_Hiperm	Permeability in I, J and K directions mulitipled by 1.4	800,000 tpa. Faults not sealing Brine salinity=45600 ppm (NaCl Equivalent) SgT based on Land Correlation C=1.95
5	3Well_LowSgt	Reference	800,000 tpa. Brine salinity=45600 ppm (NaCl Equivalent) SgT based on Land Correlation C=3.2
6	3Well_HighSalt	Reference	800,000 tpa. Faults not sealing Brine salinity=200000 ppm (NaCl Equivalent) SgT based on Land Correlation C=1.95
7	3Well_highKv	Kv=0.8*K Horizontal	800,000 tpa. Faults not sealing Brine salinity=45600 ppm (NaCl Equivalent) SgT based on Land Correlation C=1.95
8	3Well_lowKv	Kv=0.1*K Horizontal	800,000 tpa. Faults not sealing Brine salinity=45600 ppm (NaCl Equivalent) SgT based on Land Correlation C=1.96
9	3Well_001Faults	Fault Transmissibility * 0.01	800,000 tpa. Brine salinity=45600 ppm (NaCl Equivalent) SgT based on Land Correlation C=1.95
10	3WELL_holey_wonnseal	Cells adjacent to faults have the vertical permeability increased by 10 times. Wonnerup and Yalgorup in communication through the faults. No sand-on-sand communication between the Wonnerup and Yalgorup	800,000 tpa. Brine salinity=45600 ppm (NaCl Equivalent) SgT based on Land Correlation C=1.95
11	3WELL_holey	Cells adjacent to faults have the vertical permeability increased by 10 times. Communication between Wonnerup and Yalgorup through faults and sand-on-sand contact.	800,000 tpa. Brine salinity=45600 ppm (NaCl Equivalent) SgT based on Land Correlation C=1.95
12	3WELL_holey_NoYal	Cells adjacent to faults have the vertical permeability increased by 10 times. No communication between Wonnerup and Yalgorup through faults or sand-on-sand conact.	800,000 tpa. Brine salinity=45600 ppm (NaCl Equivalent) SgT based on Land Correlation C=1.95
13	3Well_holey_wonnseal_lowsol	Cells adjacent to faults have the vertical permeability increased by 10 times. Wonnerup and Yalgorup in communication through the faults.	800,000 tpa. Brine salinity=200000 ppm (NaCl Equivalent) SgT based on Land Correlation C=1.95
14	3WELL_holey_wonnseal_faults001	Fault Transmissibility * 0.01. Cells adjacent to faults have the vertical permeability increased by 10 times. Wonnerup and Yalgorup in communication through the faults.	800,000 tpa. Brine salinity=45600 ppm (NaCl Equivalent) SgT based on Land Correlation C=1.95

Table 6-1 Case Summary – Full Field Model of the Harvey Area

6.1 Case 1 - No Capillary Pressure

Drainage and imbibition capillary pressures were ignored in previous modelling studies (References 14 and 19). The impact of capillary pressures on the movement of the CO_2 plume was investigated in Case 1. In this case, the model was run without drainage or capillary pressure curves. Figure 6-1 shows the concentration of gas (i.e. gas in place) in the model. The highest concentration of gas is close to the wells and lowest is farther from the wells. Figure 6-1 compares the areal distribution of the CO_2 plume in Case 1 and the Reference Case. The result shows that there is little difference between the Reference Case and Case 1. Figure 6-2 compares the side view of the plume movement in Case 1 and the Reference Case. The difference in the shape of the plumes is indistinguishable.

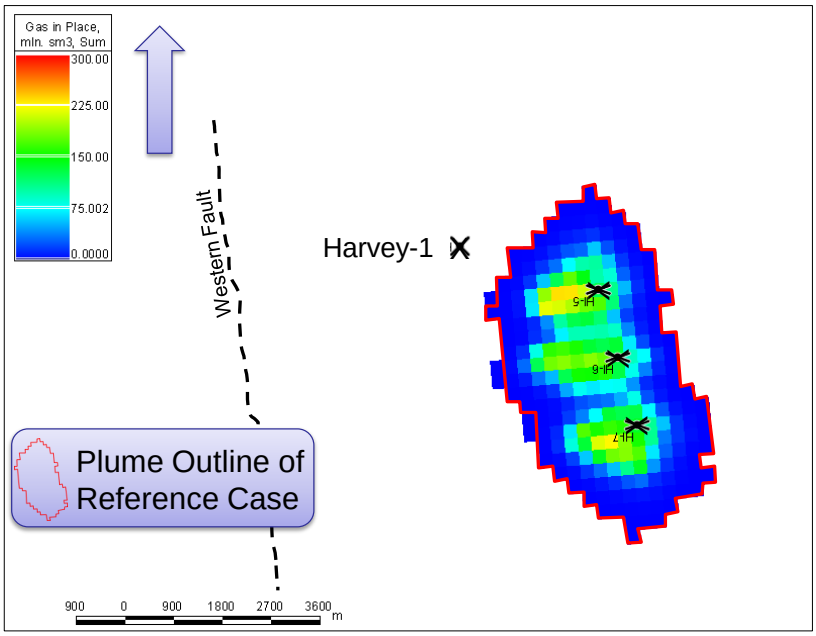

Figure 6-1 Areal View of Plume Distribution (Comparison between Reference and No PC Models)

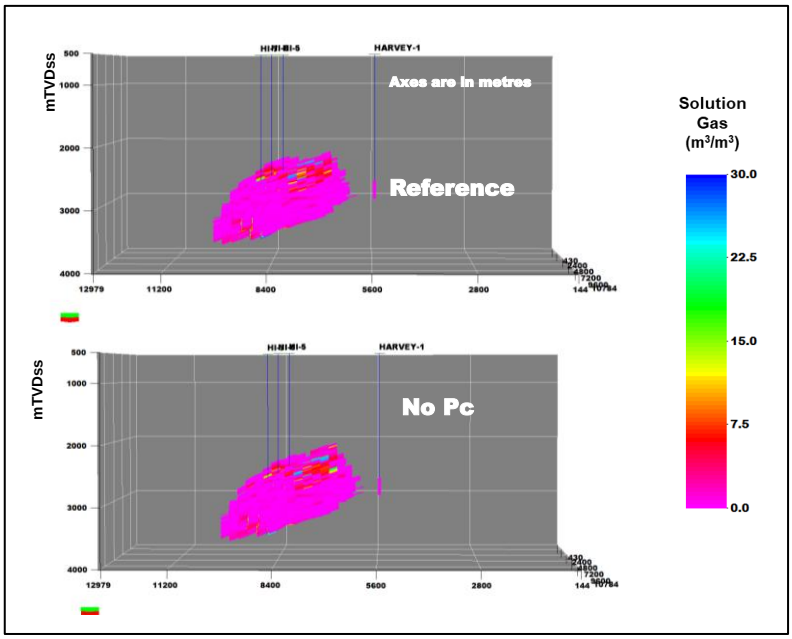

Figure 6-2 Plume Distribution Looking South (Comparison between Reference and No Pc Model @1000 years)

6.2 Case 2 – High Relative Permeability to Gas

End point relative permeability of gas is an uncertainty in fluid displacement processes as evinced by the scatter observed in (Figure 3-7). Higher end point relative permeability to the non-wetting phase would encourage the lateral and vertical movement of CO_2 in the reservoir. The impact of higher end point relative permeability was investigated by increasing the non-wetting phase end point relative permeability to 0.25. An example of the change in non-wetting phase relative permeability for SATNUM 6 is shown in (Figure 6-3). Figure 6-4 compares the areal distribution of the CO_2 plume in Case 2 and the Reference Case. The result shows that there the plume is contained in the Wonnerup and there is little difference between the Reference Case and Case 2. Figure 6-5 compares the side view of the plume movement in Case 2 and the Reference Case. The plume in the high krg migrated up dip farther than in the Reference Case.

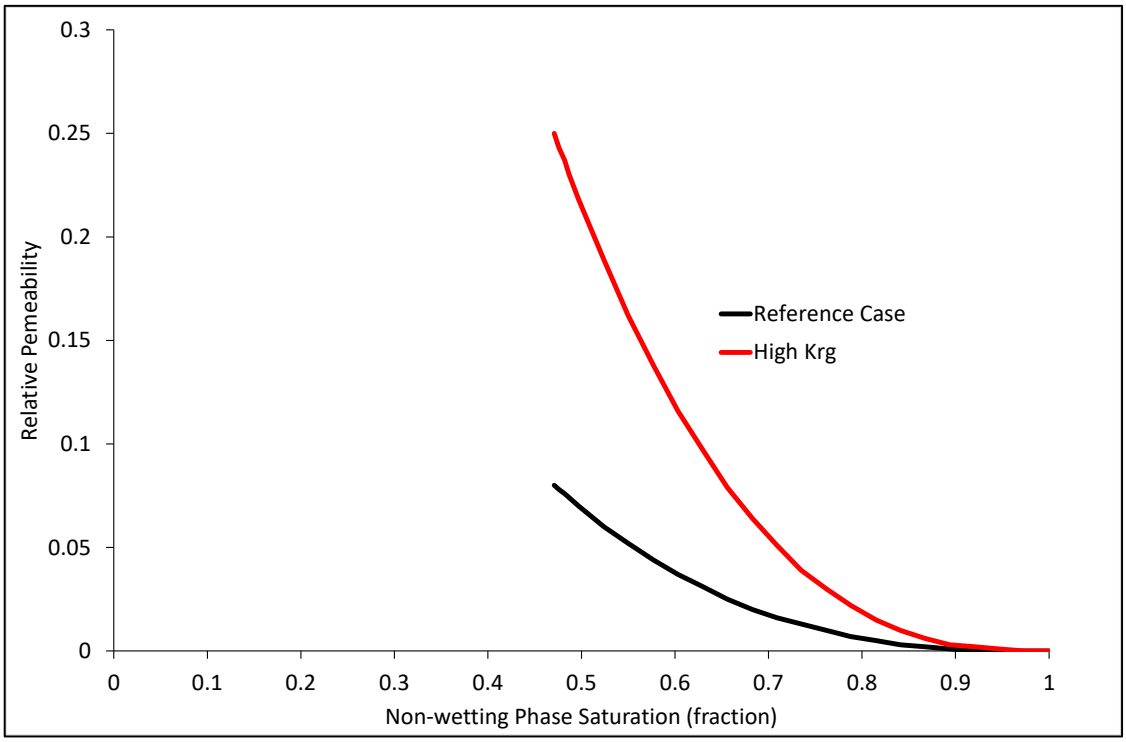

Figure 6-3 Non-Wetting Phase Relative Permeability – Comparison between Reference and Case 2

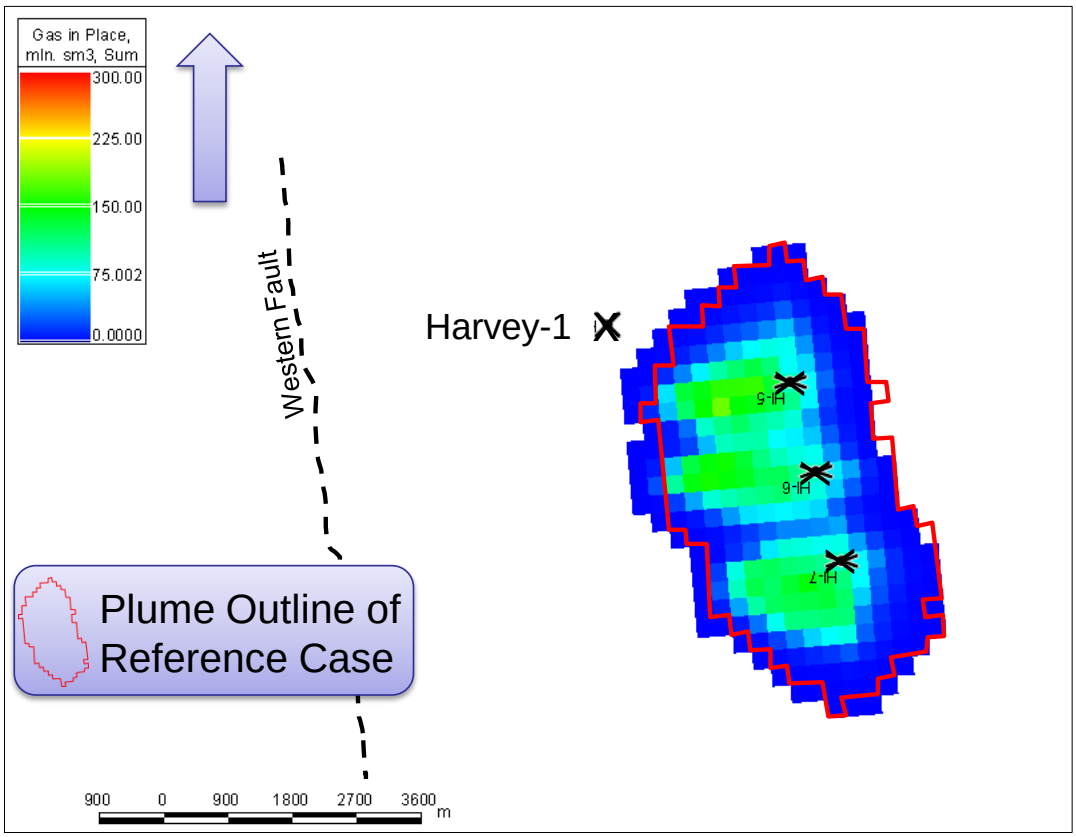

Figure 6-4 Areal View of Plume Distribution (Comparison between Reference and High Krg Models)

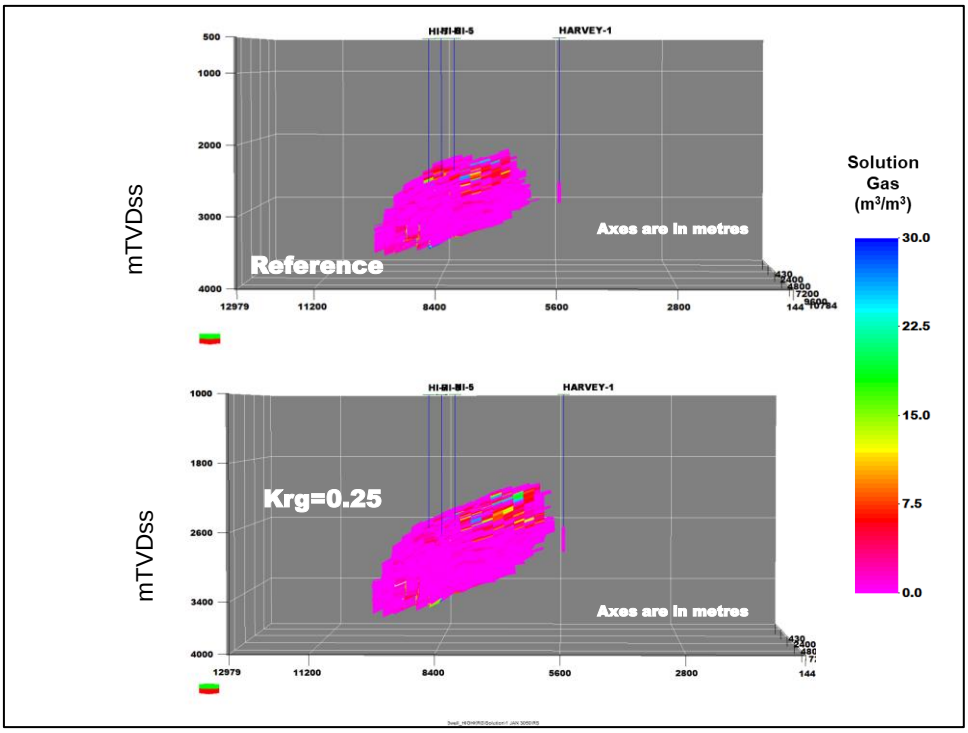

Figure 6-5 Plume Distribution Looking South (Comparison between Reference and High Krg Model @ 1000 years)

6.3 Case 3 – Homogeneous Wonnerup ("Bland" Model)

The distribution of facies for this phase of modelling (Reference 17) was influenced by the interpretation that the increased number of seismic reflectors indicated a more heterogeneous reservoir which became the "Reference Case". However, based on the only well to penetrate the entire section of the Wonnerup in the Harvey area, the Wonnerup appears more homogeneous or 'bland'. Therefore, a "Bland" case was created using the results of the GSWA Harvey-1 well which encountered ~90% net-to-gross within the Wonnerup Member.

Figure 6-6 compares the areal distribution of the CO_2 plume in the "bland" geological realisation of the Wonnerup and the Reference Case. The result shows that there is little difference in the shape of the plume between the Reference Case and Case 3. Figure 6-7 compares the side view of the plume movement in Case 3 and the Reference Case. The plume in the "bland" case migrated up dip farther than in the Reference Case but remains in the Wonnerup.

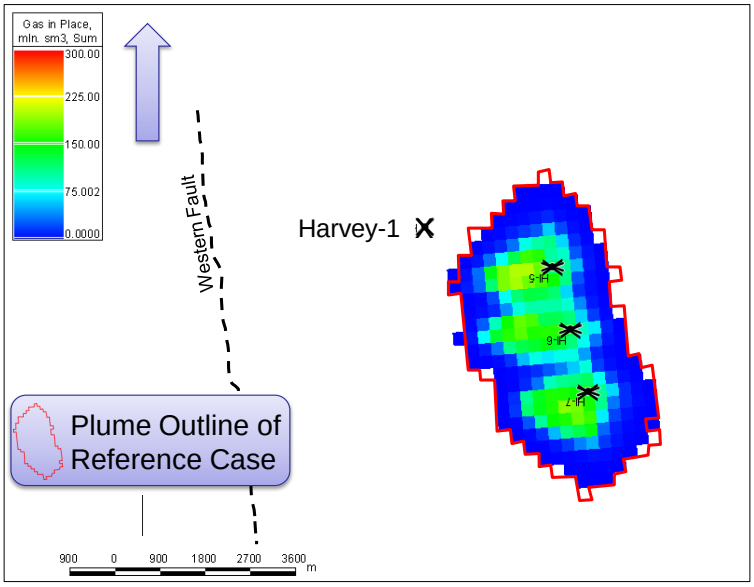

Figure 6-6 Areal View of Plume Distribution (Comparison between Reference and "Bland" Models)

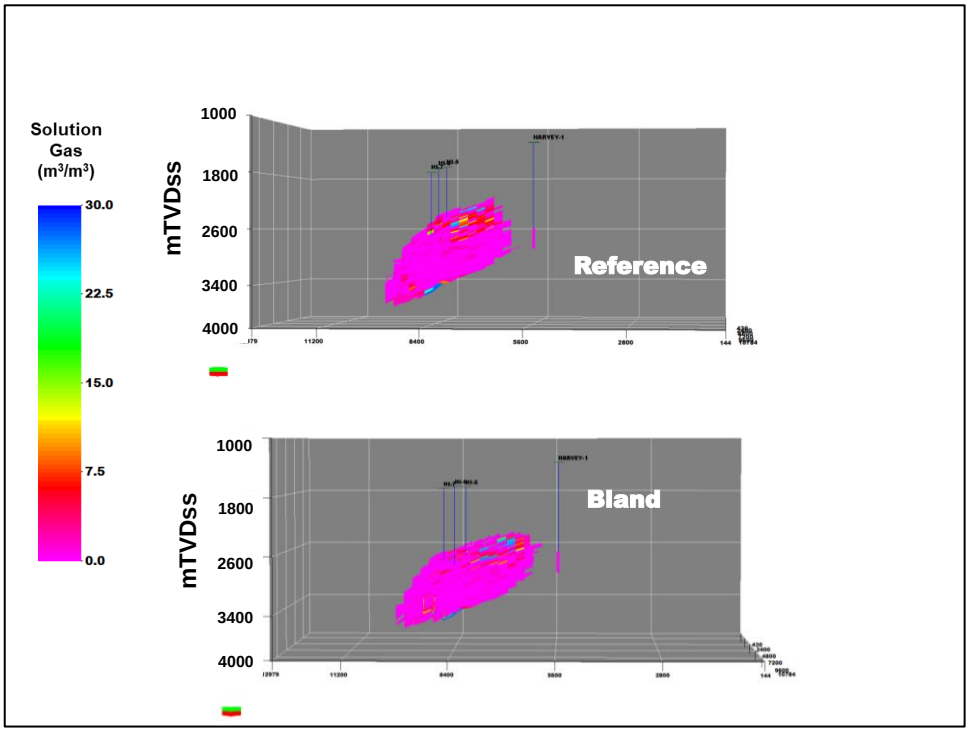

Figure 6-7 Plume Distribution Looking South (Comparison between Reference and Bland Model @1000 years)

6.4 Case 4 – High Permeability

Permeability curves were derived by building a porosity to permeability transform based on all core and Nuclear Magnetic Resonance (NMR) data. This porosity to permeability transform was applied to the porosity curve to create the permeability curve. The mean

permeability derived using this transform is 110mD which formed as our “Reference Case”. The “High Permeability” realisation was created by multiplying the permeability of all the cells by 1.4.

Figure 6-8 compares the areal distribution of the CO_2 plume in the “High Permeability” geological realisation of the Wonnerup and the Reference Case. The result shows that there is little difference in the shape of the plume between the Reference Case and Case 4. Figure 6-9 compares the side view of the plume movement in Case 4 and the Reference Case. The plume in the two cases are indistinguishable.

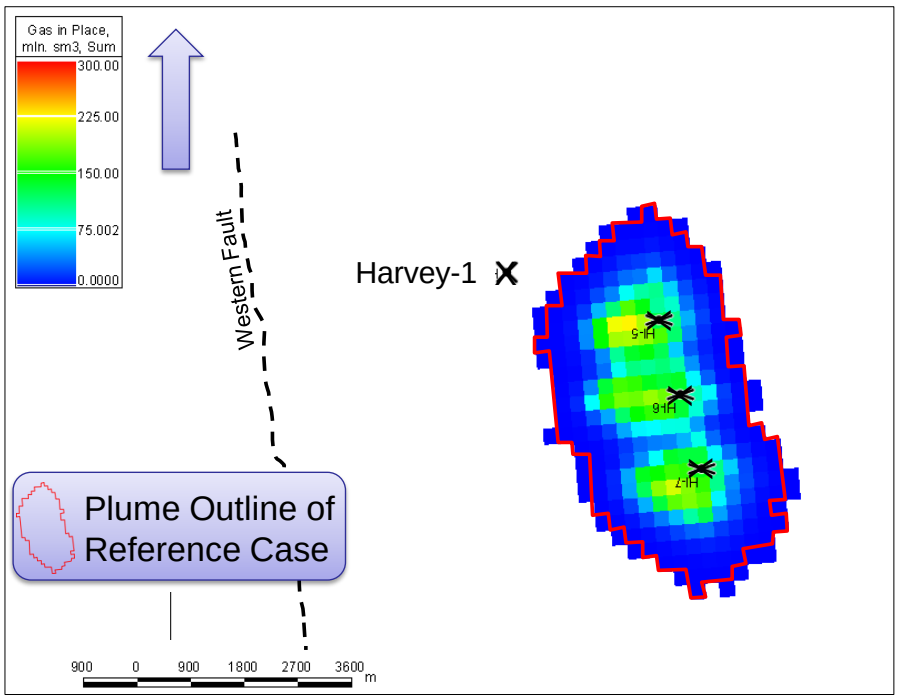

Figure 6-8 Areal View of Plume Distribution (Comparison between Reference and High Permeability Models)

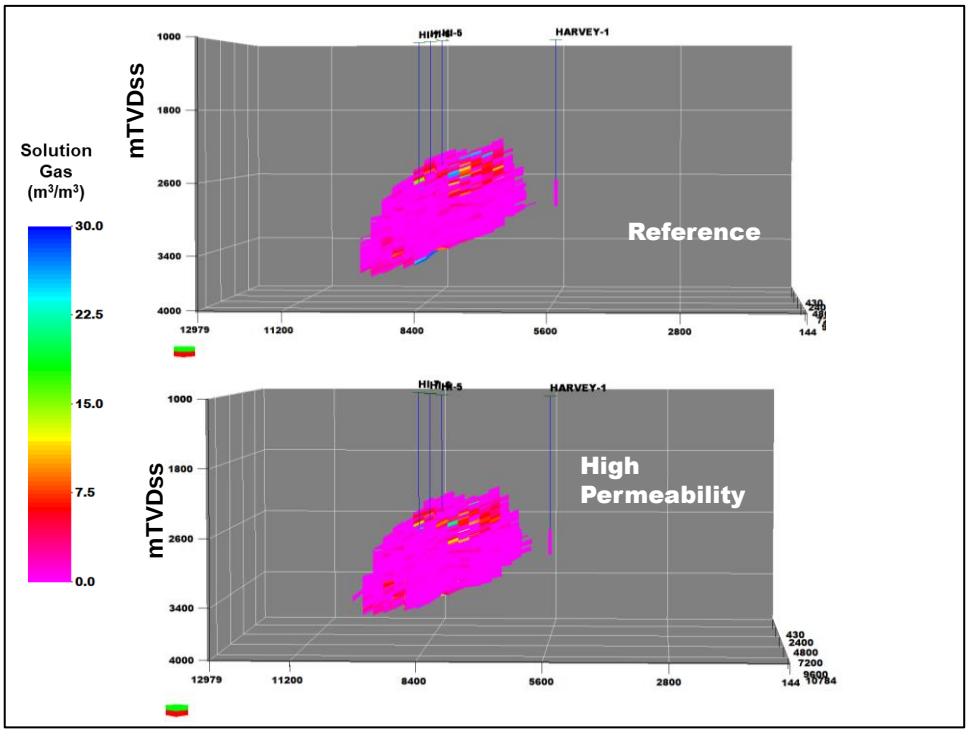

Figure 6-9 Plume Distribution Looking South (Reference and High Permeability Model @1000 years)

6.5 Case 5 – Low Trapped Gas Saturation

The Land Correlation with C=3.2 was used to generate pessimistic trapped gas saturation (Figure 6-10) for the range of permeabilities in the model. Figure 6-11 shows the reduction in trapped gas saturation for cells in the model with permeability greater than 300mD.

Figure 6-12 show that the areal extent of the CO_2 plume in Case 5 is similar to the Reference Case. Figure 6-13 shows that although the CO_2 plume in Case 5 has risen to a shallower depth than the Reference Case, the difference between the plumes is minor. Table 6-2 is a comparison of the distribution of CO_2 in Case 5 and the Reference Case.

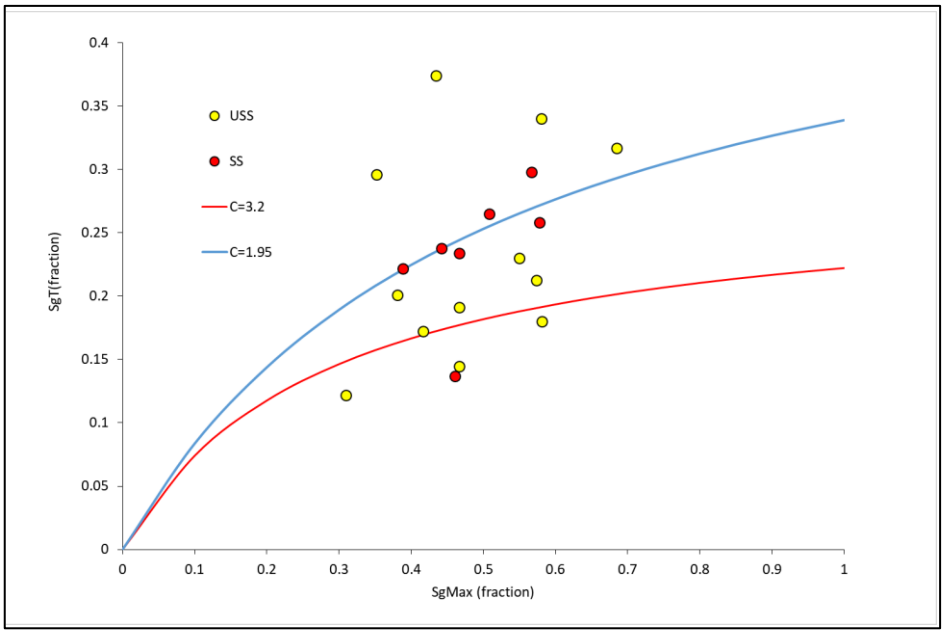

Figure 6-10 Land Correlation Parameter Used to Generate Pessimistic Sg_T

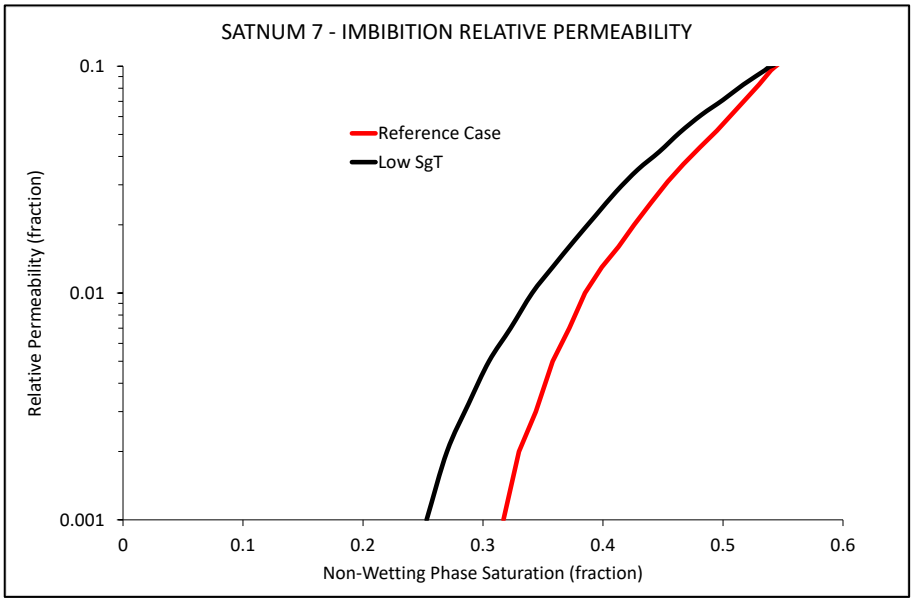

Figure 6-11 Imbibition Relative Permeability – SATNUM 7 (k > 300 mD)

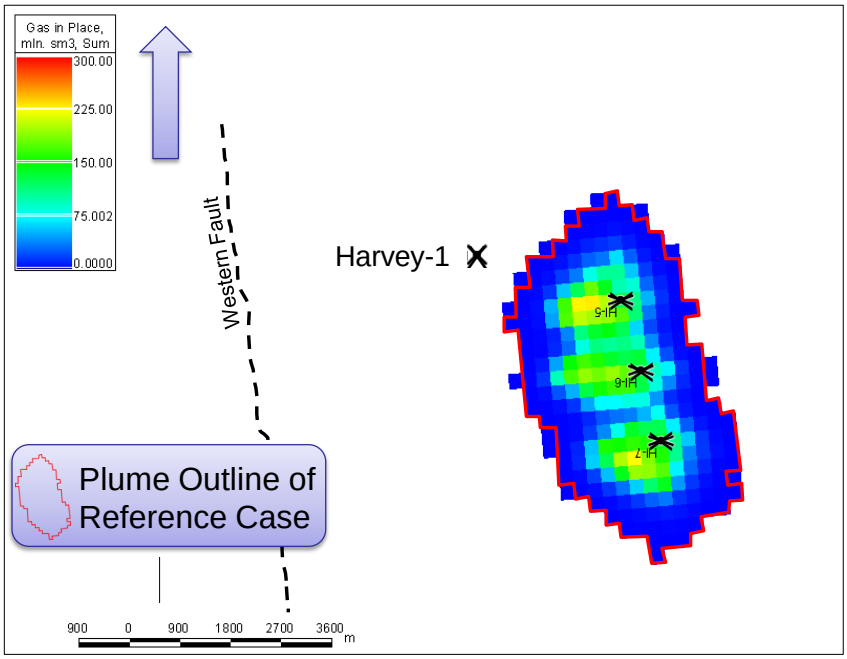

Figure 6-12 Areal View of Plume Distribution (Comparison between Reference and Low SgT Models)

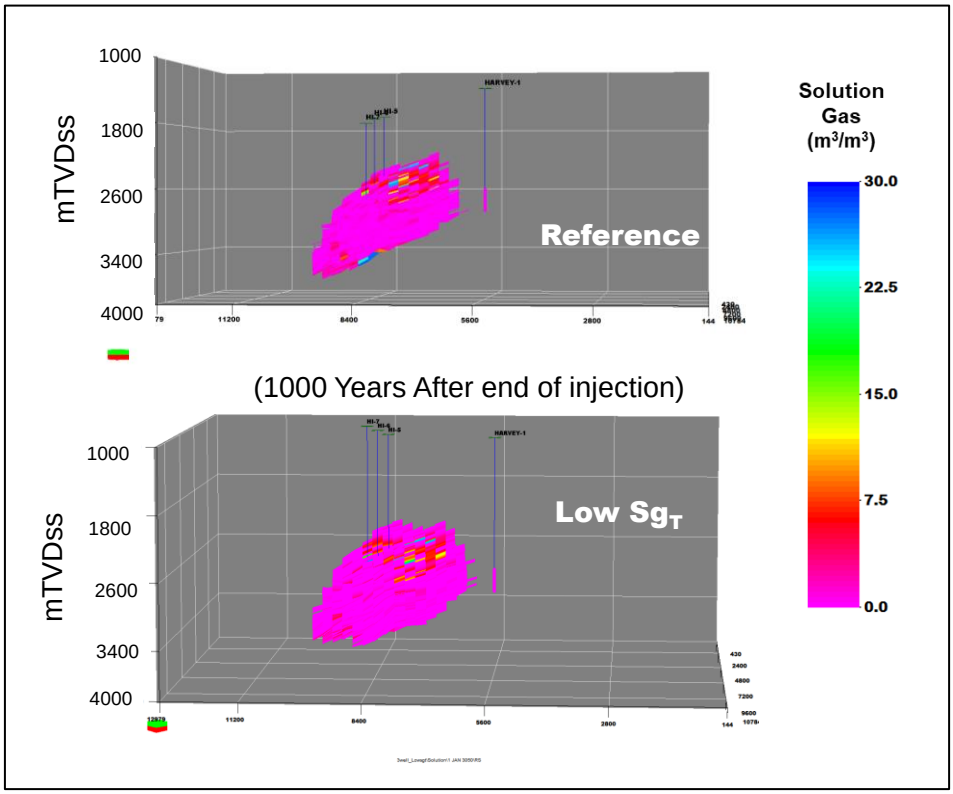

Figure 6-13 Plume Distribution Looking South (Reference and Low Sg_T Model @ 1000 years of shut-in)

Reference Case

	Supercritical CO2			
	Trapped Gas (Sm3)	Mobile Free Gas (Sm3)	Total CO2 Dissolved (Sm3)	Total CO2 (Sm3)
Gas Material Balance	4.8E+09	1.3E+07	8.5E+09	1.3E+10
% of Injected	36%	0%	64%	100%

Low Sg_T

	Supercritical CO2			
	Trapped Gas (Sm3)	Mobile Free Gas (Sm3)	Total CO2 Dissolved (Sm3)	Total CO2 (Sm3)
Gas Material Balance	4.5E+09	6.2E+06	8.9E+09	1.3E+10
% of Injected	34%	0%	66%	100%

Table 6-2 Material Balance Accounting @ 1000 years (Comparison between Reference and Low Sg_T Models)

6.6 Case 6 – Low Gas Solubility

In this scenario, the model was run assuming a brine salinity of 200 g/L H2O NaCl Equivalent to reduce the volume of CO_2 dissolved in the liquid phase to address the issue of "unknown unknowns" that could lead to uncertainty in the amount of mobile CO_2.

Figure 6-14 shows that the areal extent of the CO_2 plume in the low solubility case is smaller than the Reference Case because the lower solubility of the gas in the liquid phase results in the plume rising to a shallower depth (Figure 6-15) but still remaining in the Wonnerup. Table 6-3 is a summary of the distribution of CO_2 in the model 1,000 years after the cessation of injection. The table shows that the amount of CO_2 dissolved in the liquid phase was reduced from 64% to 37% whereas trapped gas increased from 36% to 63%. These results show that in a closed system, CO_2 that is not dissolved will be trapped.

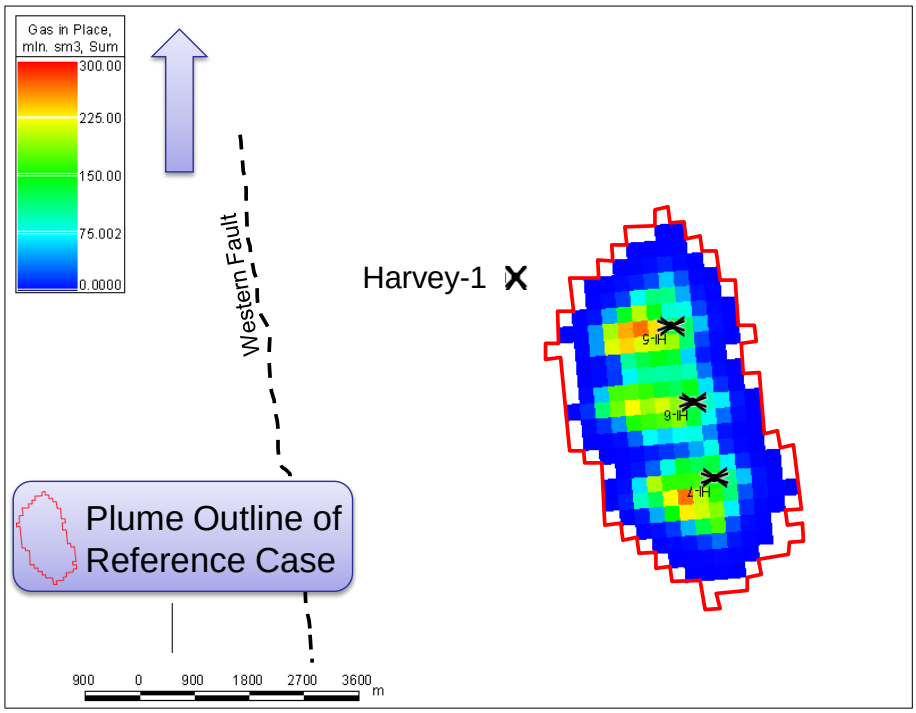

Figure 6-14 Areal View of Plume Distribution (Comparison between Reference and Low Solubility Models)

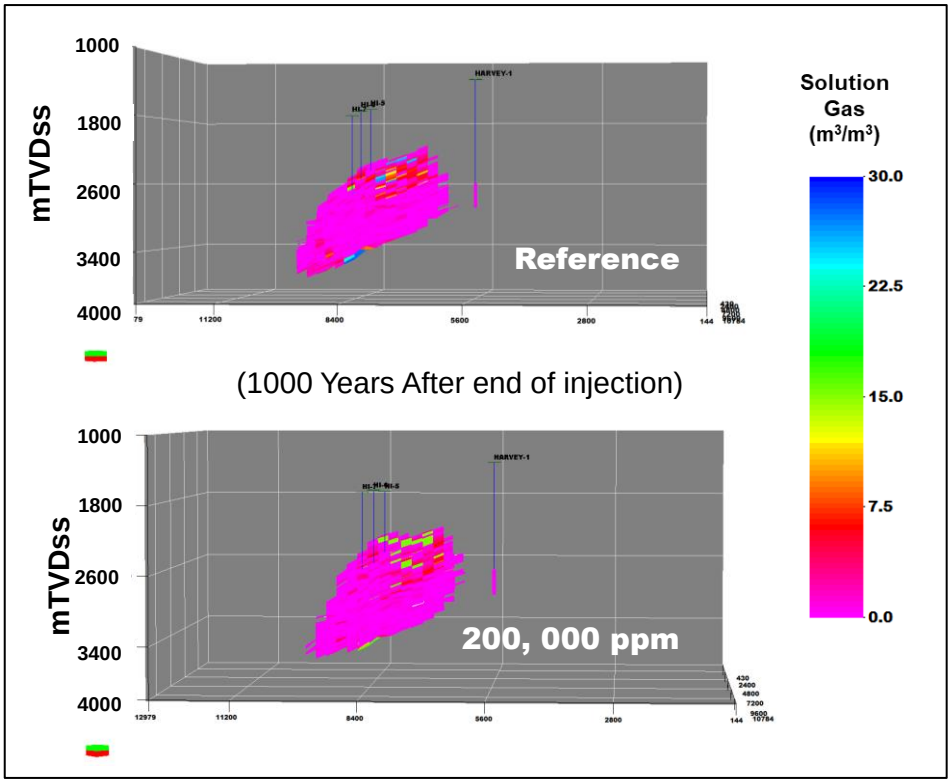

Figure 6-15 Plume Distribution Looking South –Reference and Low solubility scenario After 1000 years of shut-in

Reference Case

	Supercritical CO2			
	Trapped Gas (Sm3)	Mobile Free Gas (Sm3)	Total CO2 Dissolved (Sm3)	Total CO2 (Sm3)
Gas Material Balance	4.8E+09	1.3E+07	8.5E+09	1.3E+10
% of Injected	36%	0%	64%	100%

200,000 ppm Scenario

	Supercritical CO2			
	Trapped Gas (Sm3)	Mobile Free Gas (Sm3)	Total CO2 Dissolved (Sm3)	Total CO2 (Sm3)
Gas Material Balance	8.4E+09	8.7E+06	4.9E+09	1.3E+10
% of Injected	63%	0%	37%	100%

Table 6-3 Material Balance Accounting @ 1000 years (Comparison between Reference and Low Solubility Models)

6.7 Case 7 – High kv/kh

The ratio of vertical-to-horizontal permeability (kv/kh) in the Reference Case (Figure 6-16) varies due to the manner in which the shales and sands are distributed in the geological model. As a result, there are patches in the model where the kv/kh is low, which might act to retard the vertical migration of CO_2, and zones where the kv/kh are high, which might promote the vertical migration of CO_2. To examine the impact of a uniformly high kv/kh ratio on the flow of CO_2, the vertical permeability in the cells are made equal to 0.8 times the horizontal permeability. Figure 6-17 shows that the increase in kv/kh has little impact on the areal extent of the CO_2 plume. The increase in kv/kh did promote the migration of CO_2 vertically (Figure 6-18) but the effect was modest.

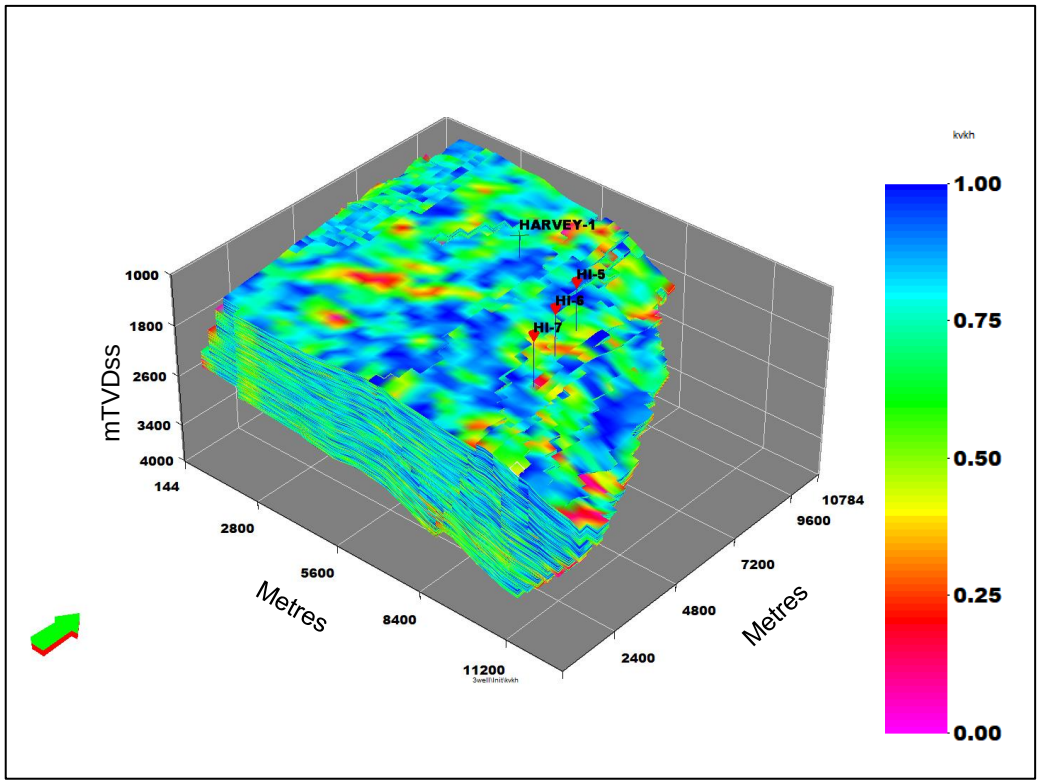

Figure 6-16 kv/kh Distribution – Wonnerup Sands (Reference Case)

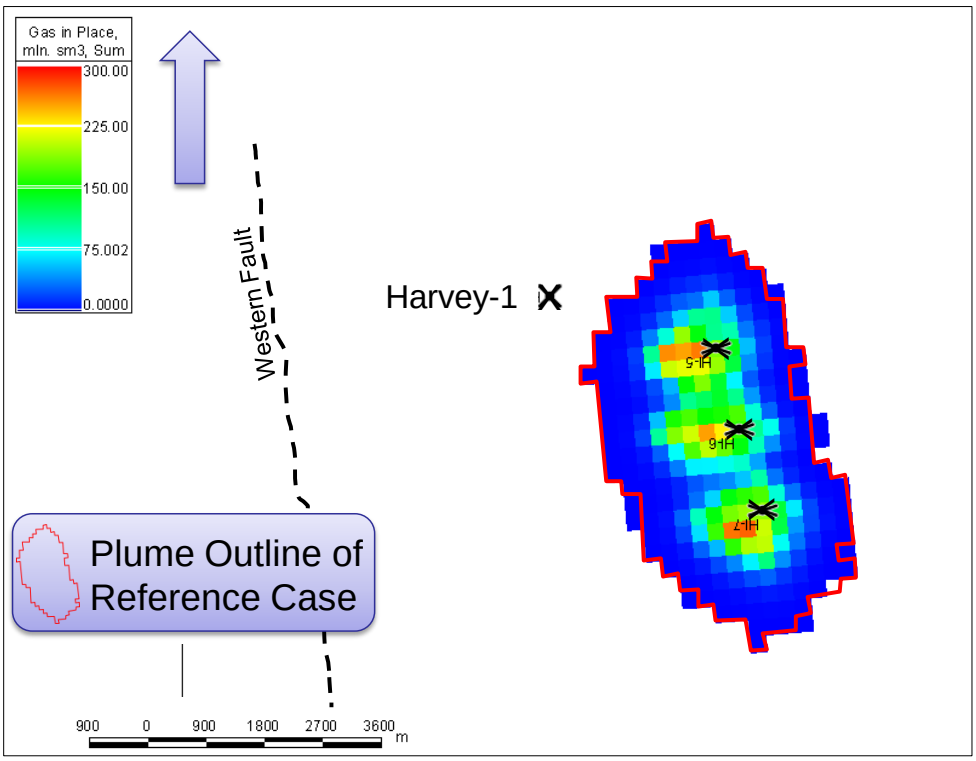

Figure 6-17 Areal View of Plume Distribution (Comparison between Reference and High kv Models)

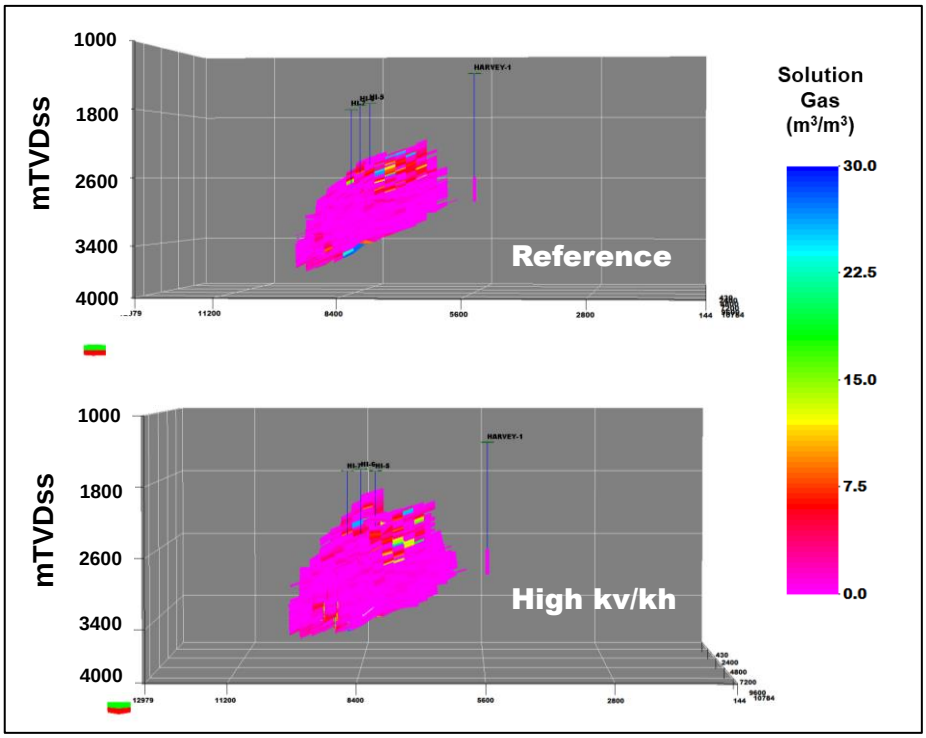

Figure 6-18 Plume Distribution Looking South –Reference and High kv/kh scenario after 1000 years of shut-in

6.8 Case 8 – Low kv/kh

To examine the impact of a uniformly low kv/kh ratio on the flow of CO_2, the vertical permeability in the cells are made equal to 0.1 times the horizontal permeability. This scenario was created to examine the impact of a low kv/kh in the Wonnerup on the lateral migration of the CO_2. Low kv/kh would promote flow of CO_2 in a lateral direction which might result in the plume reaching the "East-West" fault and substantially increase the risk of containment failure. Figure 6-19 shows that CO_2 plume in the low kv/kh scenario occupies a larger area than the Reference Case as a result of the plume being more compact (Figure 6-20) compared to the Reference Case due to more lateral movement of the gas.

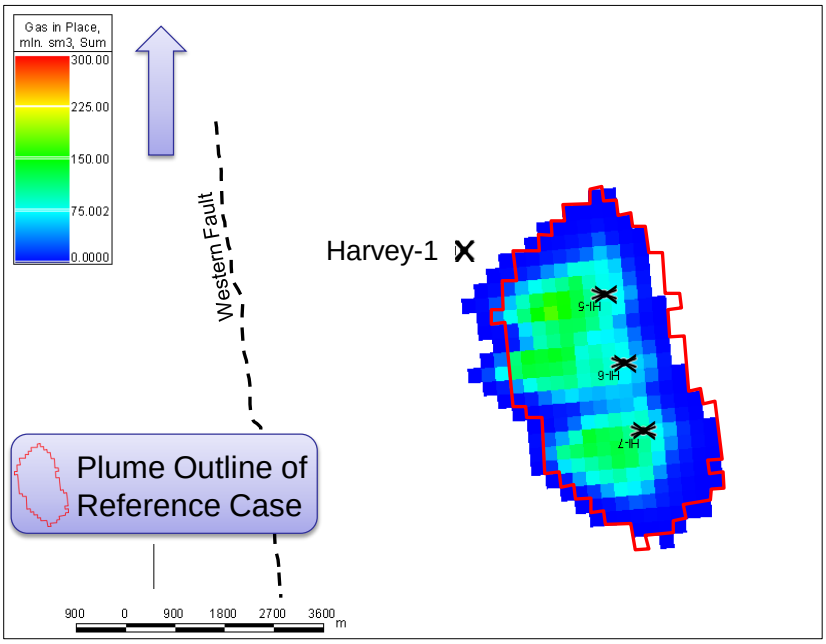

Figure 6-19 Areal View of Plume Distribution (Comparison between Reference and Low Kv Models)

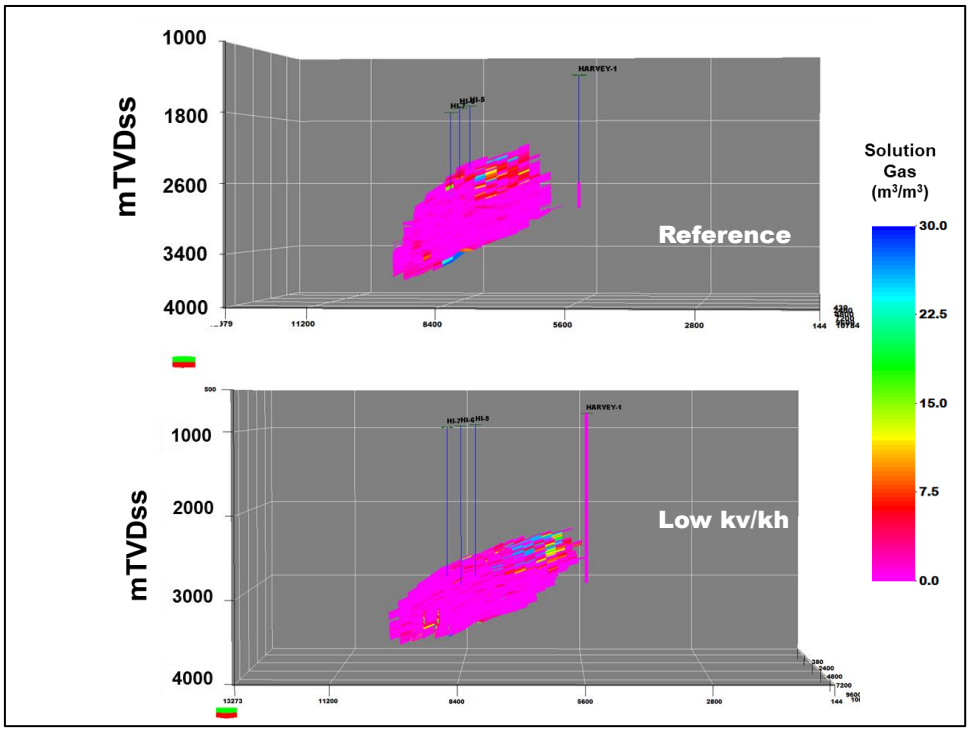

Figure 6-20 Plume Distribution Looking South –Reference and Low kv/kh scenario after 1000 years of shut-in

6.9 Case 9 – Low Fault Transmissibility

The Wonnerup is about 1,600m thick with a net-to-gross higher than 90%. The intrafield faults in the area of interest generally have displacements of a few metres and are unlikely to be

baffles or barriers to the flow of fluids. Nevertheless, cataclastic processes might result in some of the faults having lower transmissibility. To model this effect, a transmissibility multiplier of 0.01 (Figure 6-21) was used on all faults to increase the resistance to flow between the cells affected by the faults to investigate if the lower lateral transmissibility would result in the injected CO_2 preferentially flowing vertically.

Figure 6-22 shows that the CO_2 plume in Case 9 is aerially more compact than the Reference Case. The high intensity of gas concentration close to the wells indicate that the reduction in fault transmissibility encouraged the vertical migration of gas (Figure 6-23). Nevertheless, the gas is contained in the Wonnerup.

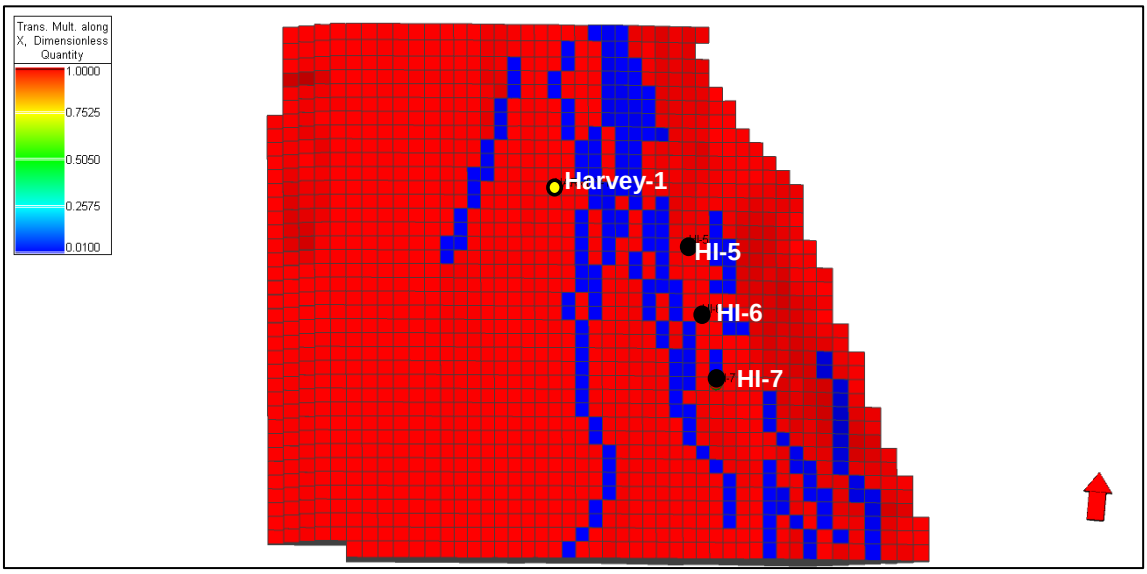

Figure 6-21 Areal View – Top Wonnerup in the Model showing transmissibility in the X-direction

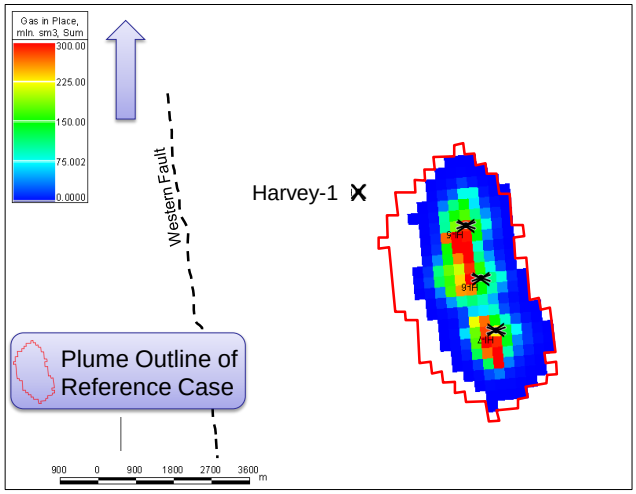

Figure 6-22 Areal View of Plume Distribution (Comparison between Reference and Low Fault Transmissibility Models)

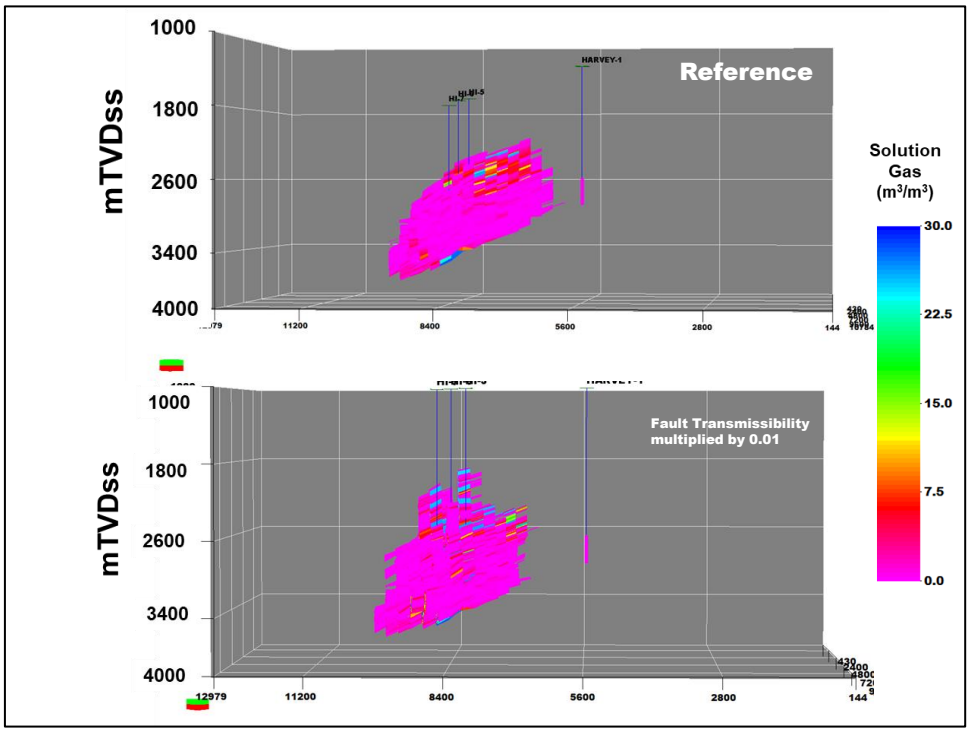

Figure 6-23 Plume Distribution Looking South - Reference and Low Fault transmissibility Model @1000 years

6.10 Case 10 – High Vertical Permeability ("Holey Faults")

The area of interest in the Harvey area is intersected by a number of faults. None of these faults are expected to form lateral barriers to flow but the areas near the faults may have enhanced vertical permeability due to fractures. The area of interest in the Harvey area is intersected by a number of faults. In Case 10, these fracture zones are modelled as areas of enhanced vertical permeability (Figure 6-24 and Figure 6-25). The vertical permeability of cells adjacent to a fault are increased 10 times.

Figure 6-26 compares the distribution of CO_2 in the Reference Case and Case 10 after 1,000 years. There is little difference in the distribution of CO_2 in between the cases. Figure 6-27 shows that the CO_2 plume has risen to a depth 1366mTVDss in the Yalgorup, the secondary containment unit. In this scenario, the Wonnerup and Yalgorup are assumed to be in communication through the faults.

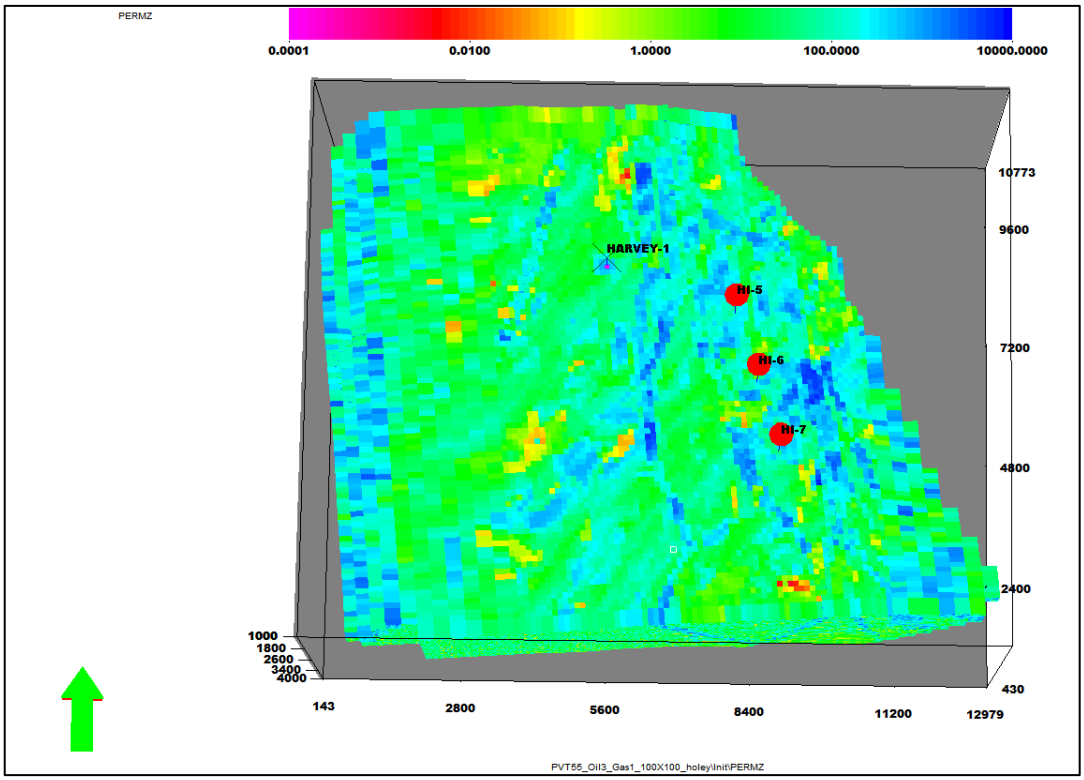

Figure 6-24 Areal View of Top Wonnerup – Permeability in the Vertical Direction

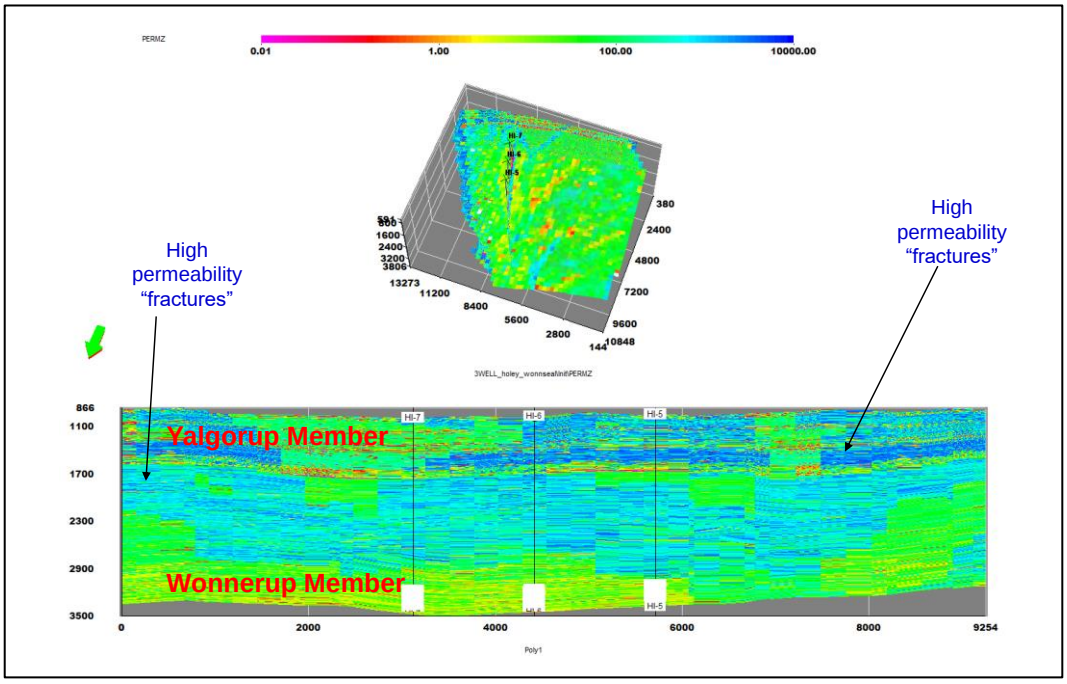

Figure 6-25 Cross-section through Injectors – Permeability in the Vertical Direction

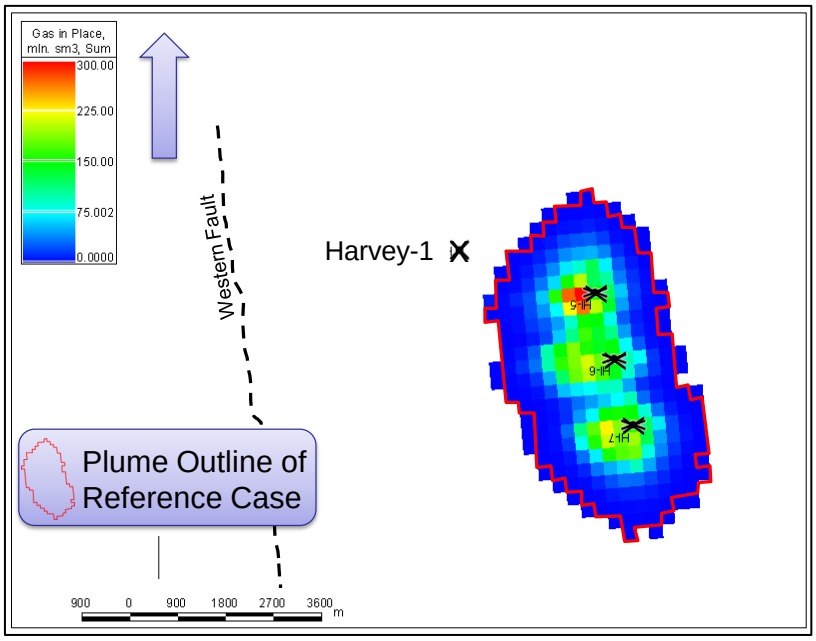

Figure 6-26 Areal View of Plume Distribution (Comparison between Reference and "Holey Faults" Models)

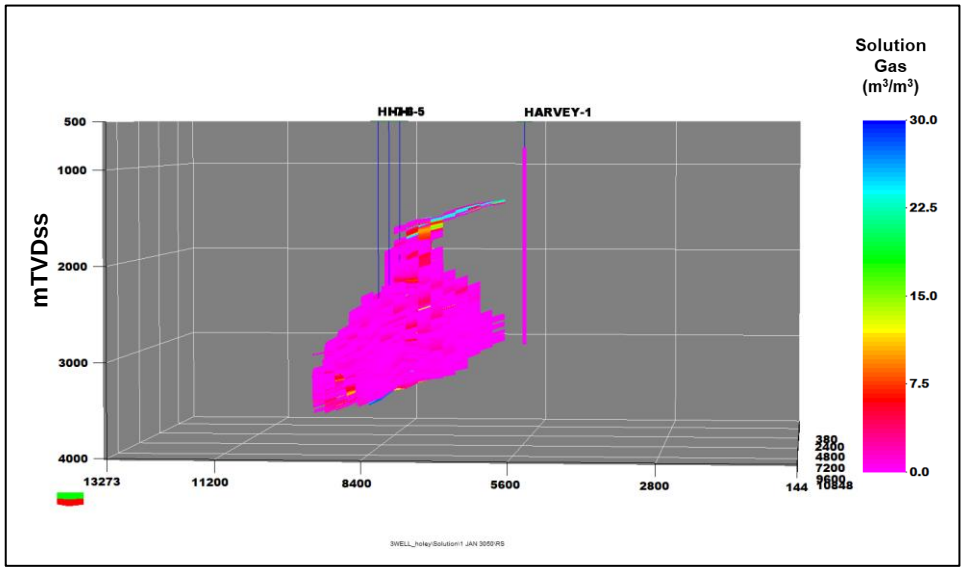

Figure 6-27 Plume Distribution Looking South @1000 years – High Vertical Permeability Scenario (Case 10)

6.10.1 Case 11 – High Vertical Permeability (Communication via Faults and sand-to-sand Contact)

In this scenario, it is assumed that communication between the Yalgorup and Wonnerup is through the faults and sand to sand contact. Figure 6-28 and Figure 6-29 show the extent of the plume in Case 11. In Figure 6-28 the areal extent of the plume is similar to the Reference Case and almost identical to the shape of the plume in Case 10. The rise of the plume in Case 11 (Figure 6-29) is almost identical to Case 10. This result indicates that vertical

movement of the CO_2 via the faults dominates and movement via sand-to-sand communication between the Wonnerup and Yalgorup.

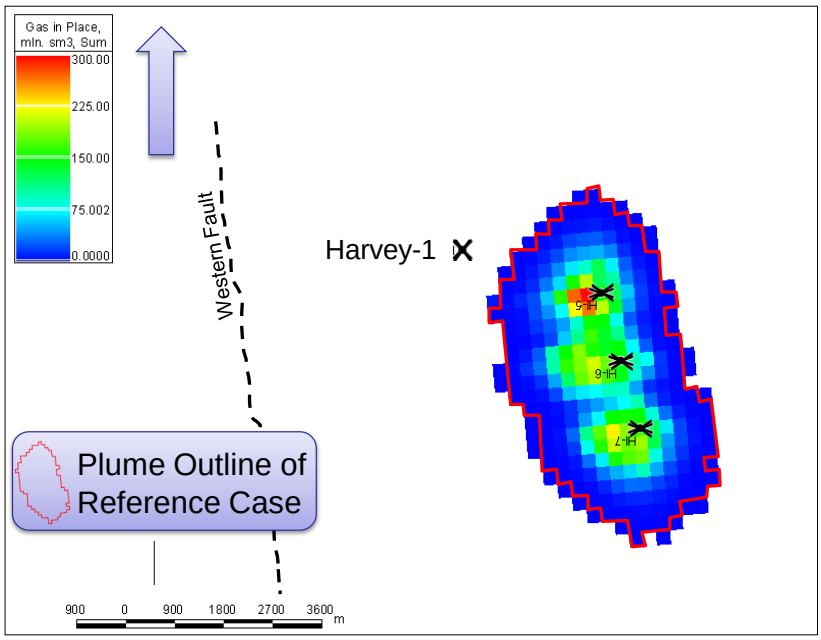

Figure 6-28 Areal View of Plume Distribution (Comparison between Reference and Case 11)

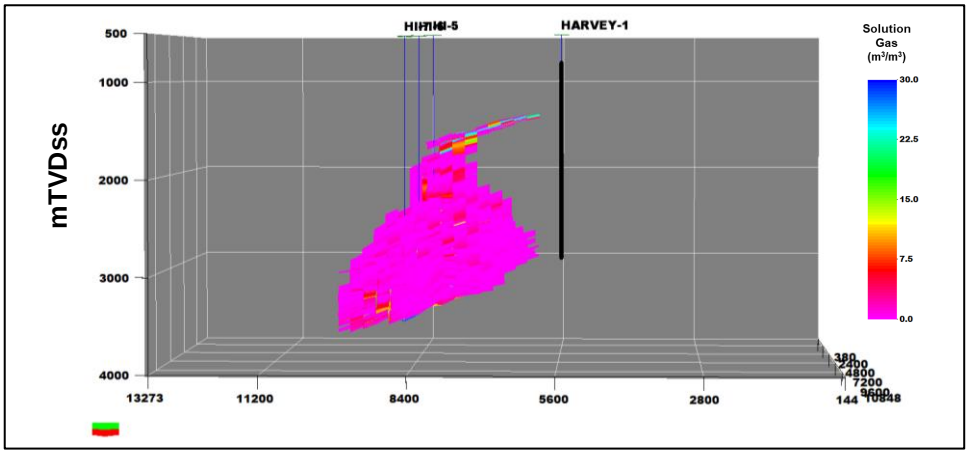

Figure 6-29 Plume Distribution Looking South @1000 years – High Vertical Permeability Scenario (Case 11)

6.10.2 Case 12 – High Vertical Permeability (Wonnerup is isolated)

In this scenario, it is assumed that there is no communication between the Yalgorup and Wonnerup. The absence of communication between the two sand members means that there is no secondary containment unit; any gas that reaches the top Wonnerup would be forced to move towards the “East-West” fault and risk containment failure.

Figure 6-30 and Figure 6-31 show the extent of the plume in Case 12. In (Figure 6-30) the areal extent of the plume is similar to Cases 10 and 11. Figure 6-31 shows that the plume has risen to a depth of 1,415mTVDss. None of the injected gas has reached the “East-West” fault.

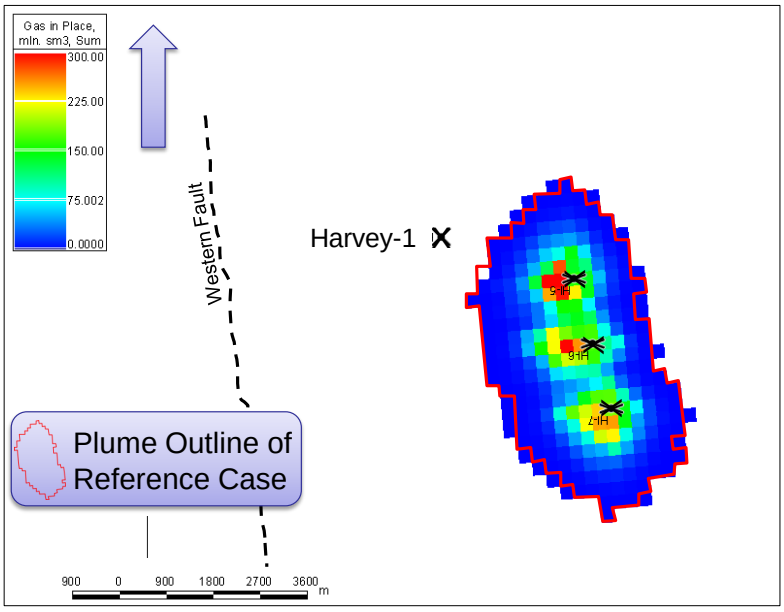

Figure 6-30 Areal View of Plume Distribution (Comparison between Reference and Case 12

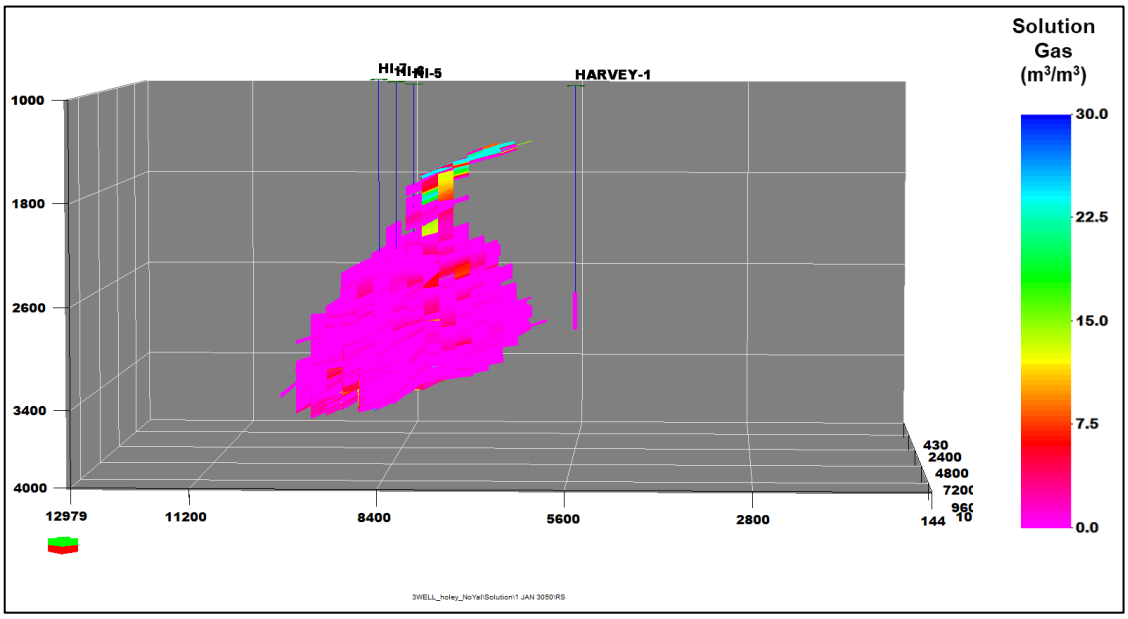

Figure 6-31 Plume Distribution Looking South @1000 years – High Vertical Permeability Scenario (Case 12)

6.11 Stress Scenarios

Stress scenarios combine two or more uncertainties to create a pessimistic but low probability outcome. Two stress scenarios were created:

- Case 13 – Combine the realisation where there are higher vertical permeability conduits close to the faults and a pessimistic view of gas solubility
- Case 14 - Combine the realisation where the faults are baffles to the lateral flow of fluids and higher vertical permeability conduits close to the faults

6.11.1 Case 13 - "Holey Faults" and Low Solubility

This scenario is a combination of Case 11 and Case 6. It combines the two uncertainties in the Harvey area: high vertical permeability adjacent to faults and low gas solubility to investigate the movement of the CO_2 plume.

- The vertical permeability of the cells adjacent to faults were increased by an order of magnitude.
- The brine salinity is assumed to be 200,000 ppm.

Figure 6-32 shows the distribution of the CO_2 plume in the model. All of the gas is within the area of interest. The shallowest level of the gas was in the Yalgorup at a depth of about 990mTVDss. Only about 2% of the injected gas is in the Yalgorup.

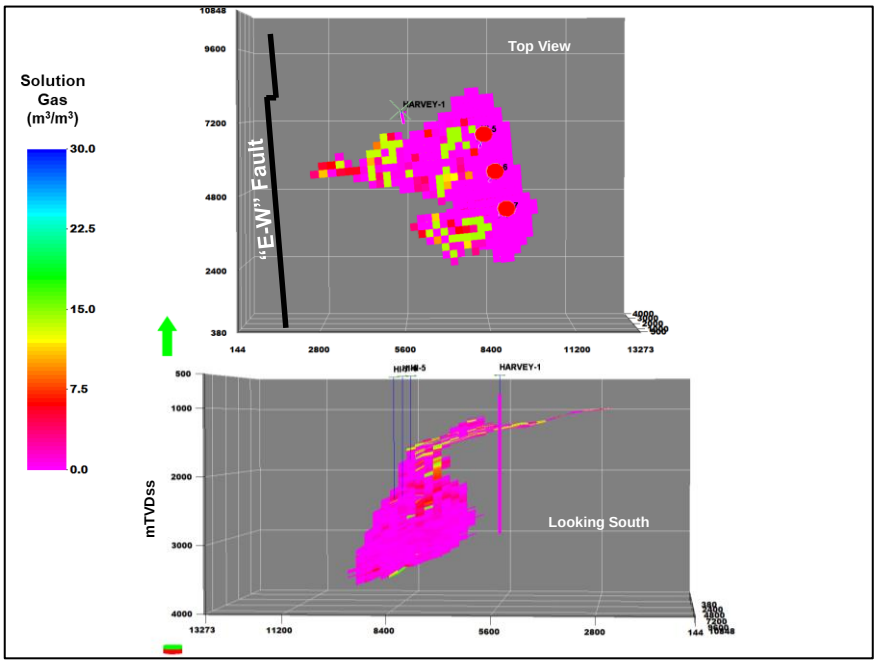

Figure 6-32 CO_2 Plume Shape of Stress Scenario – Case 13 @1000 years

6.11.2 Case 14 - "Holey Faults" and Low Fault Transmissibility

This scenario is a combination of Case 9 and Case 11. It combines two uncertainties in the Harvey area: high vertical permeability adjacent to faults and low fault transmissibility.

Figure 6-33 shows the distribution of the CO_2 plume in the model. All of the gas is within the area of interest. The shallowest level of the gas was in the Yalgorup at a depth of about 1,570mTVDss. Only about 0.3% of the injected gas is in the Yalgorup.

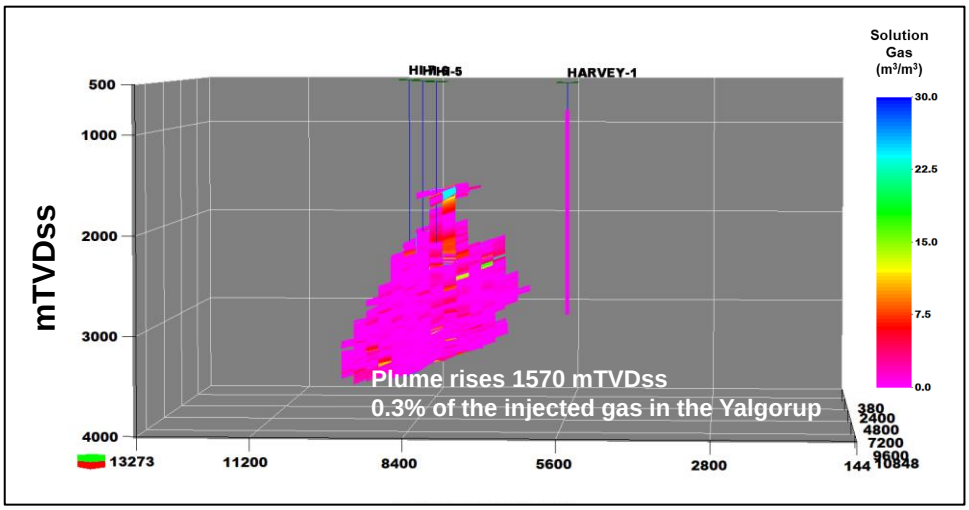

Figure 6-33 CO_2 Plume Shape of Stress Scenario – Case 14 @1000 years

7. DEVELOPMENT SCENARIOS

Table 7-1 is a summary of the development scenarios run to test the robustness of the development concept.

Case	Case Name	Geological Model	Description
1	2Well	Reference	Two injectors 800,000 tpa. Brine salinity=45600 ppm (NaCl Equivalent) Krg=0.08 SgT based on Land Correlation C=1.95
2	3Well_shallow	Reference	800,000 tpa. Brine salinity=45600 ppm (NaCl Equivalent) Krg=0.08 SgT based on Land Correlation C=1.95 Injectors perforated in middle of Wonnerup Member
3	3Well_shallow_NoYal	No communication between Wonnerup and Yalgorup through faults or sand-on-sand conact.	800,000 tpa. Brine salinity=45600 ppm (NaCl Equivalent) Krg=0.08 SgT based on Land Correlation C=1.95 Injectors perforated in middle of Wonnerup Member
4	3Well_Intermediate	Reference	800,000 tpa. Brine salinity=45600 ppm (NaCl Equivalent) Krg=0.08 SgT based on Land Correlation C=1.95 Injectors perforated about 300 metres above the Reference Case in the Wonnerup Member
5	3Well_Intermediate_NoYal	No communication between Wonnerup and Yalgorup through faults or sand-on-sand conact.	800,000 tpa. Brine salinity=45600 ppm (NaCl Equivalent) Krg=0.08 SgT based on Land Correlation C=1.95 Injectors perforated in middle of Wonnerup Member
6	8Well_3MPTA	Reference	8 injectors 3,000,000 tpa. Faults not sealing Brine salinity=45600 ppm (NaCl Equivalent) Krg=0.08 SgT based on Land Correlation C=1.95

Table 7-1 Development Scenarios – Summary of Cases

7.1 Two Well Case

A two-well development of the Harvey area was run to test the robustness of the injection scheme in the event of the loss of one well. Although the loss of one well would only be temporary, this run assumes that only two wells would be available for the life of the project.

Figure 7-1 shows that injection of 800,000tpa could not achieved for about two years due to bottom hole pressure constraints being violated. The bottom hole pressure profiles of the injectors show that displacing the low mobility water phase results in increasing bottom hole pressures until the constraint is reached. Shortly thereafter, injectivity improves as the mobility of the fluids in the near well bore region reduces as CO_2 saturation increases around the injectors; resistance to injection reduces and injection of 800,000tpa becomes achievable. Figure 7-2 shows that the reduction in injectivity has little impact on the overall volume of gas

injected. The distribution of the CO_2 plume in the model are shown in (Figure 7-3 and Figure 7-4). Figure 7-3 shows that the plume in the two-well case is more compact compared to the Reference Case as the injection is in a limited area. However, the CO_2 plume in the two-well case has gone further up dip.

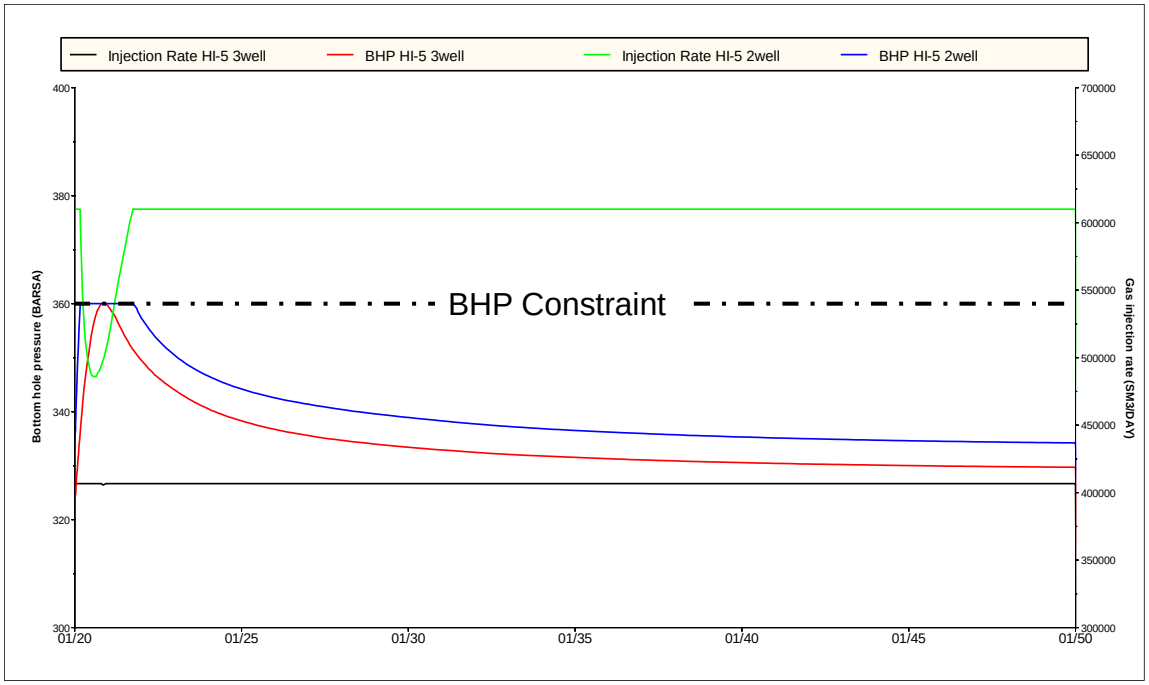

Figure 7-1 Bottom hole pressure profile during the Injection period

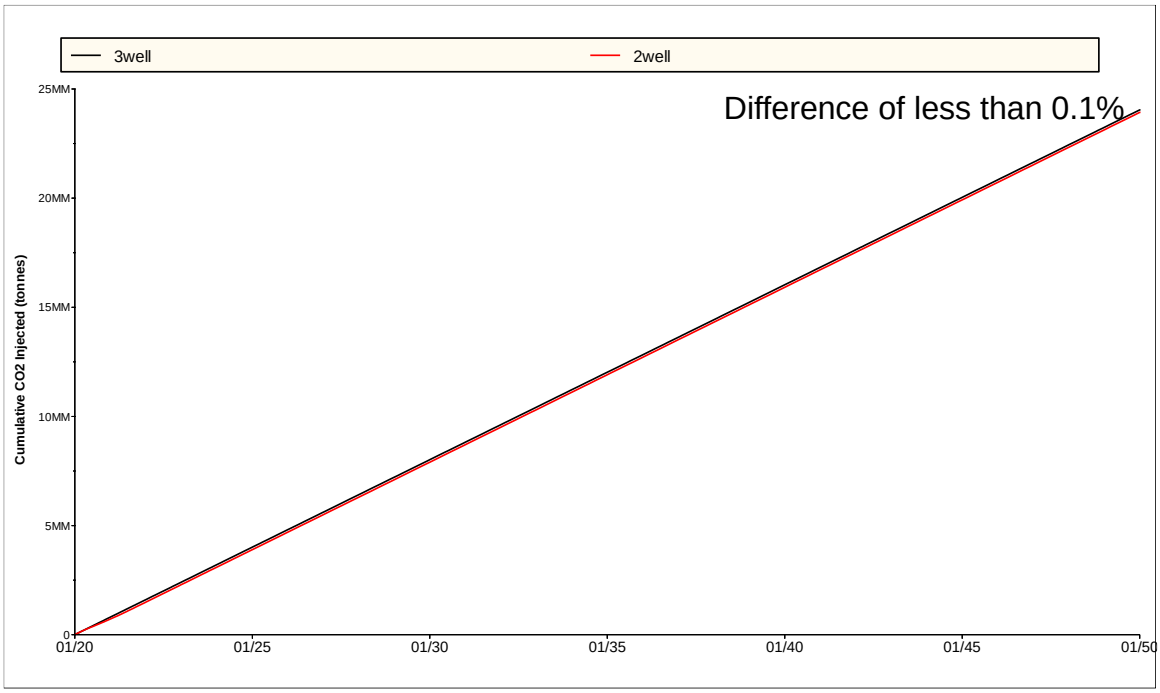

Figure 7-2 Injection Profile – Comparison of Two Well and Reference Case (Black Oil)

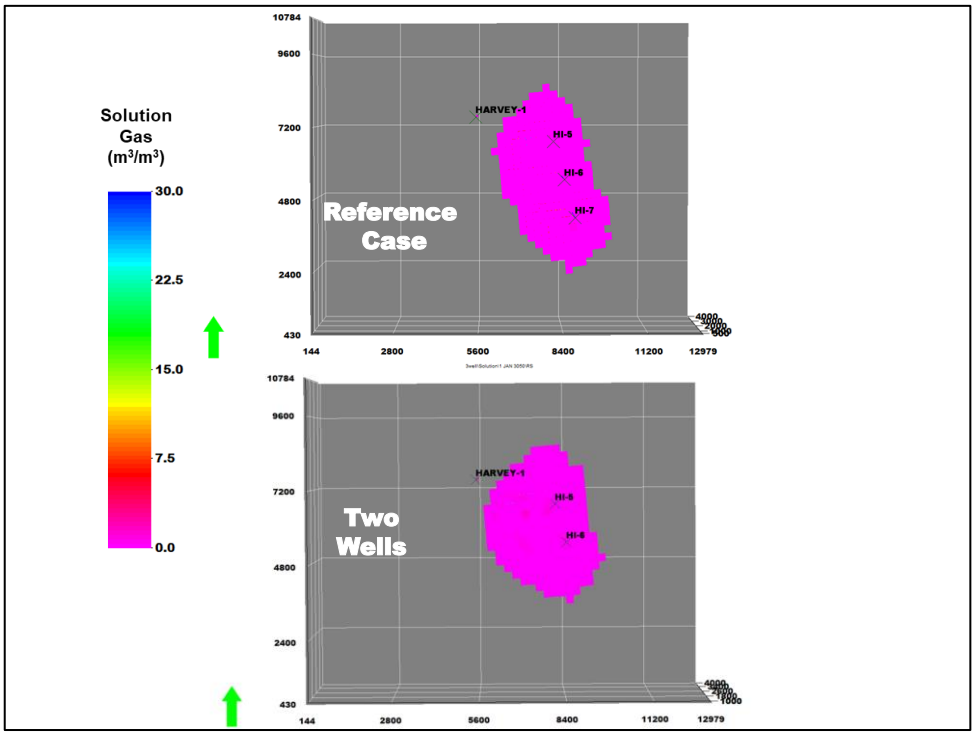

Figure 7-3 Areal View of CO_2 Plume Shape – Comparison of Two Well and Reference Case @1000 years

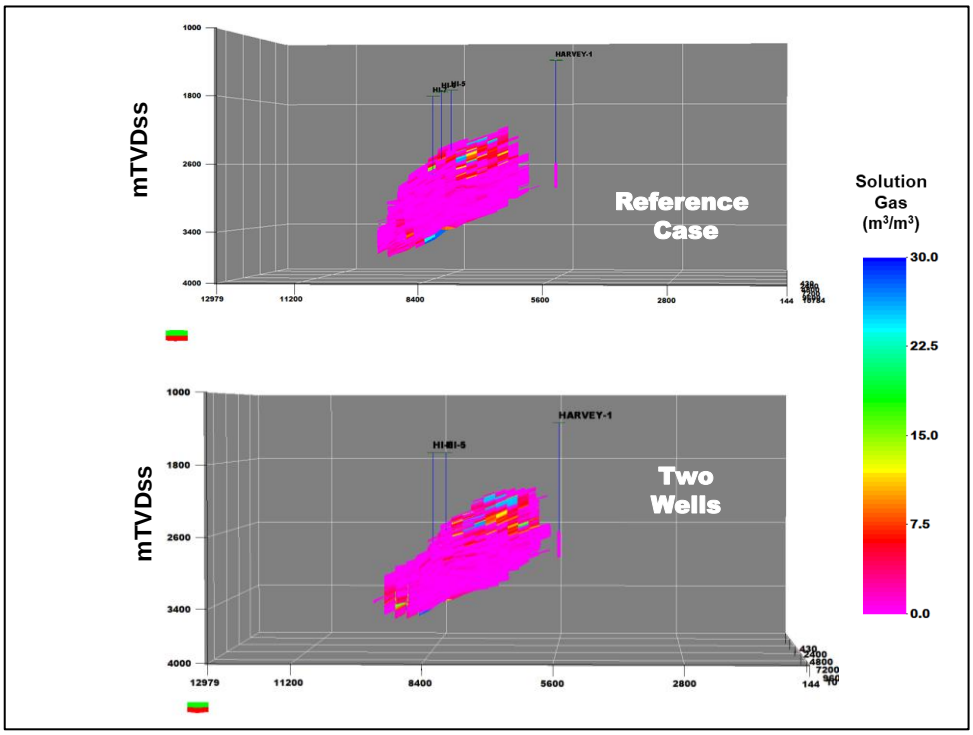

Figure 7-4 Looking South - Plume Shape of Two Well and Reference Case Scenarios @1000 years

7.2 Shallow Injection

The shallow injection scenario assumes that the injectors are perforated about 700 metres from the base of the Wonnerup at about 2,500mTVDss (Figure 7-5). Figure 7-6 shows that at the end of 1,000 years the plume was at 1,137 metres and had not reached the bounding fault to the west. About 11% of the injected CO_2 is in the Yalgorup.

Shallow injection is risky. In the event that there is no communication between the Wonnerup and Yalgorup, there is no secondary containment and the top Wonnerup acts as a ceiling and the CO_2 plume reaches the East-West fault (Figure 7-7).

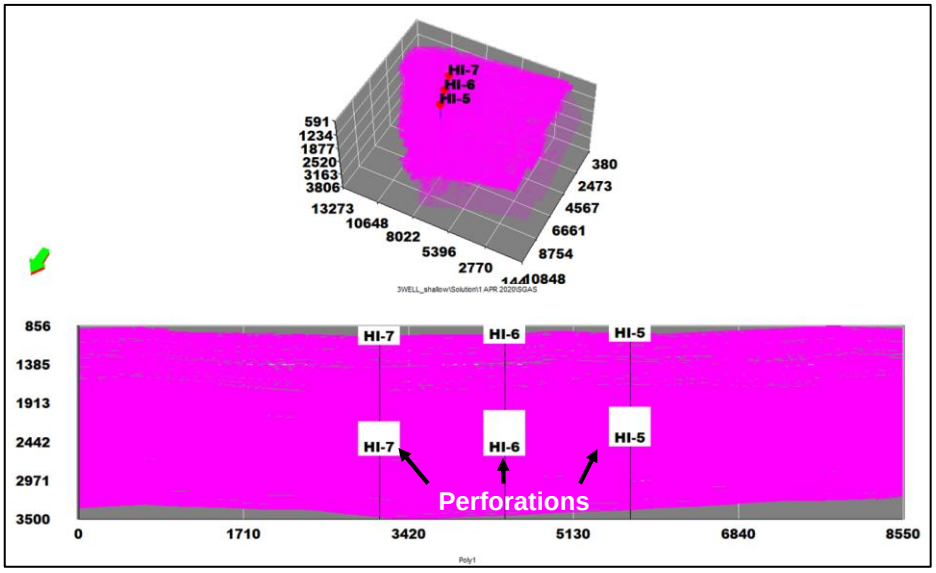

Figure 7-5 Completion Intervals – Shallow Injection Depth

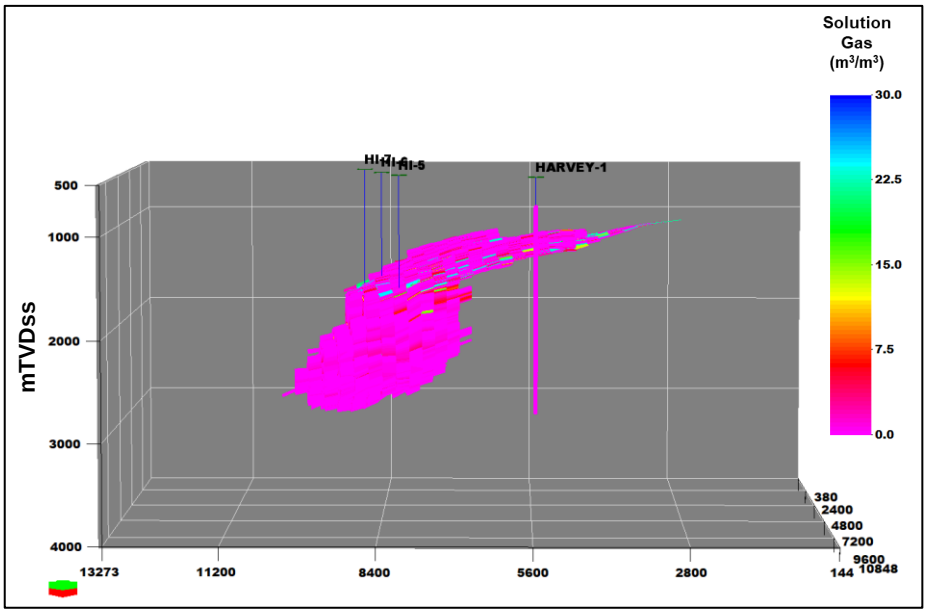

Figure 7-6 Looking South - Plume Shape of Shallow Injection Depth Scenario @1000 years

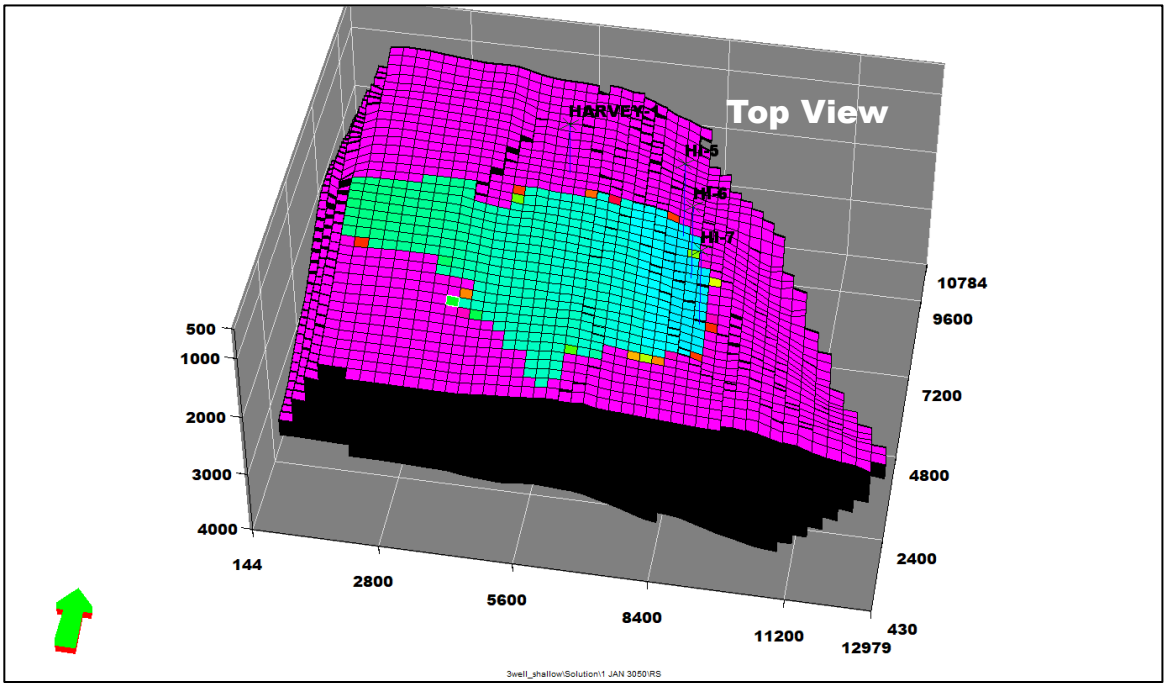

Figure 7-7 Areal View @1000 years - Shallow Injection Depth Scenario (Wonnerup and Yalgorup not in communication)

7.3 Intermediate Injection Depth

The shallow injection scenario assumes that the injectors are perforated about 300 metres from the base of the Wonnerup between 2,500 to 2,900mTVDss (Figure 7-8). Figure 7-9 shows that at the end of 1,000 years the CO_2 plume was within the Wonnerup at a depth of 1,679m.

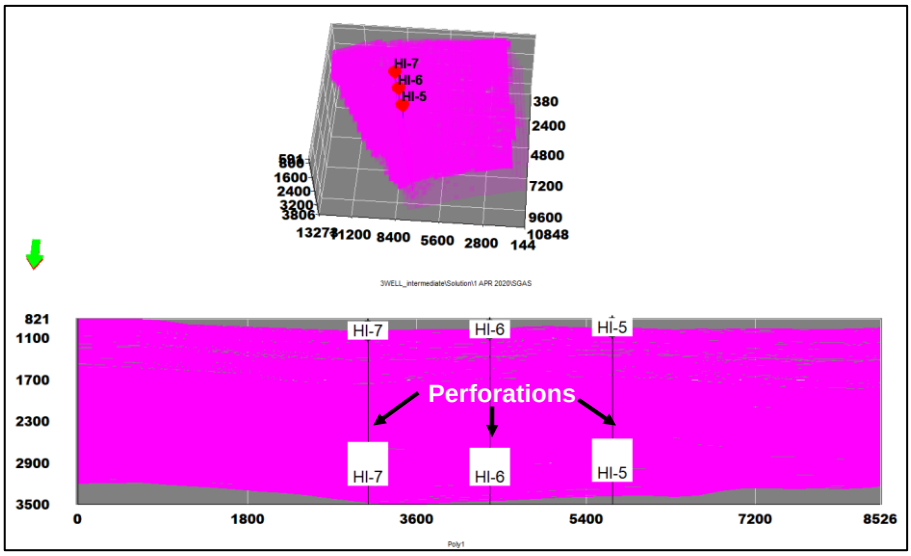

Figure 7-8 Completion Intervals – Intermediate Depth Injection Scenario

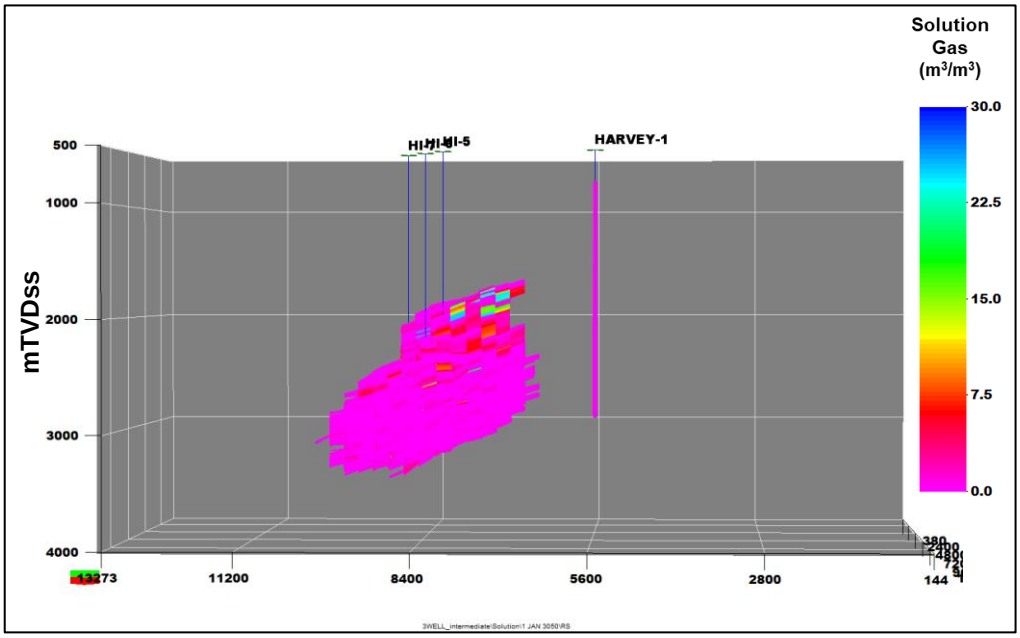

Figure 7-9 Looking South - Plume Shape of Intermediate Depth Injection Scenario

7.4 High Injection Rate

Reference 19 demonstrated that 3 million tonnes per annum of CO_2 could be injected into the Wonnerup through nine wells and up to 90 million tonnes could be sequestered over 30 years. Injection of 3 million tonnes per annum of CO_2 (3.75 times) the Reference Case required 8 wells to stay within the bottom hole pressure constraints. Figure 7-10 show the location of the 8 injection wells in the model.

Figure 7-11 shows that 3 million tonnes per annum of CO_2 could be injected into the Wonnerup and up to 90 million tonnes could be sequestered over 30 years. The slight drop in injectivity in the early years dissipates quickly as the mobility of the fluid around the well decreases due to high CO_2 saturation.

Figure 7-12 shows that, as expected, the increased mass of CO_2 injected results in an increase in the areal extent of the CO_2 plume with the plume almost reaching GSWA Harvey-1. The increase in the amount of CO_2 sequestered results in the plume rising to about 1,300mTVDss in the Yalgorup (Figure 7-13) and remaining in the secondary containment unit.

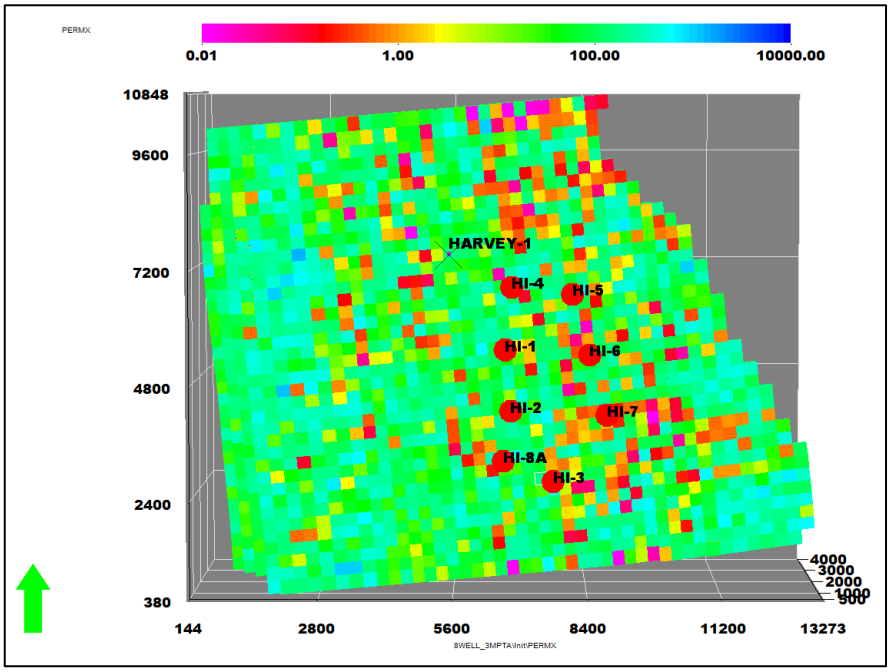

Figure 7-10 Well Locations – High Injection Scenario

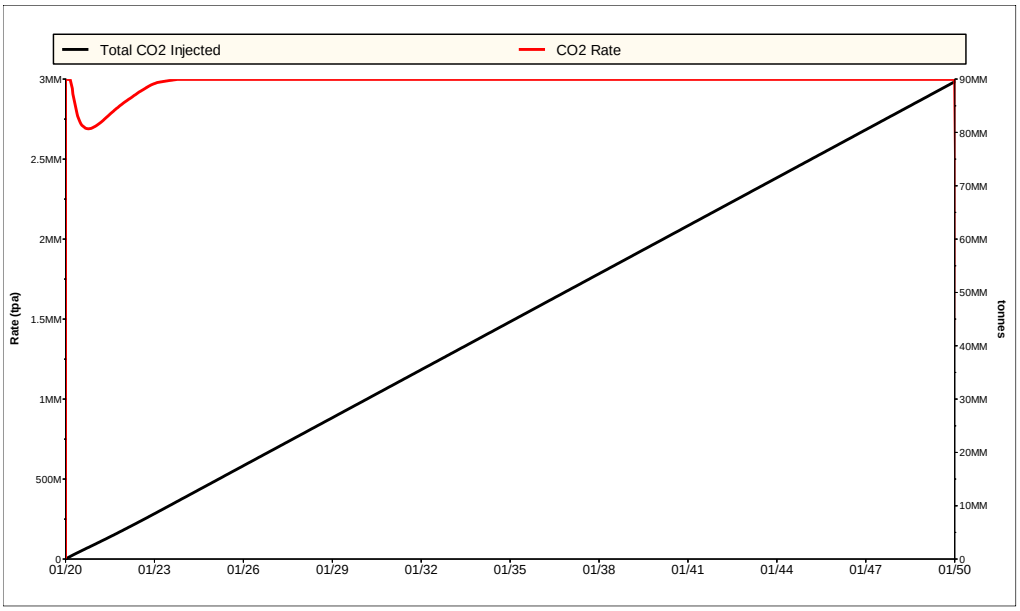

Figure 7-11 Injection Profile for High Injection Scenario

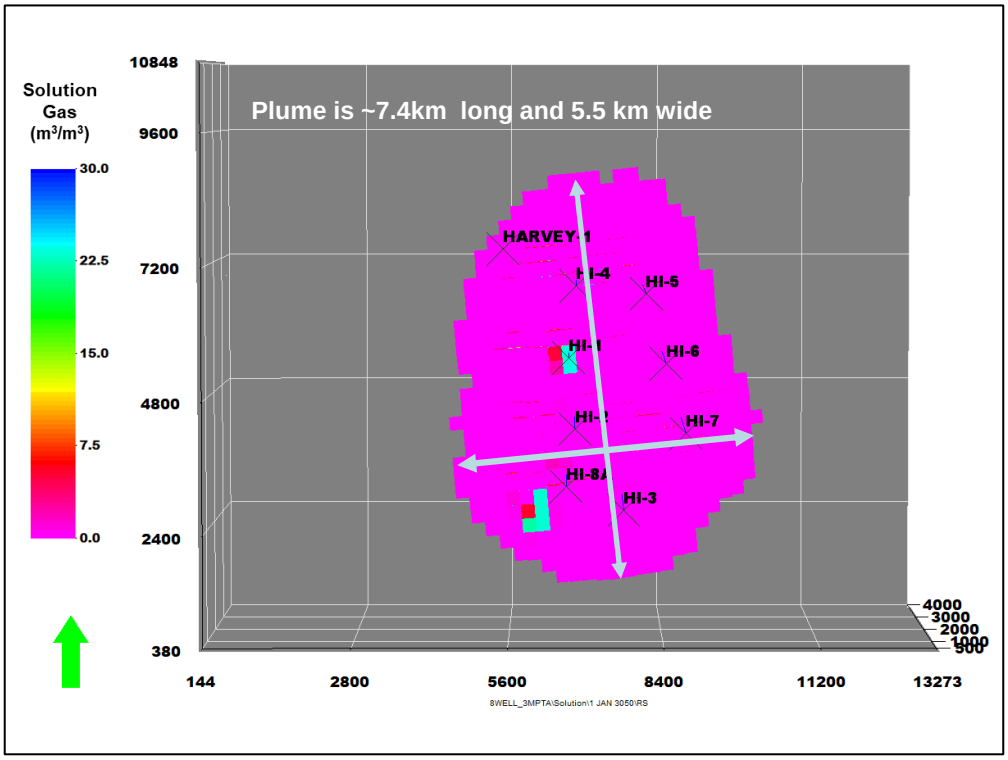

Figure 7-12 CO_2 Plume Shape – Areal view of High Injection Scenario

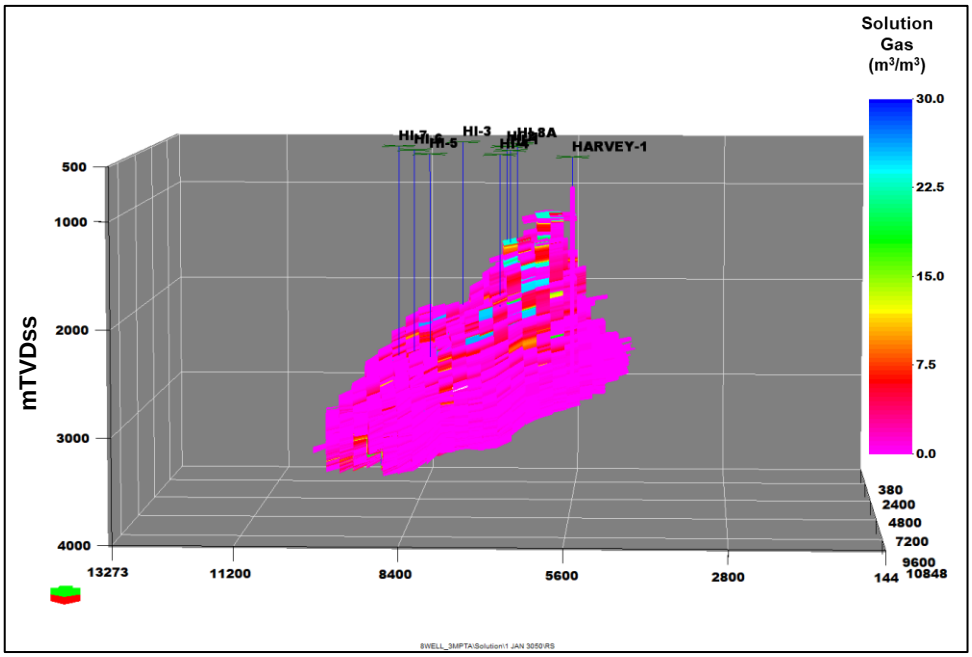

Figure 7-13 Looking South – CO_2 Plume Shape of High Injection Scenario

8. OBSERVATIONS – BLACK OIL MODELLING

The results of the black oil modelling show that it could be feasible to inject 800,000tpa of CO_2 over 30 years in the Yalgorup and Wonnerup formations in the Harvey area. Our modelling studies show that all of the injected CO_2 remains in the Area of Interest and that the main factors controlling CO_2 plume migration are:

- the solubility of CO_2 in brine

and

- The combination of the transmissibility of fluids across the faults, and high vertical permeability fracture zones close to faults.

The results of the modelling also show that communication between the Wonnerup and Yalgorup, through faults or sand-to-sand communication can result in migration of CO_2 between the members.

9. COMPOSITIONAL MODELLING

Simulations conducted using the Black Oil description of the CO_2 sequestration (Sections 0 and 6) show that it could be feasible to inject 800,000tpa of CO_2 over 30 years in the Yalgorup and Wonnerup formations in the Harvey area. As a sense check, a number of scenarios evaluated with the Black Oil model were modelled in a compositional simulator.

Compositional modelling uses a "compositional" approach based on a thermodynamically-consistent model such as a cubic equation of state (EOS) approach to simulate the physical processes during CO_2 sequestration.

9.1 Simulator Description

The full field model of the Harvey area was constructed in the compositional simulator, GEM™ (Version 2017.10). GEM is a full featured compositional simulator capable of modelling:

- Hysteresis and residual gas trapping.
- Gas solubility in aqueous phase.
- Vaporization of water during CO_2 injection.
- Detailed calculations of brine density, viscosity and accounts for solubility of CO_2 in the brine.

9.2 Model Conversion

The compositional model of the Harvey model was converted from the Black Oil model. Direct conversion of the black oil to compositional model was possible for the following:

- Model rock properties.
- Grid geometry and dimensions.
- Drainage relative permeability, drainage and imbibition capillary pressure curves.
  - The current version of GEM (v2017.10) does not allow imbibition relative permeability curves to be input. Imbibition curves are calculated using the Carlson formulation based on the trapped gas saturation.
- Well production and injection constrains.
- The Black Oil model is isothermal and reservoir temperature is only required when the PVT tables are generated.

9.3 Initialisation Parameters

The full field model was initialised with the following parameters:

- Initial Pressure (Reference 14)
  - Initial pressure based on the RCI data from GSWA Harvey-1
  - Reference pressure of 19,327 kpa at 1900m
- Reservoir Temperature (Reference 14)
  - Temperature varies with depth
  - At 800 metres the temperature is 44 °C
  - At 3000 metres the temperature is 76 °C
- The model was initialised as completely water saturated

9.4 PVT Model

The PVT model used in the simulation was constructed in WinProp™

- The model is a CO2- Brine model with an NaCl concentration of 46 g/l H_2O NaCl Equivalent
- Solubility of CO_2 in the brine is calculated using Henry's Law
- Peng-Robinson Equation of State to model the fugacities of components

9.5 Case Selection

Models for three scenarios described in Sections 0 and 6 were re-constructed in the compositional model:

- Reference Case
- Case 13 – "Holey Faults" with Low Solubility

and

- Case 14 – "Holey Faults" with Low Transmissibility Faults

9.6 Reference Case

Figure 9-1 compares the areal distribution of CO_2 in the Black Oil and compositional model. The plume in the compositional model is larger because the CO_2 has not risen as much vertically (Figure 9-2) compared to the plume in the Black Oil model. It is noteworthy that both the Black Oil and compositional model predict that the injected CO_2 remains in the Yalgorup and Wonnerup reservoirs in the Harvey area.

Figure 9-3 shows that the CO_2 is effectively immobile after about 200 years after the cessation of gas injection. Table 9-1 compares the distribution of CO_2 1000 years after the cessation of injection and shows that Black Oil model is more optimistic in solubility but more pessimistic in its results for the amount of trapped gas. The difference could be due to two factors:

- The Black Oil model is isothermal whereas the compositional model has a temperature gradient
- The current version of the compositional simulator uses Carlson's method to calculate the bounding imbibition relative permeability curve based on a value of Sg_T. In the Black Oil model, the bounding imbibition relative permeability curve is input as a table

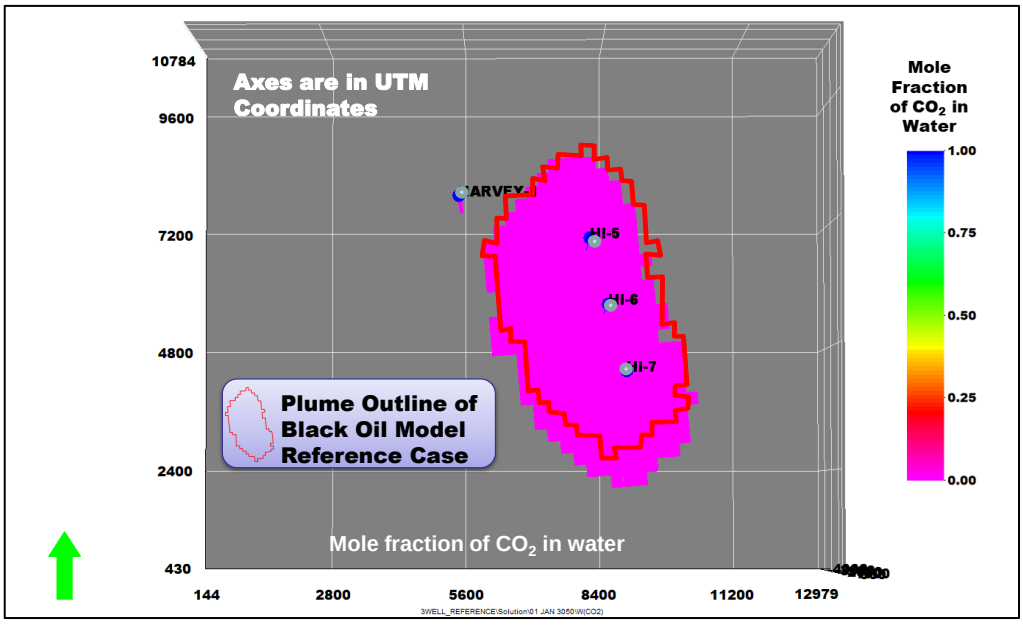

Figure 9-1 Top View Comparison of CO2 Plume @ 1000 years – Reference Case (Black Oil and Compositional)

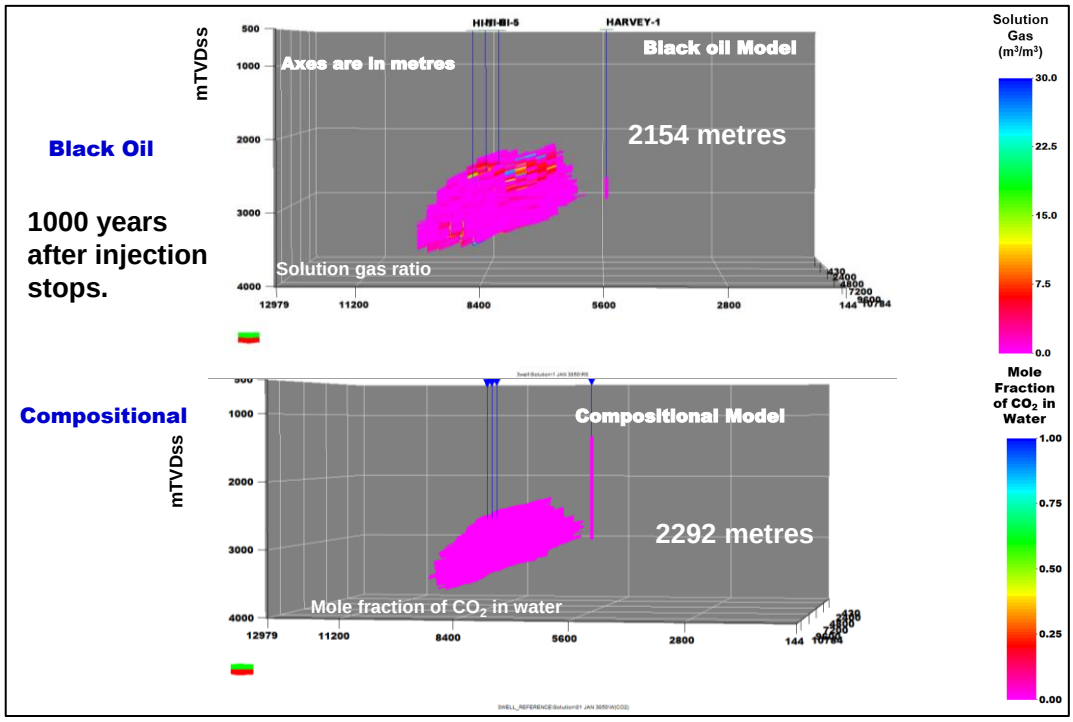

Figure 9-2 Looking South Comparison of CO2 Plume – Reference Case (Black Oil and Compositional)

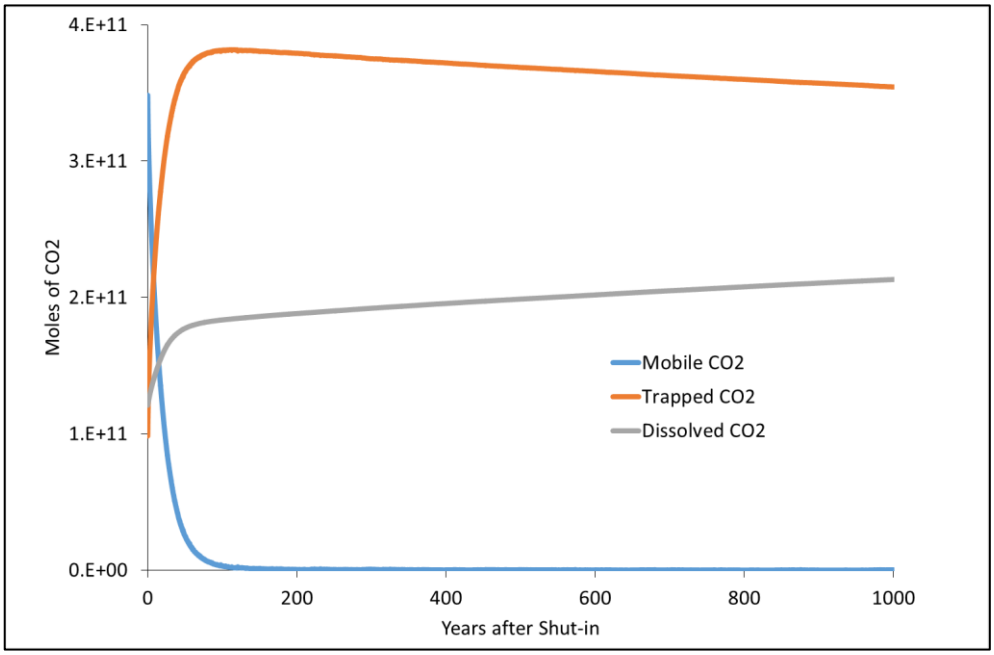

Figure 9-3 CO_2 Distribution over Time – Reference Case (Compositional Model)

(Reference Case – Black Oil Model)

	Supercritical CO2			
	Trapped Gas (Sm3)	Mobile Free Gas (Sm3)	Total CO2 Dissolved (Sm3)	Total CO2 (Sm3)
Gas Material Balance	5.4E+09	2.0E+07	7.7E+09	1.3E+10
% of Injected	40.9%	0.2%	59.0%	100%

(Reference Case - Compositional Model)

	Supercritical CO2			
	Trapped Gas (moles)	Mobile Free Gas (moles)	Total CO2 Dissolved (moles)	Total CO2 (moles)
Gas Material Balance	3.54E+11	2.37E+08	2.13E+11	5.68E+11
% of Injected	62.4%	0.0%	37.5%	100.0%

Table 9-1 Material Balance Accounting – Reference Case (Black Oil and Compositional Model)

9.7 "Holey Faults" with Low Solubility (Case 13)

Figure 9-4 and Figure 9-5 compares the shape of the CO_2 plume for Case 13 as calculated by the Black Oil and compositional models. The results of both models are similar in that they predict that injected gas would migrate to the secondary containment unit in the Yalgorup and remain in the area of interest.

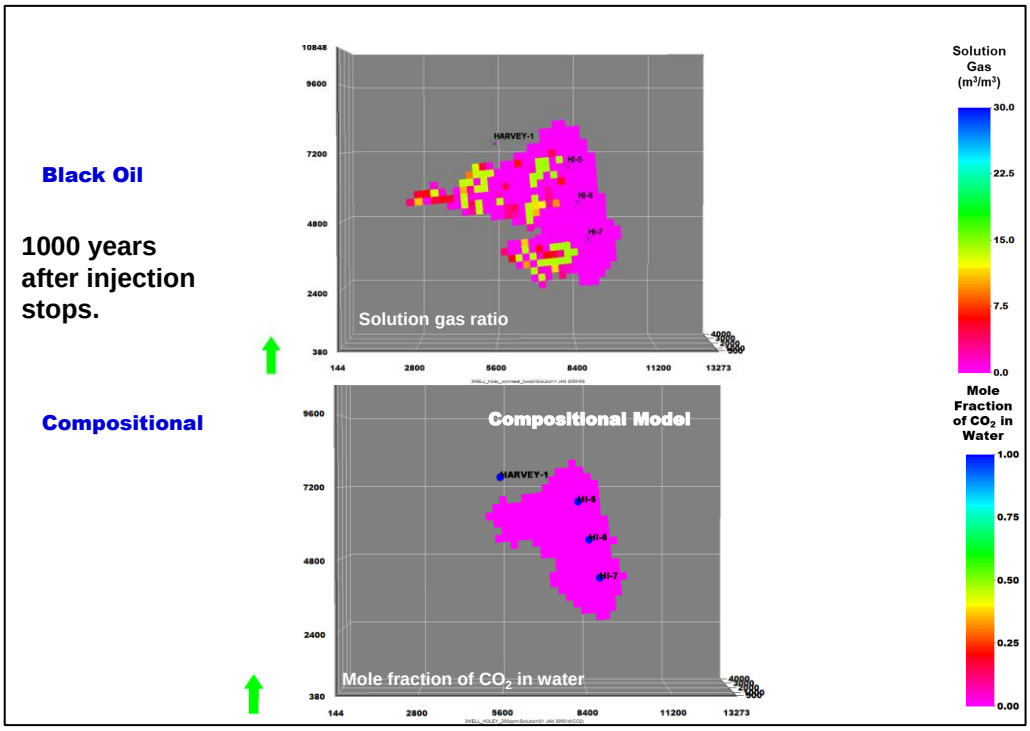

Figure 9-4 Areal View CO_2 Plume Shape of Stress Scenario

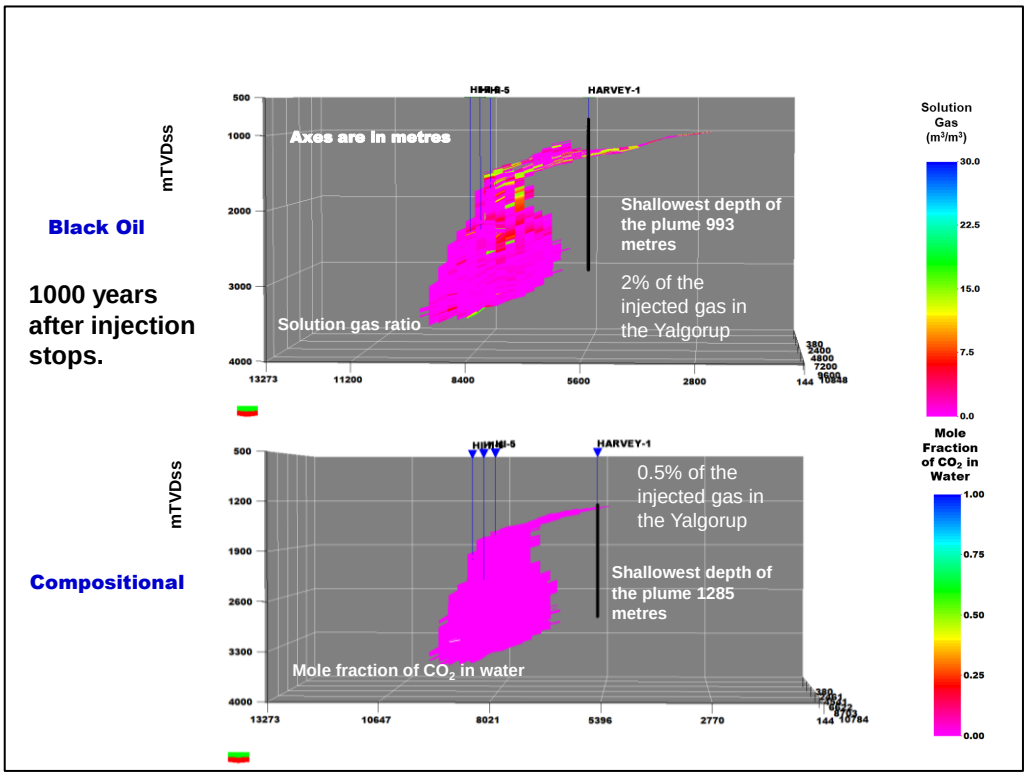

Figure 9-5 Looking South - CO_2 Plume Shape of Stress Scenario

9.8 "Holey Faults" and Low Transmissibility Faults

Figure 9-6 compares the shape of the CO_2 plume for Case 14 as calculated by the Black Oil and compositional models. The results of both models are similar in that they predict that injected gas would migrate to the secondary containment unit in the Yalgorup but remain within the area of interest. However, the compositional model predicts that the CO_2 plume would not rise as high as predicted by Black Oil model.

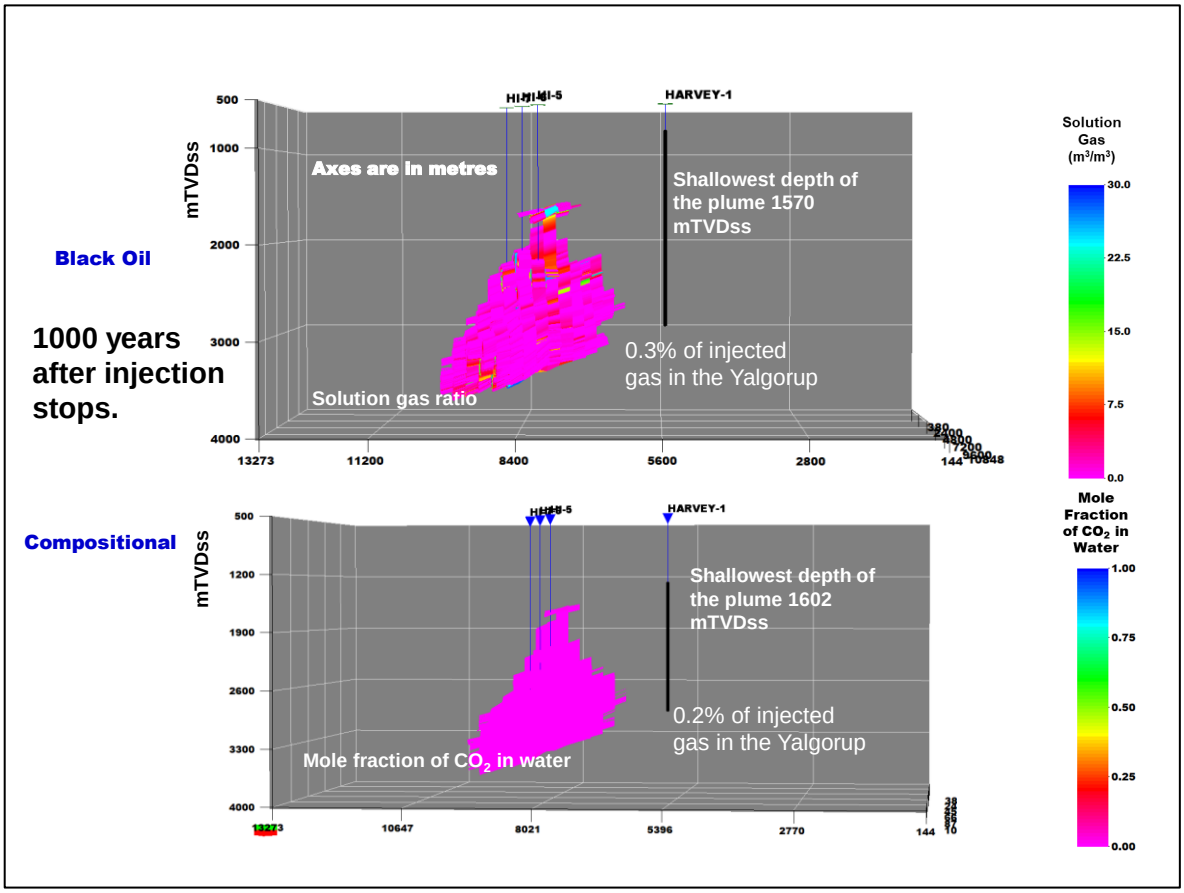

Figure 9-6 Looking South – Plume Shape of High Vertical Permeability and Low Fault Transmissibility

10. OBSERVATIONS – COMPOSITIONAL MODELLING

Our modelling shows that the description of the CO_2 plume in the compositional models are similar to those predicted using the Black Oil models. These results confirm that the Black Oil formulation can effectively model CO_2 sequestration in the Harvey area and indicate that it could be feasible to inject 800,000tpa of CO_2 over 30 years in the Yalgorup and Wonnerup formations in the Harvey area.

The results of the compositional modelling also show that communication between the Wonnerup and Yalgorup, through faults or sand-to-sand communication, can result in migration of CO_2 between the members. Nevertheless, the injected CO_2 remains within the area of interest even in pessimistic and low probability geological and fluid flow realisations.

11. REFERENCES

1. Zhan, Y.: "2D Seismic Interpretation of the Harvey Area, Southern Perth Basin, Western Australia" GSWA Record 2014/7

2. Core Laboratories, "Final Special Core Analysis – Selected Samples from Wells: DMP Harvey-1, DMP Harvey-3, and DMP Harvey-4." HOU-1703703, February 2018

3. Core Laboratories Petroleum Services Division. "Advanced Core Analysis Study Department of Mines and Petroleum Harvey-3." HOU-150878, January 2016

4. Burnside, N. M. and Naylor, M., "Review and implications of relative permeability of CO_2/brine systems and residual trapping of CO_2", International Journal of Greenhouse Gas Control, 23, pp. 1-11

5. Land, C.: "Comparison of Calculated with Experimental Imbibition Relative Permeability." SPEJ (Dec. 1971), pp. 419-425.

6. Delle Piane, C., Olierook, H.K.H., Timms, N.E., Saeedi, A., Esteban, L., Rezaee, R., Mikhaltsevitch, V., Lebedev, Maxim. 2013. "Facies-based rock properties distribution along the Harvey 1 stratigraphic well." CSIRO Report Number EP133710

7. Brooks, R.H. and Corey, A.T.: "Hydraulic Properties of Porous Media," Hydrology Papers No. 5, Colorado State University, March 1964.

8. Purcell, W.R.: "Capillary Pressures – Their Measurement Using Mercury and the Calculation of Permeability", Trans. AIME, (1949), 186, 39.

9. Li, K. and Horne, R.N.:"A Universal Capillary Pressure Model: Verification and Application", Geothermal Resources Council Transactions, Vol. 28, September 2004.

10. Li, K..:"Generalized Capillary Pressure and Relative Permeability Model Inferred from Fractal Characterization of Porous Media, SPE 89874, Presented at the SPE Annual Technical Conference and Exhibition, Houston, Texas, USA, 26-29 September 2004.

11. Personal Communication, Louise Stelfox and David Lim, May 2016

12. Core Laboratories Australia. "Water Analysis Report for DMP Harvey-4." AFL 2015018

13. Rockwater. "Harvey-3 Lesueur Formation Fluid Sampling", August 2015

14. ODIN Reservoir Consultants: “Black Oil Modelling of CO2 Sequestration and Model Upscaling in the Harvey Area”, Report for Department of Mines and Petroleum, WA, DMIRS/2018/5, December 2017.

15. Seyedmohammad Shariati Pour, Gillian E. Pickup, Eric James, Niklas Heinemann: ”Flow Simulation of CO_2 Storage in Saline Aquifers Using Black Oil Simulator”, CMTC-151042-MS, presented at the Carbon Management Technology Conference, 7-9 February, 2012, Orlando, Florida, USA

16. Hassan Hassanzadeh, Mehran Pooladi-Darvish, Adel M. Elsharkawy, David W. Keith, Yuri Leonenko: “Predicting PVT data for CO_2–brine mixtures for black-oil simulation of CO2 geological storage”, International Journal of greenhouse gas control 2 (2 0 0 8) 6 5 – 77

17. ODIN Reservoir Consultants: “Static Model of the Harvey Area”, Report for Department of Mines and Petroleum, WA, DMIRS/2018/6, June 2018.

18. ODIN Reservoir Consultants: “Static Model of the Harvey Area”, Report for Department of Mines and Petroleum, WA, DMP/2016/4, July 2016.

19. ODIN Reservoir Consultants: “Dynamic Modelling of CO_2 Sequestration in the Harvey Area”, Report for Department of Mines and Petroleum, WA, DMP/2016/5, July 2016.